STUDIES ON
SOME NEW COMPLEXES OF IRON, COBALT, NICKEL AND COPPER

Thesis submitted to the
Cochin University of Science and Technology
in partial fulfilment
of the requirements for the degree of

DOCTOR OF PHILOSOPHY

in

CHEMISTRY

under the Faculty of Science

by

A. R. KARTHIKEYAN

DEPARTMENT OF APPLIED CHEMISTRY
COCHIN UNIVERSITY OF SCIENCE AND TECHNOLOGY
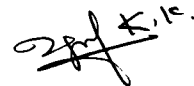KOCHI - 682 022

APRIL 1992

CERTIFICATE

This is to certify that the thesis bound herewith is an authentic record of research work carried out by the author under my supervision in partial fulfilment of the requirements for the degree of Doctor of Philosophy of Cochin University of Science and Technology.

Kochi 682022

27th April 1992

Dr.K.K.MOHAMMED YUSUFF
(Supervising Teacher)

The thesis deals with our studies on some metal complexes of interesting Schiff bases and also on some mixed ligand complexes. The Schiff base ligands used in the present study are those formed by the condensation of 2-aminocyclopent-1-ene-1-dithiocarboxylic acid (ACDA) with benzaldehyde, salicylaldehyde, quinoxaline-2-carboxaldehyde or with polymer bound benzaldehyde. Another Schiff base ligand derived from quinoxaline-2-carboxaldehyde and crosslinked polystyrene functionalized with amino group, PSBQC, has also been used in the present study. The ligands involved in the synthesis of the mixed ligand complexes are dimethylglyoxime, 1-benzyl-2-phenylbenzimidazole (BPBI), 2-alkyl derivatives of ACDA and N,N'-bis(salicylaldehyde)ethylenediimine (Salen).

The thesis is divided into eight chapters. Chapter 1 is a brief discussion on the stereochemistry and electronic properties of iron(III), coblat(II), cobalt(III), nickel(II) and copper(II) complexes. Scope of the present investigation is also given at the concluding section of this chapter.

The details of the preparation and purification of the ligands, reagents etc., employed in the study are

i

given in chapter 2. Furthermore, the informations regarding various characterization techniques employed are also given in this chapter.

New Schiff base ligands have been synthesized by condensing ACDA with benzaldehyde or salicylaldehyde. Some iron(III), cobalt(II), nickel(II) and copper(II) complexes of these ligands have been synthesized and characterized. Studies on these new complexes are presented in chapter 3. Chapter 4 of the thesis deals with our studies on some new iron(III), cobalt(II), nickel(II) and copper(II) complexes of a Schiff base derived from ACDA and quinoxaline-2-carboxaldehyde.

Iron(III), cobalt(II), nickel(II) and copper(II) complexes of a polymer bound Schiff base (formed by condensation of ACDA with polymer bound benzaldehyde) have been synthesized. Thermal behaviour of these complexes were investigated by the techniques of thermogravimetry (TG), derivative thermogravimetry (DTG) and by differential scanning calorimetry (DSC). Details on these studies are given in chapter 5. Chapter 6 of the thesis deals with our studies on iron(III), cobalt(II), nickel(II) and copper(II) complexes of another interesting polymeric Schiff base ligand, PSBQC. Thermal studies of the complexes are also included in this chapter.

Furthermore, a few mixed ligand complexes of Fe(III), containing Salen and ACDA or its alkyl derivatives such as isopropyl and n-butyl were synthesized and characterized. Studies on these complexes are presented in chapter 7.

Chapter 8 of the thesis describes our studies on some mixed ligand complexes which are synthesized by reacting cobaloxime with a bulky ligand, BPBI, in n-butanol medium. This chapter has two sections. Section A deals with the synthesis and characterization of the complexes and Section B deals with thermal decomposition kinetic studies.

Results presented in this thesis have been published/are under publication as indicated below:

1. "Mixed ligand complexes of cobaloxime with a bulky ligand, 1-benzyl-2-phenylbenzimidazole", K.K.M.Yusuff and A.R.Karthikeyan, Synth. React. Inorg. Met.-Org. Chem., 21 (6 & 7), 903 (1991).

2. "Thermal decomposition kinetics of mixed ligand complexes of cobaloxime with 1-benzyl-2-phenylbenzimidazole", K.K.M.Yusuff and A.R.Karthikeyan, Thermochim. Acta, (in press).

3. Iron(III), cobalt(II), nickel(II) and copper(II) complexes of new Schiff bases derived from 2-amino-cyclopent-1-ene-1-dithiocarboxylic acid and benzaldehyde or salicylaldehyde", (communicated).

4. "Iron(III), cobalt(II), nickel(II) and copper(II) complexes of a Schiff base ligand derived from quinoxaline-2-carboxaldehyde and 2-aminocyclopent-1-ene-1-dithiocarboxylic acid" (under preparation).

5. "Iron(III), cobalt(II), nickel(II) and copper(II) complexes of a Schiff base derived from polymer bound benzaldehyde and 2-aminocyclopent-1-ene-1-dithio-carboxylic acid", (under preparation).

CONTENTS

* * *

Chapter 1

INTRODUCTION AND SCOPE OF THE PRESENT INVESTIGATION

Today the study of coordination compounds has emerged as one of the major center of attraction for the inorganic chemist. It covers a comprehensive range of fascinating and theoretical applications. In synthetic work they continue to provide a challenge in the laboratory In industry coordination compounds play key roles in homogeneous[1-7] and heterogeneous[8-12] catalysis, purification of water,[13] analytical chemistry,[14] solvent extraction,[15-17] photography,[18] metallurgy[19] and electrochemistry.[20-21] They are also used as dyes[22,23] and also used for the formulation and improvement of semiconductors,[24] superconductors,[25] advanced ceramic materials[26] and pharmaceuticals.[27-29] They are essential in many life processes such as oxygen transfer and metal ion control.[30-31] In fact the rapidly developing field of bioinorganic chemistry is centered on the presence of metal complexes in the biological systems.[34-36] Moreover, the study of coordination compounds has enabled the inorganic chemist to make significant progress in refining the concept of chemical bonding and to explain the influence that bonding has on the various properties of the compounds.

Majority of the coordination compounds are those of transition elements. Among the transition elements the main transition group or d block includes the elements that have partly filled d orbitals either in the ground state of the free atom or in one or more of their chemically important ions. The d orbitals "project well out to the periphery of the atoms and ions so that the electrons occupying them are strongly influenced by the surroundings of the ions, and in turn are able to influence the environments very significantly".[37]

As the present investigation is confined to the studies on some complexes of iron(III), cobalt(II), cobalt(III), nickel(II) and copper(II), a brief discussion on the stereochemistry and electronic properties of the complexes of these metal ions is presented here.

1.1 COORDINATION CHEMISTRY OF IRON(III)

Iron(III) forms a variety of cationic, neutral and anionic complexes. It shows a high preference for hard bases, especially for O-donor ligands. Majority of the complexes favour an octahedral coordination, a number of complexes exist in other geometries also. Physical techniques such as EPR, Mössbauer and vibrational spectra can give a good deal of information about the electronic and molecular structure of these complexes.

Octahedral complexes of iron(III) usually exist in high or low spin state. The ferric ion has five 3d electrons so that $t_{2g}^3 e_g^2$ (S = 5/2), $t_{2g}^4 e_g^1$ (S = 3/2) or t_{2g}^5 (S = 1/2) ground states may arise. Systems with S = 3/2 are known, in relatively few cases, when there is a strong tetragonal field.[38,39] Fe(III) is high spin with $t_{2g}^3 e_g^2$ configuration in nearly all its octahedral complexes except those with the strongest ligands.

Magnetic susceptibility measurements afford excellent means of determining the ground state term.[40] Ions with a $^6A_1$ ground state (S = 5/2) have moments close to 5.92 BM predicted by the spin only formula for an orbital singlet. As there are no other states with the same spin multiplicity, large deviations cannot occur due to the mixing in of excited states into the ground state although high order perturbations are probably responsible for slight deviations from this spin only value. Deviations may also arise due to impure materials or dimer formation whereby antiferromagnetic interaction can lead to low μ_{eff} values.

Magnetic moment values of complexes with S = 3/2 ground state are around 4.0 BM which is very close to the spin

only value expected for 3 unpaired electrons. The ground
term in these systems is probably $^4A_2$, and hence only a small
orbital contribution to the moment is expected in these
cases.[41]

For systems with S = 1/2, the ground state in an
octahedral field is $^2T_{2g}$. Thus temperature dependent
orbital contribution to the moment is expected. Figgis[42]
has calculated the variation of μ_{eff} with temperature as a
function of the axial field, also making allowance for
covalency. Moments reported lie in the range 2.0-2.6 BM at
ambient temperatures and they usually decrease upon cooling.
Fe(III) tetrahedral complexes are very rare. There are few
reports of square pyramidal Fe(III) complexes. One typical
example[43] is [Fe(S$_2$CNR$_2$)$_2$Cl] which exhibits a μ_{eff} value of
~4.0 BM corresponding to three unpaired electrons with no
orbital contribution.

Dithiocarbamates and Schiff base complexes provide
many good examples of spin crossover and low spin-high spin
equilibria.[44] Trivalent iron dithiocarbamate complexes
have been extensively studied because of their anomalous
magnetic properties. Whether the $^6A_2$ (for the high spin
complex) or the $^2T_2$ (for the low spin complex) term is the

ground state depends on the magnitude of the ligand field splitting energy Δ . There is a balance of the energy terms Δ and P., (the mean pairing energy) which determines whether the complex is high spin or low spin. For $\Delta < P$, a high spin ground state results, and for $\Delta > P$ a low spin ground state results. There will be an equilibrium between the two states, when $\Delta = P$. If the difference in energy between the two states, ΔE is of the order of KT, then the relative populations of the two states will vary with the temperature of the sample. In the Fe(III) dithiocarbamate series of complexes,[45] $[Fe(R_1R_2 \, dtc)_3]$, ΔE can be varied by suitable choice of substituents R_1 and R_2. Although these substituents are well removed from the FeS_6 molecular core, they can appreciably affect the electronic parameters of the central iron atom and of the surrounding crystal field of the sulphur atom by the conjugated system of the ligand. The evidence for spin crossover equilibria can be obtained by carrying out temperature dependent magnetic suscepti-bility measurements.

1.1.1 Electronic Spectra

For the high spin complex the ground state is $^6A_1$ in a weak ligand field. There are no other sextuplet states, so that all excited states of the d^5 ion have a

different spin multiplicity to the ground state and transitions to them are spin forbidden. Hence the absorption bands due to d-d transitions are extremely weak. These bands are probably made possible by the mixing up of spin quartet excited states and the ground state via spin orbit coupling. High spin d-d spectra are generally more difficult to assign, the reason for this is that charge transfer absorption occurs at lower energy in the ferric complexes due to the high positive charge and thus obscures most of the d-d bands.[46]

Few data are available for S = 3/2 systems. Many transitions are spin allowed. Moreover, there is likely to be a good deal of enhancement of molar extinction coefficient values through overlap with charge transfer bands.

Spin allowed transitions are possible when $^2T_2$ becomes the ground state. Ewald et al.[47] have examined the spectral transitions in the visible and UV regions of a number of low-spin iron-sulphur complexes. They could obtain reasonable 10 Dq values of ca, 20,000-25,000 cm^{-1} although the molar extinction coefficient values (upto 10^3) are usually high due to the overlap with charge transfer bands.

1.2 COORDINATION CHEMISTRY OF COBALT(II) AND COBALT(III)

Cobalt(II) forms numerous complexes mostly either octahedral or tetrahedral.[37] Five coordinate and square planar complexes are also known. Tetrahedral complexes of cobalt(II) are more in number than for other transition metal ions. This is mainly due to the fact that, for the d^7 ion, ligand stabilization energies disfavour the tetrahedral configuration relative to the octahedral one to a smaller extent than for any other d^n configuration.

Magnetic moment values for the high spin octahedral complexes lie between 4.7 and 5.2 BM.[48] Because of the intrinsic orbital angular momentum in the octahedral ground state, there is considerable orbital contribution to the magnetic moment.

Low spin cobalt(II) octahedral complexes are rare. These species possess a $t_{2g}^6 e_g^1$ configuration and because of the presence of an electron in antibonding e_g^* orbitals they would be unstable. Furthermore, the complexes are subject to strong Jahn-Teller distortions. Thus they tend to lose ligands and form low spin four or five coordinate species.[49]

Square planar complexes are low spin with magnetic moments of 2.2-2.7 BM. Their spectra are complex and neither magnetic nor spectral properties of such compounds have been studied in detail.

Five coordinate high spin (with three unpaired electrons) and low spin (with one unpaired electron) complexes are found to have either trigonal bipyramidal[50-52] or square pyramidal structures or structures with intermediate configurations.[53,54] The strength of the ligand field, which determines the magnitude of the splitting, is important in determining the spin state. However, the nephelauxetic effect of the donor atoms is much more important since it can reduce the separation between the free ion terms by as much as 50%. As a result of this, the crossover point between high and low spin ground terms may occur at relatively small values of 10 Dq. The nephelauxetic reduction is a function of the electronic delocalization on the ligand and covalency of the metal-ligand bond, which are related to the softness and π-bonding ability of the donor atoms. Thus high-spin complexes are generally formed with hard donors (N, O, Cl etc.) and low-spin complexes are formed with soft donors (P, As, I etc.).[45]

For Co(II) tetrahedral complexes the ground state acquires orbital angular momentum only indirectly through mixing with the $^4T_2$ state by a spin-orbit coupling perturbation. The magnetic moment values are often observed in the range 4.4-4.7 BM.[37]

1.2.1 Electronic Spectra of Cobalt(II) Complexes

For high spin d^7 systems, the ground state term is with a low lying ^4P excited term. Six coordinate octahedral or pseudo-octahedral species will exhibit three transitions.[37]

$$\nu_1 = {}^4T_{1g}(F) \longrightarrow {}^4T_{2g}(F)$$

$$\nu_2 = {}^4T_{1g}(F) \longrightarrow {}^4A_{2g}(F) \text{ and}$$

$$\nu_3 = {}^4T_{1g}(F) \longrightarrow {}^4T_{1g}(P)$$

None of which corresponds in energy with 10 Dq, however, the energy difference $\nu_2 - \nu_1$ is exactly equal to 10 Dq. Unfortunately the ν_2 transition is usually very weak as it is a two electron transition, and rarely unequivocally observed.

Tetrahedral complexes also exhibit three transitions: $\nu_1 = {}^4A_2 \longrightarrow {}^4T_2$, $\nu_2 = {}^4A_2 \longrightarrow {}^4T_1(F)$, $\nu_3 = {}^4A_2 \longrightarrow {}^4T_1(P)$

and all three can be observed, though ν_1 lies at low energy in the near infrared. Both octahedral and tetrahedral complexes display rich spin forbidden transitions, whose intensity is often enhanced by intensity stealing.

The complexes of Co(III) are numerous. Almost all Co(III) complexes are octahedral, though a few tetrahedral, planar and square antiprismatic complexes are known. Six coordinate complexes of cobalt(III) which make up over 99% of known cobalt(III) complexes are invariably low spin and diamagnetic, (with $^1A_{1g}$ ground state term).

1.2.2 Electronic Spectra of Cobalt(III) Complexes

The $^1A_{1g}$ state originating in one of the high energy singlet states of the free cobalt(III) ion drops very rapidly and crosses the $^5T_{2g}$ state (the ground state term in very weak ligand field) at a very low values of L.F.S.E. Thus almost all the known octahedral complexes have low spin configuration, and the d-d transitions from $^1A_{1g}$ ground state of these complexes to other singlet states are possible. The commonly observed two bands are $\nu_1 = {}^1A_{1g} \longrightarrow {}^1T_{1g}$, $\nu_2 = {}^1A_{1g} \longrightarrow {}^1T_{2g}$.

1.3 COORDINATION CHEMISTRY OF NICKEL(II)

The +2 oxidation state is undoubtedly the most prolific oxidation state for nickel. The absence of any other oxidation states of comparable stability for nickel implies that compounds of Ni(II) are largely immune to normal redox reactions.

The coordination number of Ni(II) rarely exceeds 6 and its principal stereochemistries are octahedral, tetrahedral, square planar, square pyramidal and trigonal bipyramidal.[48]

Octahedral nickel(II) complexes have two unpaired electrons and the magnetic moments range from 2.9-3.4 BM depending on the magnitude of the orbital contribution. In an octahedral field three spin allowed transitions are expected because of the splitting of the free ion ground ^3F term and the presence of the ^3P term, and the three bands are

$$\nu_1 \quad = \quad ^3A_{2g} \longrightarrow {}^3T_{2g} \quad = \quad 10 \ Dq$$

$$\nu_2 \quad = \quad ^3A_{2g} \longrightarrow {}^3T_{1g}(F)$$

$$\nu_3 \quad = \quad ^3A_{2g} \longrightarrow {}^3T_{1g}(P)$$

For regular tetrahedral complexes, the magnetic moment values are in the range 3.5-4.0 BM, and for the more

distorted ones the moments are in the range 3.0-3.5 BM.[37] In the electronic spectra of these complexes, three transitions are observed. They are $\nu_1 = {}^3T_1(F) \longrightarrow {}^3T_2(F)$, $\nu_2 = {}^3T_1(F) \longrightarrow {}^3A_2(F)$, $\nu_3 = {}^3T_1(F) \longrightarrow {}^3T_1(P)$. The spectra are more intense than the octahedral complexes and bands are often split by spin-orbit coupling to an extent which can make unambiguous assignments difficult.

A considerable number of both trigonal bipyramidal[55-57] and square pyramidal complexes occur,[58] and high and low-spin complexes of each geometry are known. For high spin square pyramidal complexes, spectra are basically similar to the six coordinate tetragonal systems. There are relatively few square pyramidal low spin nickel(II) complexes. Three transitions are usually observed for such complexes while two are observed for the low spin trigonal bipyramidal complexes. Of these three, namely ${}^1A_1 \longrightarrow {}^1B_1$, ${}^1A_1 \longrightarrow {}^1E$ and ${}^1A_1 \longrightarrow {}^1A_2$, only transition to ${}^1E$ is orbitally allowed.

Of the four coordinate complexes of Ni(II), square planar stereochemistry are the most numerous. They are diamagnetic especially with strong ligands or when steric hindrance impedes high coordination numbers. Diamagnetism

is a consequence of eight electrons being paired in the four
lower lying d orbitals. The upper orbital is $d_{x^2-y^2}$ in
square planar complex with monodentate ligands, where the
x, y cartesian coordinates pass through the Ni-L bonds. If
bidentate ligands are used the x, y coordinates usually
bisect these ligands. Under such circumstances the upper
orbital is d_{xy}. The four lower orbitals are often so close
together in energy, that individual transitions therefrom to
the upper d level, cannot be distinguished. Hence a single
absorption band is usually observed. However, in many cases
a weak shoulder or peak may appear on each side of the main
stronger absorption band.[59]

1.4 COORDINATION CHEMISTRY OF COPPER(II)

Most Cu(I) compounds get easily oxidised to Cu(II)
compounds, but further oxidation to Cu(III) is more
difficult. The d^9-configuration makes Cu(II) subject to
Jahn-Teller distortion if placed in an environment of cubic
symmetry and this has profound effect on all its
stereochemistry.[37] Tetragonally distorted octahedral
coordination and square coordination cannot be sharply
differentiated. Because of the relatively low symmetry of
the environment in which the Cu^{2+} ion is characteristically

found, detailed interpretation of the spectra and magnetic properties are somewhat complicated. The magnetic moments of Cu(II) complexes are in the range 1.75-2.20 BM regardless of stereochemistry and independently of temperature except at extremely low temperature. Majority of the complexes exhibit single absorption band in the region 11,000-16,000 cm^{-1}. The d^9 ion is characterized by large distortion from octahedral symmetry and the band is unsymmetrical being the result of a number of transitions which are by no means easy to assign unambiguously. The T ground term of the tetrahedrally coordinated ion implies an orbital contribution to the magnetic moment and a value in excess of spin only value (1.73 BM) is obtained.

The E ground term of the octahedrally coordinated ion is expected to yield a moment in excess of 1.73 BM because of mixing of the excited T term into the ground term. Moments of magnetically dilute compounds are in the range 1.9-2.2 BM. Compounds whose geometry approaches octahedral have moments at the lower end, and those with pseudotetrahedral have moments at the higher end, however these values cannot be used safely unless supported by other evidences.[48]

1.4.1 Electron Spin Resonance

The copper(II) ion has an effective spin of $S = 1/2$ and associated spin angular momentum of $M_S = \pm 1/2$ leading to a doubly degenerate spin energy state in the absence of a magnetic field. On application of a magnetic field this degeneracy is removed and transition occurs between the two levels given by the condition $h\nu = g\beta H$, where β is the Bohr Magneton, H, the magnetic field, h, the Planck's constant, ν, the frequency of radiation and g, the Lande splitting factor. For a free electron, g has the value 2.0023, whilst for an electron in a ligand field the value may often differ from 2.0023. In a cubic environment only one 'g' value will be obtained while in axial and rhombic crystal fields two and three different g-values are obtained respectively. The g values of copper(II) complexes can be measured in two ways. The measurement involving polycrystalline powder is the most rapid experimental method but only yields approximate g values.[60-67] The single crystal technique yields[68-70] the most accurate g values. Both techniques will only yield the local molecular g values.[71,72] The factors which determine the nature of EPR spectrum observed are (1) the electronic ground state of the complex; (2) the symmetry of the effective ligand field about the copper(II) ion;

(3) the mutual orientations of the local molecular axes of the individual copper(II) complex molecules in the unit cell. If all the tetragonal axes are aligned parallel then the crystal g values accurately reflect the local copper(II) ion environment g values. For the axial spectra[73] the empirical parameter, G (which is equal to $g_\parallel - 2/g_\perp - 2$) is nearly 4.0 and a $d_{x^2-y^2}$ ground state is indicated in such cases. The g values for a regular trigonal bipyramidal stereochemistry have been shown to be equivalent to those for a compressed tetragonal distortion and a low g value slightly greater than 2.00 is shown with a d_{z^2} ground state.[74] If the tetragonal axes in the unit cell are not aligned parallel then the observed crystal g values are not simply related to the g values of the local copper(II) ion environment.[73] In the case of known crystal structures the observed g values may be related to the local g values.[72] The local g values cannot be specified precisely if the crystal structure is unknown. The three types of EPR spectra observed for copper(II) complexes are: isotropic spectra, axial spectra and rhombic spectra.

Isotropic Spectra

Such a spectrum would suggest the presence of a copper(II) ion in

1. A regular static octahedral or tetrahedral stereochemistry, neither of which can occur in practice.

2. A regular octahedral stereochemistry undergoing a dynamic[75] or pseudo-rotational type of Jahn-Teller distortion.[76]

3. $[Cu(L)_x]$ complexes of lower symmetry than octahedral undergoing free rotation.

4. A complex containing grossly misaligned tetragonal axes.[77]

Axial Spectra

Two types of axial spectra are observed depending on the value of the lowest g factor. The spectra with lowest g value greater than 2.04 can be observed for a copper(II) ion in

1. Axial symmetry with all the principal axes aligned parallel. Such a spectrum is expected in complexes with elongated tetragonal-octahedral, square planar, or square based pyramidal stereochemistries. In these axial spectra, the g values are stated by the expression

$G = g_\parallel - 2/g_\perp - 2 = 4.0$. If $G > 4.0$, then, the local tetragonal axes are aligned parallel or only slightly misaligned. If $G < 4.0$, significant exchange coupling[78] is present and misalignment is appreciable.

2. Rhombic symmetry with slight misalignment of the tetragonal axes.

3. Rhombic symmetry with the tetragonal axes elongated but in which the inplane rhombic component is small and the powder technique is insufficiently sensitive to resolve the two planar components.

4. Compressed tetragonal or trigonal bipyramidal molecules occupying two non-equivalent sites, with the principal axes inclined at 90°, (this situation has not been observed).

The spectra with lowest $g < 2.03$ can be observed for a copper(II) ion in

1. Axial symmetry with all the principal axes aligned parallel and would be consistent with compressed tetragonal-octahedral or trigonal-bipyramidal stereo-chemistries as in Ba_2CuF_6.[79]

2. Compressed rhombic symmetry with the slight misalignment of the tetragonal axes.

3. Compressed rhombic symmetry with the tetragonal axes aligned parallel.

Rhombic Spectra

Two types of spectra may be observed, depending upon the value of the lowest g factor. A spectrum with lowest g value greater than 2.04 can be observed for a copper(II) ion in

1. Elongated rhombic symmetry with all the axes aligned parallel and would be consistent with elongated rhombic octahedral, rhombic squareplanar or distorted square based pyramidal stereochemistries.

2. Elongated axial symmetry with slight misalignment of the principal axes.[80] The spectrum with lowest g value less than 2.03 is observed for a copper(II) ion in

    i) compressed rhombic symmetry with all of the axes aligned parallel; such type of spectra can be observed in complexes with compressed rhombic octahedral, cis-distorted octahedral or distorted trigonal-bipyramidal stereochemistries.[81]

ii) compressed axial or rhombic symmetry with slight misalignment of the axes.[82]

1.5 SCOPE OF THE PRESENT INVESTIGATION

Owing to the diverse application of coordination compounds in chemistry and technology, there exists continuing interest in the synthesis and characterization of these compounds, especially those of 3d transition metals. Further, Schiff base ligands offer considerable scope for designing novel complexes of catalytic interest, as they can provide a square planar arrangement about the metals like copper(II) and nickel(II) ions for interaction with the reactants. Cobaloximes, being square planar, are also capable of interacting with the reactant through the vacant coordination sites. Eventhough catalytic studies were not included as a part of our investigation it was our intention to synthesize some new complexes which might later find application as oxidation catalysts. In view of these, complexes involving the following ligands were selected for the present study.

1. Schiff base ligands formed by condensation of 2-amino-cyclopent-1-ene-1-dithiocarboxylic acid with benzalde-hyde (ACB), salicylaldehyde (ACS) and quinoxaline 2-carboxaldehyde (ACQ).

2. Polymeric Schiff base ligands derived from quinoxaline 2-carboxaldehyde and crosslinked polystyrene function- alized with amino group (PSBQC) and 2-aminocyclopent-1- ene-1-dithiocarboxylic acid with polymer bound benzalde- hyde (PACB).

3. 2-aminocyclopent-1-ene-1-dithiocarboxylic acid (ACDA) and its isopropyl and n-butyl alkyl derivatives and N,N'-bis(salicylaldehyde)ethylenediimine (salen).

4. 1-benzyl-2-phenylbenzimidazole (BPBI) and dimethyl- glyoxime.

Several new complexes with the above mentioned ligands have been prepared and characterized by various physicochemical techniques like elemental analysis, conductance and magnetic measurements and infrared and electronic spectral studies. In a few cases studies involving ^{1}H-NMR (section 8.3.3), EPR (sections 3.3.4, 4.3.4, 5.3.4 & 6.3.4) or cyclic voltammetry (section 8.3.4), have been carried out. Thermal decomposition studies like TG and DTA/DSC (sections 5.3.5, 6.3.5 & 8.4) have also been carried out in the case of few complexes.

Chapter 2

EXPERIMENTAL TECHNIQUES

Details about the general reagents used, preparation of ligands and various analytical and physico-chemical methods employed for the characterization of the metal complexes are discussed in this chapter. Procedural details regarding the synthesis of metal complexes are given in the appropriate chapters.

2.1 REAGENTS

The following metal salts were used: $FeCl_3$ (Aldrich, 98% pure); $CoNO_3 6H_2O$ (E.Merck, GR); $CoCl_2 6H_2O$ (E.Merck, GR); $CoBr_2$ (Aldrich, 98% pure); $NiCl_2 6H_2O$ (BDH, GR); $NiBr_2$ (Aldrich, 98% pure), $CuCl_2 2H_2O$ (E.Merck, GR).

Isopropylamine (Fluka), N-butylamine (Fluka), ethylenediamine (Merck), cyclopentanone (Merck), carbon disulphide (Merck), Hexamine (Loba), benzaldehyde (Merck), salicylaldehyde (SRL), n-butanol (Merck), Ninhydrin (Himedia), dimethylglyoxime (BDH), 25% ammonia solution (BDH) and 2% crosslinked chloromethylated polystyrene (Fluka) were used for the present work.

Quinoxaline-2-carboxaldehyde was prepared[83] according to the following procedure:

Glacial acetic acid (6 ml), o-phenylenediamine (21.6 g, 0.2 mol), hydrazine hydrate (5 ml, 0.1 mol) and a pinch of sodium bicarbonate were added to a solution of D-glucose (36 g, 0.2 mol) in water (50 ml), and the mixture was heated under reflux for 5 h on a boiling water bath. The solution was then cooled in ice, and the precipitated product, 2-(D-arabinotetrahydroxybutyl)quinoxaline, was filtered and washed with water. This product was further purified by recrystallization from hot water. The recrystallized 2-(D-arabinotetrahydroxybutyl)quinoxaline (5.0 g, 0.02 mol) was mixed with sodium metaperiodate (13 g, 0.06 mol) in water (300 ml) and glacial acetic acid (10 ml), and the mixture was kept at room temperature with occasional shaking for 16 h. It was then filtered and the filtrate was neutralized with sodium bicarbonate. The neutral solution was extracted with ether. The ether extract was then dried with anhydrous sodium sulphate, filtered and evaporated to dryness. The resulting residue was recrystallized from petroleum ether to give pure quinoxaline-2-carboxaldehyde (yield = 60%, m.p. = 107°C).

Preparation of Aldehyde Resin

The polymer bound benzaldehyde was prepared[84] in the following way. A mixture of chloromethylated polystyrene beads (20 g, 3.8 m equiv. Cl/g), dimethyl sulphoxide (300 ml) and sodium bicarbonate (19 g) was stirred at 138-140°C for 12 h, till the side chain of the beads get oxidised. The resultant resin was filtered, washed with hot ethanol, methylene chloride and benzene (50 ml x 2 min. x 3 times) and dried in vacuo over anhydrous calcium chloride. A portion of the test sample gave yellow colour to the beads on treatment with 2,4-dinitrophenyl hydrazine reagent indicating the presence of aldehyde group (yield 18.75 g, aldehyde capacity 3.67 m. mol/g).

Preparation of Aminomethyl Polystyrene[85] from Chloromethyl Polystyrene Resin

Chloromethyl polystyrene (11 g) were suspended in DMF (200 ml), Hexamethylenetetramine (11.2 g) and potassium iodide (13.28 g) were added to this suspension and heated with stirring under reflux at 100°C in an oil bath for 10 h. The resin was filtered, washed with 6 N HCl and water. It was then stirred with a solution of NaOH (10%, 150 ml) for 2 h, filtered, washed several times with water and methanol (50 ml x 3 min. x 4 times) and dried in vacuum to

constant weight. A test portion of the resin on heating with Ninhydrin reagent (12 ml) gave a deep blue colour. (yield = 4.5 g).

Unless otherwise specified, all other reagents used were of analytical reagent grade. The solvents employed were either of 99% purity or purified by known laboratory procedures.[86]

2.2 PREPARATION OF LIGANDS

2.2.1 2-Aminocyclopent-1-ene-1-dithiocarboxylic Acid (HACDA)

The reagent was prepared following a modified procedure[88] of Takeshima et al.[87] Cyclopentanone (22.2 ml, 0.25 mol) and 25% aqueous ammonia (100 ml) were taken in a stoppered conical flask. The flask was cooled to 0°C by keeping it in a bath containing a freezing mixture of ice and salt. Carbondisulphide (15 ml, 0.25 mol) was then added slowly with constant stirring to this cooled solution. The flask was shaken in an automatic shaker for 8 h, while keeping the same in the freezing bath. Ammonium salt of HACDA was separated as a yellow solid, which was filtered and washed with diethylether. The ammonium salt

is not stable at room temperature; it loses ammonia on standing. However, the acid form is more stable and was prepared by dissolving the crude product in water and slowly neutralising with 2 N acetic acid under ice-cooling. The yellow crystals separated were collected, washed with water and dried over anhydrous calcium chloride (yield = 60%), m.p. = 98°C, decomp).

2.2.2 Alkyl Derivatives of HACDA

Alkyl derivatives of HACDA were prepared by the transamination reaction[88] of HACDA. HACDA (7.9 g, 0.06 mol) and alkylamine, 8 ml (0.01 mol) of i-PrNH$_2$ (i-Pr = isopropyl) or 10 ml (0.01 mol) of n-BuNH$_2$ (n-Bu = Butyl) were dissolved in methanol (100 ml), and the solution was refluxed for one hour. After cooling the solution to room temperature, water (200 ml) was added and the solution was filtered to remove any solid impurities. To this filtrate, 2 N acetic acid was added till the yellow product was separated. The crude product was then recrystallised from acetone (yield = 60%, m.p. = 122°C and 128°C respectively).

2.2.3 Schiff bases Derived from 2-aminocyclopent-1-ene-1-dithiocarboxylic Acid and Benzaldehyde or Salicylaldehyde or Quinoxaline-2-carboxaldehyde

The Schiff bases were prepared by refluxing equimolar quantities of HACDA (7.9 g, 0.05 mol) and the

aldehyde(benzaldehyde (5.3 g, 0.05 mol) or salicylaldehyde (6.1 g, 0.05 mol) or quinoxaline-2-carboxaldehyde (8.4 g, 0.05 mol)) in methanol on a water bath for 6-8 h. The solid separated was filtered, washed with methanol dried over anhydrous $CaCl_2$ and recrystallised from acetone (Yield = 60% and m.p. = 115°C, 140°C, > 300°C respectively).

2.2.4 Schiff Base Derived from 2-aminocyclopent-1-ene-1-dithiocarboxylic acid and Aldehyde Resin

A mixture of the aldehyde resin (10 g) and 2-aminocyclopent-1-ene-1-dithiocarboxylic acid (15 g) in methanol (200 ml) were refluxed at 90°C on a water bath for 4 h. The reaction mixture was then cooled, filtered and washed successively with DMF, ethanol, methanol and chloroform. It was then dried under vacuum. Test with Borsche's reagent was negative (Yield = 12 g).

2.2.5 Schiff Base Derived from Quinoxaline-2-carboxaldehyde and Aminomethyl Polystyrene

A mixture of aminomethyl polystyrene (10 g) and quinoxaline-2-carboxaldehyde (15 g) in methanol (200 ml) were refluxed at 90°C on a water bath for 4 h. The reaction mixture was then cooled, filtered and washed successively with DMF, ethanol, methanol and chloroform. It was then dried under vacuum (Yield = 12.5 g).

2.2.6 N,N'-bis(Salicylaldehyde)ethylenediimine[89] (Salen)

With a set up consisting of an Erlenmeyer flask topped by a dropping funnel and a Dean stark-type receiver with a condenser, a solution of salicylaldehyde (3.66 g, 0.03 mol) in benzene (25 ml) was mixed with a solution of ethylenediamine (0.9 g, 0.015 mol) in benzene (50 ml) taken in the dropping funnel. The solution of ethylenediamine was added drop by drop at room temperature into the stirred reaction mixture. The yellow precipitate of the Schiff base separated out was filtered and dried over anhydrous calcium chloride (Yield = 70%, m.p. 122°C).

2.2.7 1-Benzyl-2-phenylbenzimidazole

This ligand was prepared by adopting the procedure reported in the literature,[90] with slight modifications. Details about the preparation are given below:

o-Phenylenediamine (10.8 g, 0.1 mol) and benzalde-hyde (21.2 g, 0.2 mol) were separately dissolved in glacial acetic acid (50 ml) and mixed. The mixture was kept aside for 12 h. It was then filtered and the filtrate was poured into crushed ice. After 2 h, the mother liquor was

decanted off. The product formed was washed several times with water by decantation and was recrystallized from 50% ethanol (Yield = 60%, m.p. = 134°C).

2.3 ANALYTICAL METHODS

2.3.1 Estimation of Metals

In all the cases, the organic part of the transition metal complexes was completely eliminated before estimation of metals. In the case of the polymer bound metal complexes, this was done by treating the complexes with aqua regia for 24 h at 100°C. The resulting solution was filtered and the metal concentration in the solution was determined by using the following spectrophotometric methods.[14] Iron was estimated by the thiocyanate method. For the determination of cobalt the method involving nitroso-R-salt[14] was employed. Nickel was estimated by extracting the red nickelous dimethylglyoximate in chloroform and measuring the absorbance at 366 nm. Copper was determined by extraction of its diethyldithiocarbamate complex in carbon tetrachloride and measuring the absorbance of the extract at 435 nm.[14]

The following procedure was used for eliminating the organic part of the sulphur containing complexes:

A known weight of the metal complex (0.2-0.3 g) was treated with conc. nitric acid (25 ml) and bromine in carbon tetrachloride (20 ml). This mixture was kept for about 3 h. It was then evaporated to dryness on a water bath and converted to its sulphate by fuming with a few drops of conc. sulphuric acid several times. The resulting metal sulphate was dissolved in water and was used for the estimation of the metal.

A uniform procedure was adopted for eliminating the organic part of all other complexes. A known weight of the metal complex (0.2-0.3 g) was treated with conc. sulphuric acid (5 ml) followed by conc. nitric acid (20 ml). After the reaction subsided, perchloric acid (5 ml, 60%) was added. This mixture was maintained at the boiling temperature for 3 h on a sand bath. The clear solution thus obtained was evaporated to dryness. After cooling, conc. nitric acid (15 ml) was added and evaporated to dryness on a water bath. The residue was dissolved in water and this neutral solution was used for the estimation of metals.

Gravimetric procedures[14] were adopted for the estimation of iron, cobalt and nickel. Iron in the complex was estimated by precipitating the metal with ammonia

solution and igniting the resulting hydroxide to ferric oxide. Cobalt was estimated by precipitating it as $[Co(C_5H_5N)_4](SCN)_2$ using ammonium thiocyanate and pyridine. Nickel was precipitated as nickel dimethylglyoximate complex by the addition of an alcoholic solution of dimethylglyoxime and excess of ammonia solution. Iodometric method[14] was employed for the estimation of copper in the complex.

2.3.2 CHN Analyses

Microanalyses for carbon, hydrogen and nitrogen were done on a Perkin-Elmer 2400 CHN elemental analyser or on a Heraeus CHN elemental analyser.

2.3.3 Estimation of Halogen and Sulphur[14]

Halogen content was determined by peroxide fusion of the sample, followed by volumetric estimation using Volhard's method. For sulphur estimation, the complexes were fused with Na_2CO_3 and Na_2O_2 and the resulting sulphate was determined gravimetrically as barium sulphate.

For the estimation of chlorine in the polymer sample, the following procedure was adopted. The polymer

supported sample (3 g) was digested with pyridine (5 ml) for 2 h at 100°C. Then the mixture was quantitatively transferred to a conical flask containing 50% acetic acid (30 ml) and conc. nitric acid (5 ml). To this solution, standard silver nitrate solution was added with stirring and then the mixture was allowed to stand for 5 minutes. Afterwards, about 50 ml of water was added to this followed by toluene. The solution was mixed thoroughly, using a stirrer. The excess of silver nitrate was back titrated with standard ammonium thiocyanate solution.

2.4 PHYSICO-CHEMICAL METHODS

2.4.1 Conductance Measurements

The molar conductance of the complexes in nitro-benzene were determined at 28 ± 2°C using a Thoshniwal or Elico IR 9500 conductivity bridge with a dip type cell and a platinized platinum electrode.

2.4.2 Magnetic Susceptibility Measurements

The magnetic susceptibility measurements were done at room temperature (28 ± 2°C) using EG & G PARC model 155 vibrating sample magnetometer or on a simple Gouy-type magnetic balance. The Gouy tube was standardized using

$[Hg(Co(CNS)_4]$ as recommended by Figgis and Nyholm.[91] The effective magnetic moment was calculated using the equation,

$$\mu_{eff} = 2.84 \ (X_m^{Corr} \ T)^{\frac{1}{2}} \ BM$$

where T is the absolute temperature and X_m^{Corr} is the molar susceptibility corrected for diamagnetism of other atoms in the complex using Pascal's constants.[92-95]

2.4.3 Electronic Spectra

Electronic spectra were taken in solution (in the case of soluble complexes) or in the solid state by mull technique following a procedure recommended by Venanzi.[96] The procedure is as given below:

Small filter paper strips were impregnated with a paste of the sample in nujol mull. These were placed over the entrance to the photocell housing. A nujol treated filter paper strip of similar size and shape was used as the blank.

The spectra were recorded on a Hitachi U-3410 Spectrophotometer or on a Shimadzu UV-160 A Spectrophotometer.

2.4.4 Infrared Spectra

Infrared spectra of the ligand and complexes in the region 4000-600 cm^{-1} were taken both in nujol mull and as KBr discs on a Perkin-Elmer PE-983 infrared spectrophotometer. The far infrared spectra of the complexes in the region 600-200 cm^{-1} were taken in polyethylene matrix on a Polytech FIR-30 Fourier far IR Spectrophotometer.

2.4.5 ^{1}H NMR Spectra

The proton nuclear magnetic resonance spectra of complexes were taken in CDCl$_3$ using Hitachi R-600 FT NMR Spectrophotometer. Tetramethylsilane (TMS) was employed as the internal reference.

2.4.6 EPR Spectra

The X-band EPR spectra of a few complexes in chloroform or chloroform-toluene mixture or powder spectra were recorded at room temperature as well as at liquid nitrogen temperature using Varian E-112 X/Q band EPR Spectrophotometer. Powder spectra of the polymer bound metal complexes at room temperature were also taken. Spectra were calibrated using diphenyl picrylhydrazyl (DPPH) as a field marker.

2.4.7 Cyclic Voltammogram

Cyclic voltammogram was recorded using EG & G PARC model 362 scanning potentiostat and EG & G PARC model RE 0091 X-Y recorder. An undivided cell was used for the study. A platinum sheet (20 mm x 20 mm) was used as the auxillary electrode. A platinum button electrode of area 4 mm^2 was used as the working electrode and saturated calomel electrode (SCE) as the reference electrode. The complex was dissolved in acetonitrile solvent. The supporting electrolyte was 0.1 M LiClO$_4$ in acetonitrile. The cell was flushed with oxygen free nitrogen.

2.4.8 Thermogravimetry (TG)

The TG curves were obtained on a Dupont 990 thermal analyser at a heating rate of 10°C min^{-1} in nitrogen atmosphere using a platinum crucible. The mass of the samples used was in the range 5-10 mg.

2.4.9 Differential Thermal Analysis (DTA)

The DTA curves were obtained on Dupont 990 thermal analyser under the operational conditions mentioned above. The reference substance used for DTA measurements was $\propto Al_2O_3$.

2.4.10 Differential Scanning Calorimetry (DSC)

DSC measurements were carried out in nitrogen atmosphere at a heating rate of 10°C min^{-1} on a Delta DSC-7 instrument. The sample masses used were of the order of 0.5-2 mg.

IRON(III), COBALT(II), NICKEL(II) AND COPPER(II) COMPLEXES OF NEW SCHIFF BASES DERIVED FROM 2-AMINOCYCLOPENT-1-ENE-1-DITHIOCARBOXYLIC ACID AND BENZALDEHYDE OR SALICYLALDEHYDE

3.1 INTRODUCTION

The coordination chemistry of transition metal complexes of chelating agents with sulphur-nitrogen donor sites has been an area of great interest for a number of years.[97,98] The ligand systems having soft sulphur and hard nitrogen atoms are chemically very versatile. In many of such complexes both nitrogen and sulphur atoms are involved in the bond formation to the metal while in some others the bond formation is either through nitrogen or through sulphur. An interesting ligand belonging to this group is the deprotonated form of 2-aminocyclopent-1-ene-1-dithiocarboxylic acid (ACDA). Reports of a number of complexes of this ligand have appeared in the literature.[97,98] However, complexes of Schiff bases derived from ACDA have not yet been studied. We have synthesized a new Schiff base derived from ACDA and benzaldehyde (ACB) and also another one from ACDA and salicylaldehyde (ACS). Studies on the Fe(III), Co(II), Ni(II) and Cu(II) complexes of ACB and Cu(II) and Ni(II) complexes of ACS are presented in this chapter.

3.2 EXPERIMENTAL

3.2.1 Materials

Details about the preparation and purification of the ligands, ACB and ACS are given in chapter 2.

3.2.2 Synthesis of the Complexes

The metal chelates were prepared by refluxing equimolar amounts of the ligand (0.01 mol – 2.46 g for ACB and 2.63 g for ACS) and the metal chloride (0.01 mol – 1.62 g of $FeCl_3$, 2.38 g of $CoCl_2 \cdot 6H_2O$, 2.36 g of $NiCl_2 \cdot 6H_2O$ or 1.7 g of $CuCl_2 \cdot 2H_2O$) in acetone on a water bath for 3-4 h. The complex separated was washed with acetone and dried over anhydrous $CaCl_2$ (Yield = 50-60% for the iron complex and 60-70% for the other complexes).

3.2.3 Analytical Methods

Details about the analytical methods and other characterization techniques are given in chapter 2.

3.3 RESULTS AND DISCUSSION

All the complexes are coloured crystalline substances. The complexes of ACB are moderately soluble in nitrobenzene, dimethylformamide, dimethylsulphoxide, aceto-

Table 3.1: Analytical data

Complex (Empirical formula)	Colour	C (%) Found (Calc.)		H (%) Found (Calc.)		N (%) Found (Calc.)		M (%) Found (Calc.)		X (%) Found (Calc.)		S (%) Found (Calc.)	
[Fe(ACB)(H$_2$O)$_2$(OH)Cl] [C$_{13}$H$_{17}$ClFeNO$_3$S$_2$]	Black	39.00	(39.95)	4.28	(4.38)	3.52	(3.58)	14.29	(14.30)	9.00	(9.08)	16.00	(16.39)
[Co(ACB)(Cl)(H$_2$O)] [C$_{13}$H$_{14}$ClCoNOS$_2$]	Brown	44.16	(43.50)	4.00	(3.93)	4.02	(3.90)	16.00	(16.40)	9.01	(9.08)	17.32	(17.80)
[Ni(ACB)(Cl)(H$_2$O)] [C$_{13}$H$_{14}$ClNiNOS$_2$]	Red	42.52	(43.50)	3.82	(3.93)	3.85	(3.90)	15.42	(15.59)	10.01	(9.89)	18.01	(17.86)
[Cu(ACB)(Cl)(H$_2$O)] [C$_{13}$H$_{14}$ClCuNOS$_2$]	Black	43.04	(42.96)	3.79	(3.88)	3.62	(3.85)	15.00	(15.38)	9.80	(9.76)	18.01	(17.62)
[Cu(ACS)(Cl)(H$_2$O)] [C$_{13}$H$_{14}$ClCuNO$_2$S$_2$]	Dark Brown	41.00	(41.10)	3.69	(3.72)	3.58	(3.60)	16.00	(16.70)	9.28	(9.30)	16.50	(16.80)
[Cu(ACS)(Br)(H$_2$O)] [C$_{13}$H$_{14}$BrCuNO$_2$S$_2$]	Dark Brown	36.86	(36.63)	3.29	(3.33)	3.20	(3.30)	14.96	(15.00)	18.72	(18.86)	15.00	(15.10)
[Ni(ACS)(Cl)(H$_2$O)] [C$_{13}$H$_{14}$ClNiNO$_2$S$_2$]	Red	41.62	(41.68)	3.73	(3.77)	3.66	(3.74)	15.60	(15.68)	9.30	(9.47)	17.00	(17.10)
[Ni(ACS)(Br)(H$_2$O)] [C$_{13}$H$_{14}$BrNiNO$_2$S$_2$]	Red	38.00	(37.25)	3.28	(3.37)	3.26	(3.34)	14.00	(14.01)	18.92	(19.00)	15.40	(15.28)

nitrile and are slightly soluble in chloroform. The complexes of ACS are insoluble in most of the solvents. However, they are found to be slightly soluble in DMSO, DMF and nitrobenzene. The analytical data (Table 3.1) shows that the complexes have the general empirical formulae $[MLCl(H_2O)]$ (when L = ACB and M = Co(II), Ni(II) or Cu(II) and $[ML'X(H_2O)]$ (when L' = ACS; X = Cl or Br and M = Cu(II) or Ni(II). The iron complex has the empirical formula $[Fe(ACB)Cl(OH)(H_2O)_2]$. The molar conductance values suggest that all the complexes are non-electrolytes in nitrobenzene (Table 3.2).

3.3.1 Magnetic Susceptibility Measurements

Magnetic moment values of the complexes are presented in Table 3.2. For the iron complex the magnetic moment value was found to be 3.6 BM which lies in between that expected for a high spin (5.9 BM) and a low spin ($\sim$2.3 BM) octahedral complex. This anomalous value might be due to spin crossover phenomenon[99]; however, we could not confirm this by carrying out a temperature dependent magnetic measurement studies, as facilities for this could not be made available to us. This phenomenon has been observed in the case of iron(III) dithiocarbamate complexes.[98]

Table 3.2: Molar conductance and magnetic moment data

Compound	Molar conductance ($ohm^{-1}cm^2mol^{-1}$)	Magnetic moment (BM)
$[Fe(ACB)(H_2O)_2(OH)Cl]$	2.0	3.6
$[Co(ACB)(Cl)(H_2O)]$	1.8	4.4
$[Ni(ACB)(Cl)(H_2O)]$	1.7	Diamagnetic
$[Cu(ACB)(Cl)(H_2O)]$	2.1	1.7
$[Cu(ACS)(Cl)(H_2O)]$	2.6	1.7
$[Cu(ACS)(Br)(H_2O)]$	2.2	1.7
$[Ni(ACS)(Cl)(H_2O)]$	2.2	Diamagnetic
$[Ni(ACS)(Br)(H_2O)]$	2.4	Diamagnetic

the magnetic moment value of 4.4 BM for the Co(II) complex
indicates a tetrahedral structure.[100] A square planar
structure for the Ni(II) complexes is indicated by the
diamagnetic nature of the complex. The magnetic moments of
simple Cu(II) complexes are generally in the range
1.73-2.20 BM regardless of their stereochemistry. The low
magnetic moment value around 1.7 BM for the Cu(II)
complexes suggests that the complexes are not tetrahedral.
Possible structure for these 4 coordinated complexes might,
therefore, be a square planar one.

3.3.2 Electronic Spectra

Solid state electronic spectra of the complexes
are shown in Figs.3.1 to 3.8 and the spectral data are
given in Table 3.3. The spectrum of the iron(III) complex
displays five bands. The bands observed at 44050 cm^{-1} and
41000 cm^{-1} can be assigned to the intra-ligand transitions
and the bands at 36100 cm^{-1}, 31750 cm^{-1} and 24000 cm^{-1}
might be due to charge transfer transitions. The d-d bands
are not observed in the present case and in fact they are
generally not observed in most of the iron(III) complexes.
Because of the greater oxidising power of iron(III),
ligand to metal charge transfer bands often appear in the
visible region and obscure the very low intensity d-d
bands.[101]
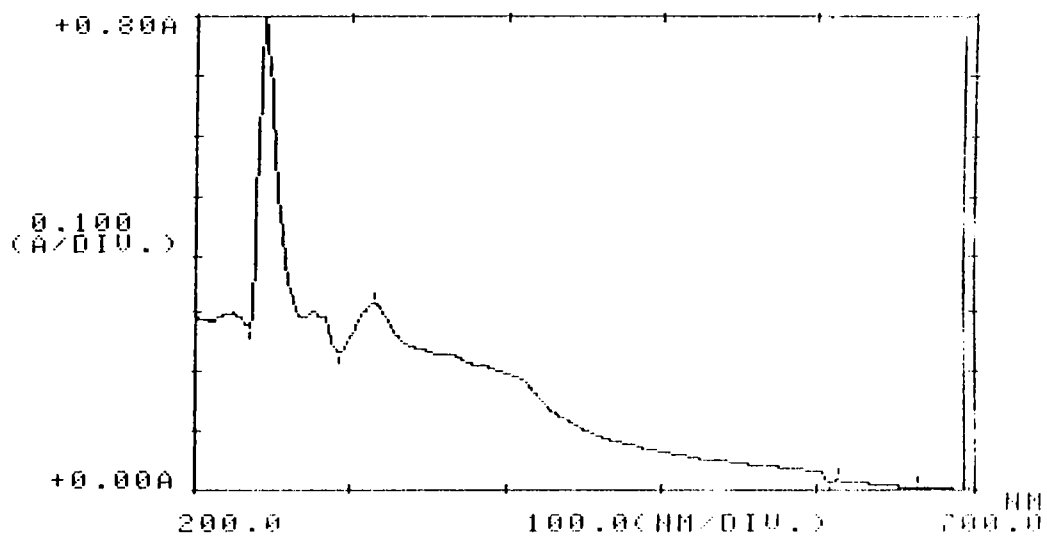
Fig.3.1: Electronic Spectrum of [Fe(ACB)(H$_2$O)$_2$(OH)Cl]
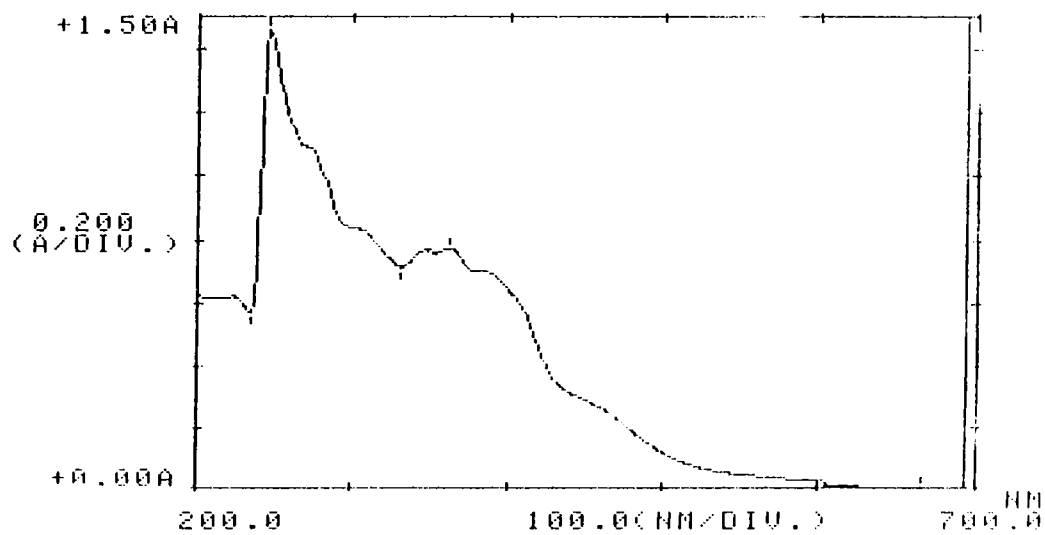
Fig.3.2: Electronic Spectrum of [Co(ACB)Cl(H$_2$O)]
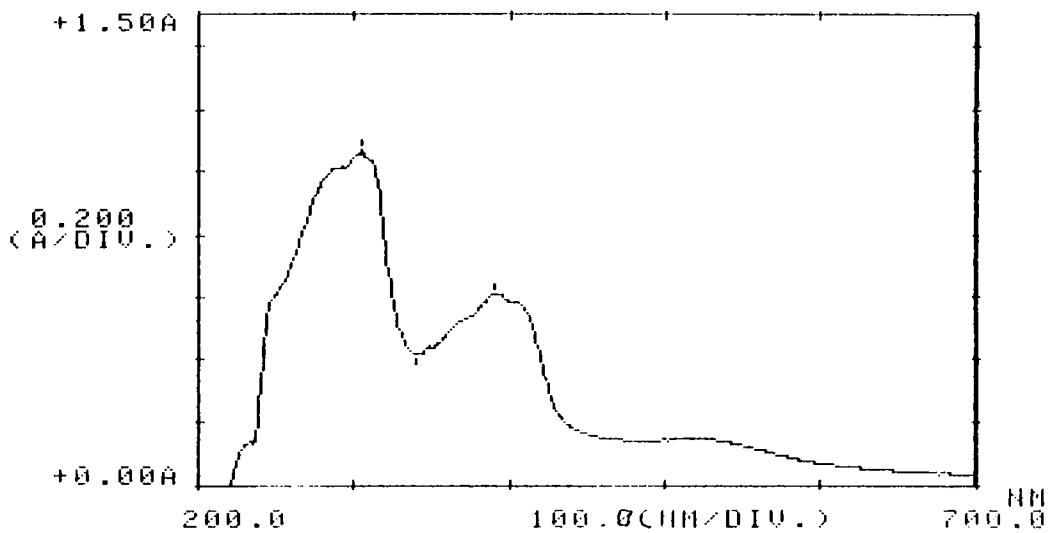
Fig.3.3: Electronic Spectrum of [Ni(ACB)Cl(H$_2$O)]
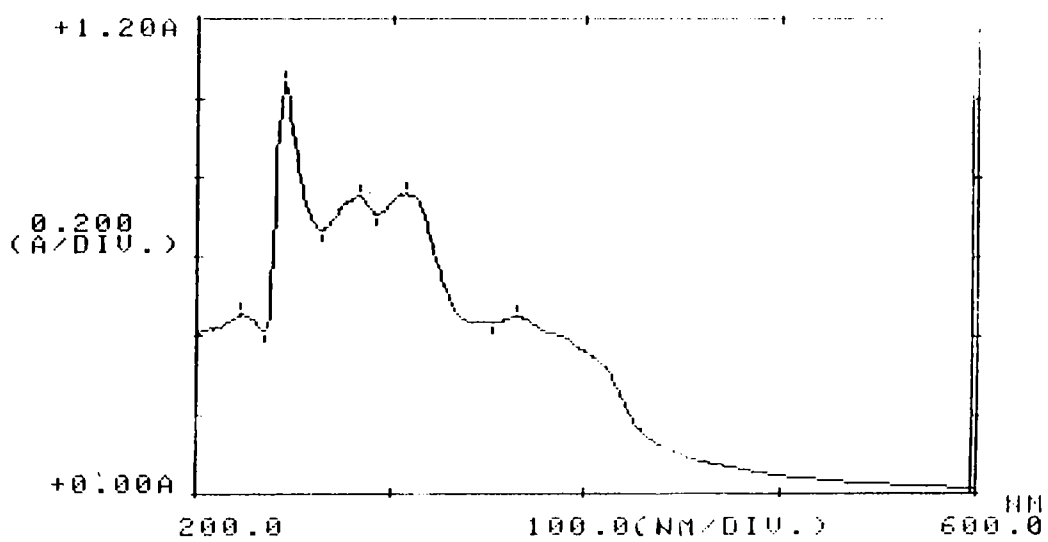
Fig.3.4: Electronic Spectrum of [Cu(ACB)Cl(H$_2$O)]
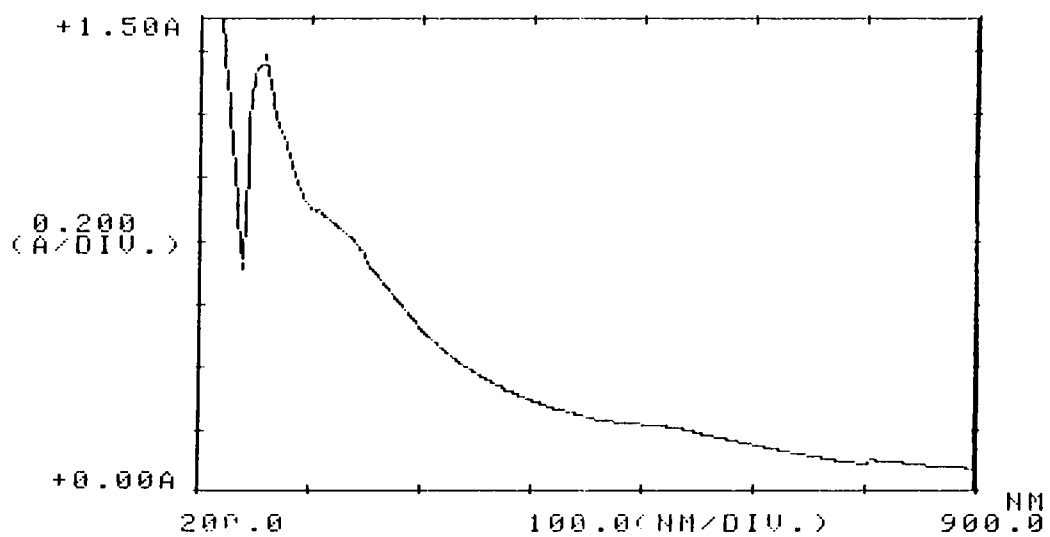
Fig.3.5: Electronic Spectrum of [Cu(ACS)Cl(H$_2$O)]
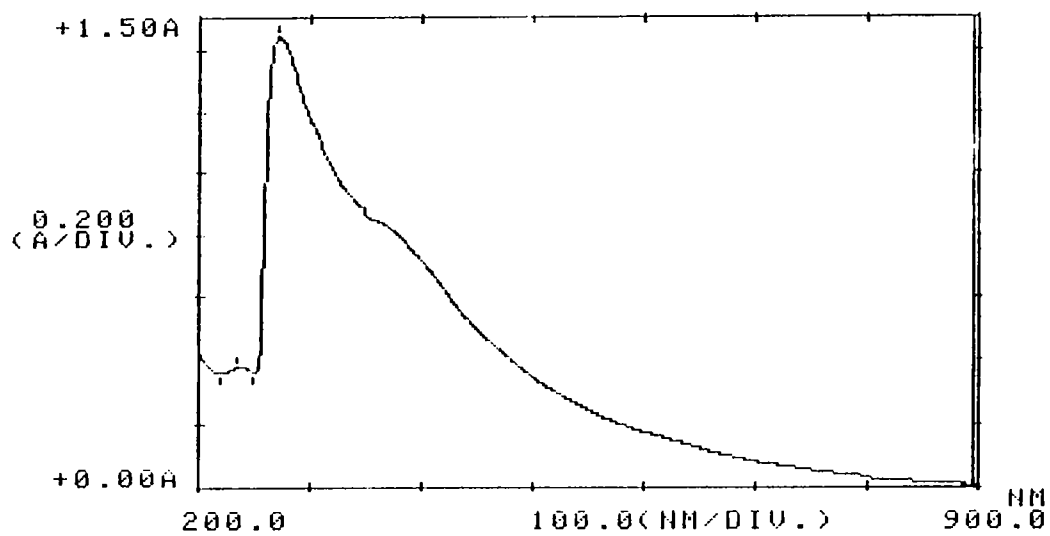
Fig.3.6: Electronic Spectrum of [Cu(ACS)Br(H$_2$O)]
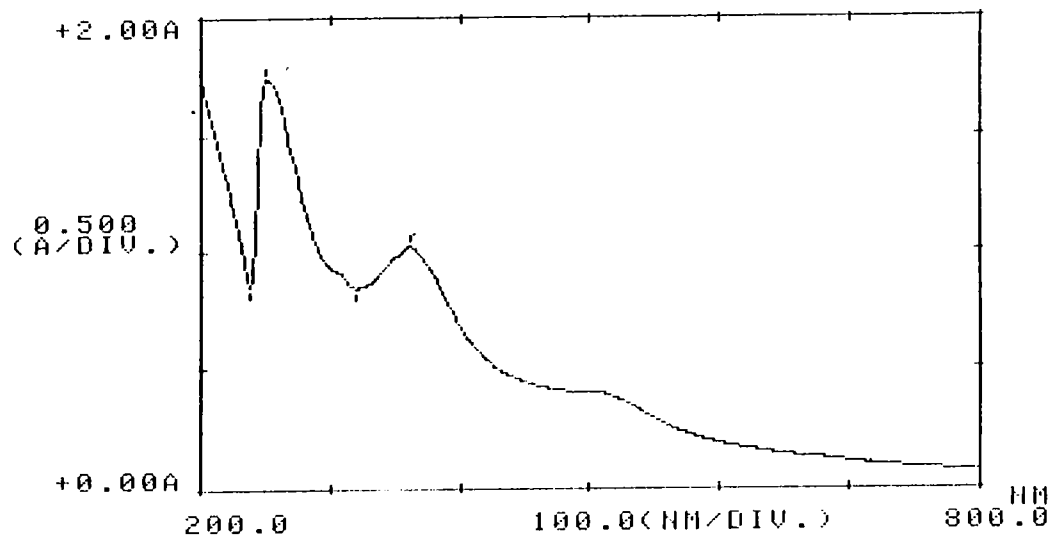
Fig.3.7: Electronic Spectrum of [Ni(ACS)Cl(H$_2$O)]
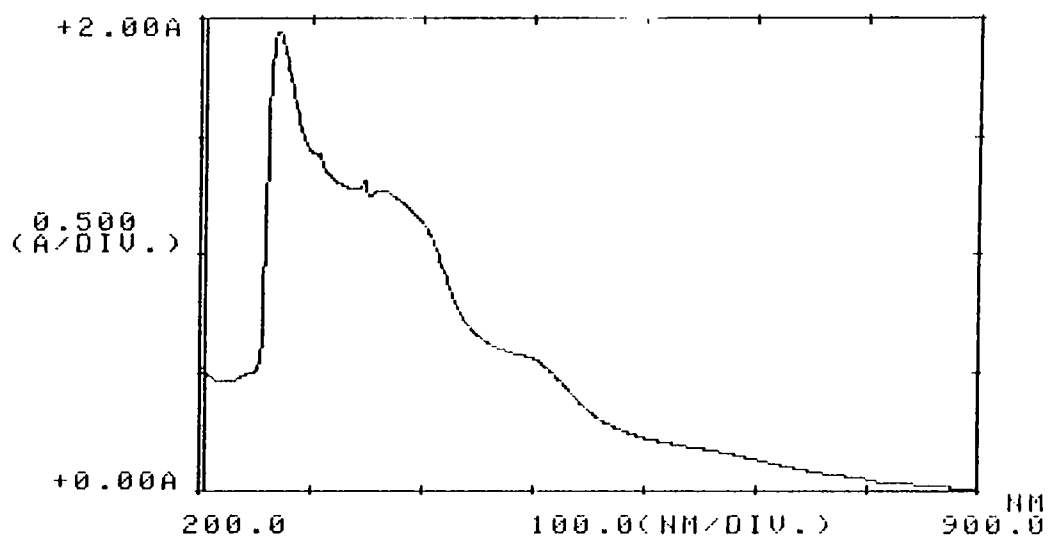
Fig.3.8: Electronic Spectrum of [Ni(ACS)Br(H$_2$O)]

Table 3.3: Electronic spectral data

Compound	Abs. Max. (cm^{-1})	Tentative assignments
(1)	(2)	(3)
$[Fe(ACB)Cl(H_2O)_2(OH)]$	44050	Intra-ligand transition
	40980	"
	36100	Charge transfer transition
	31750	"
	24000	"
$[Co(ACB)(Cl)(H_2O)]$	44050	Intra-ligand transition
	40650	"
	36500	Charge transfer transition
	27625	"
	22200	$^4A_2 \longrightarrow {}^4T_1(P)$
	7100	$^4A_2 \longrightarrow {}^4T_1(F)$
	5100	$^4A_2 \longrightarrow {}^4T_2$
$[Ni(ACB)(Cl)(H_2O)]$	44050	Intra-ligand transition
	40800	"
	32900	Charge transfer transition
	25600	"
	18950	$^1A_{1g} \longrightarrow {}^1B_{1g}$

(1)	(2)	(3)
$[Cu(ACB)(Cl)(H_2O)]$	44850	Intra-ligand transition
	40815	"
	35200	Charge transfer transition
	25800	d–d transition
$[Ni(ACS)(Cl)(H_2O)]$	39850	Intra-ligand transition
	27800	Charge transfer transition
	19600	$^1A_{1g} \longrightarrow {}^1B_{1g}$
$[Ni(ACS)(Br)(H_2O)]$	37000	Intra-ligand transition
	27600	Charge transfer transition
	20000	$^1A_{1g} \longrightarrow {}^1B_{1g}$
$[Cu(ACS)(Cl)(H_2O)]$	38800	Intra-ligand transition
	30800	Charge transfer transition
	16000	d–d transition
$[Cu(ACS)(Br)(H_2O)]$	42550	Intra-ligand transition
	36800	Charge transfer transition
	32300	"

The Co(II) complex exhibits low energy bands expected for the tetrahedral complexes at 7100 cm^{-1} and 5100 cm^{-1}. The band around 7100 cm^{-1} is broad and can be assigned to $^4A_2 \longrightarrow {}^4T_1$ (F) and the band at 5100 cm^{-1} may be due to $^4A_2 \longrightarrow {}^4T_2$ transition. Furthermore, the complex shows a band around 22200 cm^{-1} which may be due to $^4A_2 \longrightarrow {}^4T_1$ (P) electronic transition.[101] The bands observed at 27600 cm^{-1} and 36500 cm^{-1} are due to charge transfer and those at 40700 cm^{-1} and 44000 cm^{-1} are due to intra-ligand transitions.

The electronic spectrum of the nickel(II) complex of ACB show a broad band in the region 18000-25000 cm^{-1} (18950 cm^{-1}) which may be assigned to the $^1A_{1g} \longrightarrow {}^1B_{1g}$ transition.[102] The band at 25600 cm^{-1} and 32900 cm^{-1} can be assigned to charge transfer transition. The band observed around 44000 cm^{-1} and 40800 cm^{-1} are due to the intra-ligand transitions.

The Cu(II) complex of ACB shows bands around 44850 cm^{-1} and 40800 cm^{-1} due to intra-ligand transitions. The expected d-d transitions for square planar complex are not obtained. The very broad charge transfer band observed

around 35200 cm^{-1} and 32500 cm^{-1} might have obscured the d-d transitions. However, a shoulder observed at 25800 cm^{-1} may be due to $^2B_{1g} \longrightarrow {}^2A_{1g}$ transition.[103]. Both B_{1g} and B_{2g} states have been assigned as the ground state for copper(II) complexes with D_{4h} symmetry. The details about the ordering of the excited states are still uncertain. Two of the prevailing energy level diagrams are given below:

$$
\begin{array}{ll}
\underline{\overline{\quad\quad\quad}} & ^2E_g \\[1em]
\underline{\quad\quad\quad\quad} & ^2B_{1g} \\[1em]
\underline{\quad\quad\quad\quad} & ^2A_{1g} \\[1em]
\underline{\quad\quad\quad\quad} & ^2B_{2g}
\end{array}
\qquad\qquad
\begin{array}{ll}
\underline{\quad\quad\quad\quad} & ^2A_{1g} \\[1em]
\underline{\overline{\quad\quad\quad}} & ^2E_g \\[1em]
\underline{\quad\quad\quad\quad} & ^2B_{2g} \\[1em]
\underline{\quad\quad\quad\quad} & ^2B_{1g}
\end{array}
$$
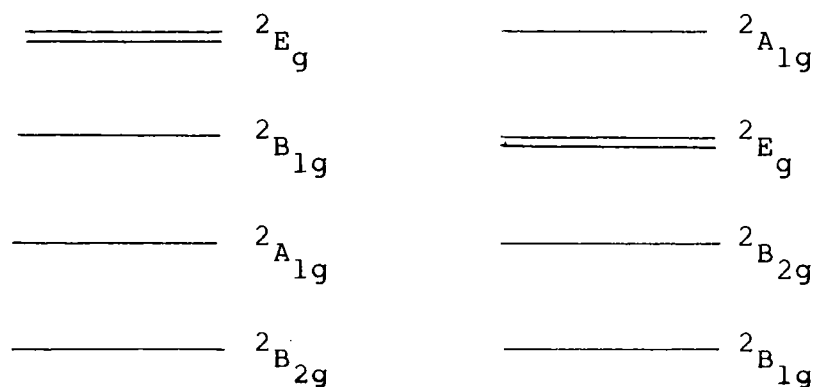
Whatever be the energy level diagram, three electronic transitions are expected for Cu(II) ion in D_{4h} symmetry. However, all the transitions have been seldom observed. They occur as a single broad band.

The Cu(II) complexes of ACS show bands around 38800 cm^{-1} and 42550 cm^{-1} due to intra-ligand transition.

Very broad charge transfer bands were observed at 30800 cm^{-1}, 32300 cm^{-1} and 36800 cm^{-1}. A shoulder observed at 16000 cm^{-1} may be due to d-d transition.

For the nickel(II) complexes of ACS ligand, bands observed at 37000 cm^{-1} and 39850 cm^{-1} are due to intra-ligand transitions. Bands observed around 27700 cm^{-1} are, due to charge transfer transition. The band observed in the region 18000-25000 cm^{-1} may be assigned to the $^1A_{1g} \longrightarrow {}^1B_{1g}$ transition.

3.3.3 Infrared Spectra

The infrared spectral data of the ligands and complexes are given in Table 3.4 and 3.5. All the complexes show a band in the region 3350-3460 cm^{-1} due to ν(OH) of water molecule.[104] Further a double hump around 3020-3040 cm^{-1} and a sharp band at 840 cm^{-1} due to coordinated water molecule[105] are also seen in the spectra of the complexes. Thus the IR spectra clearly reveal the presence of coordinated water molecule. Presence of water is also confirmed from TG studies.

The COH deformation band[106] in ACS ligand occurs at 1250 cm^{-1}. In the spectra of the nickel and copper

Table 3.4: Infrared absorption frequencies (cm^{-1})

ACB	I	II	III	IV	Tentative Assignments of the more relevant bands
(1)	(2)	(3)	(4)	(5)	(6)
--	3550m	3400m	3380m	3430m	
--	3025m	3030m	3020m	3040m	ν(O-H)
--	2350w	2355w	2355w	2340w	
1650m	1620m	1610m	1620m	1630m	ν(C=N)
1595m	1595m	1595m	1595s	1595s	
1565m	1570s	1570m	1570m	1565m	
1555m	1560sh	1560sh	1560sh	1560sh	
1540m	1540s	1530sh	1540s	1540sh	
1485s	1490m	1495m	1495m	1490m	
1460s	1465s	1465s	1465s	1465sh	ν(C=C)+ δ(CH_2)
1445s	1450s	1455s	1455s	1440s	
1370s	1390m	1385m	1380m	1380m	
1360sh	1360m	1360s	1355m	1355m	
1320s	1320m	1330m	1330s	1330m	ν(C-N) + ν(C-S)
1300m	1310m	1310m	1310m	1310m	
1265m	1275m	1275m	1270m	1270m	ν(C-S) + ν(C-N)
1200m	1210m	1205m	1210m	1210sh	
1175m	1180m	1180w	1190m	1180m	
1150w	1155w	1150w	1165w	1155w	
1125w	1130w	1130w	1135w	1130w	
1075m	1080w	1070w	1060w	1070sh	ρ(CH_2)
1025m	1035w	1025w	1020w	1025w	
1010w	1010w	1010w	1010w	1010w	
--	990m	990m	990m	990m	
960m	--	--	--	--	ν(CSS)
--	930m	935m	930m	930m	

(Contd...)

(1)	(2)	(3)	(4)	(5)	(6)
910m	910m	910m	910m	910m	
--	840m	835m	840m	840m	δ(H-O-H)
760w	760m	750m	750s	750s	
680s	690sh	690sh	690sh	690s	
665w	665w	655w	655w	665sh	
605w	605w	605w	610w	610s	
--	500w	490m	495m	495m	ν(M-O)
--	460w	450w	450w	455w	ν(M-N)
--	370s	360s	380s	385s	ν(M-S)
--	260m	265m	270m	265m	ν(M-Cl)
--	215m	215m	210m	215m	

s = strong ;   m = medium ;   w = weak ;   sh = shoulder

I = [Fe(ACB)(H$_2$O)$_2$(OH)Cl] ;   II = [Co(ACB)(Cl)H$_2$O]

III = [Ni(ACB)(Cl)H$_2$O]   ;   IV = [Cu(ACB)(Cl)H$_2$O]

Table 3.5: Infrared absorption frequencies (cm^{-1})

ACS	I	II	III	IV	Tentative Assignments of the more relevant bands
(1)	(2)	(3)	(4)	(5)	(6)
--	3400m	3450m	3340m	3340m	ν(O-H)
3350m	2930m	2940m	2930m	2935	ν(O-H) Hydrogen bonded
1620m	1600s	1590s	1590s	1590s	ν(C=N)
1560m	1560m	1560m	1560m	1560m	
1500w	1490w	1480w	1480w	1480w	
1470s	1465s	1460s	1460s	1460s	
1440s	1445s	1450s	1450s	1450s	
1380m	1385m	1400m	1380m	1380m	
1290w	1310w	1300w	1300w	1300w	
1250m	1250m	1250m	1250m	1250m	δ(COH)
1210m	1210m	1220m	1210m	1220m	
1180w	1180w	1180w	1170w	1180w	
1160w	1155w	1150w	1150w	1155w	
1140w	1130w	1120w	1120w	1120w	

(Contd...)

(1)	(2)	(3)	(4)	(5)	(6)
--	970m	970m	970m	965m	
950m	--	--	--	--	γ(CSS)
--	925m	925m	925m	925m	
--	850w	850w	850w	850w	δ(H-O-H)
750s	750m	750m	760m	750m	
715m	715m	715m	720m	715m	
680m	680m	680m	680m	680m	
630w	630w	620w	610w	610m	
--	500w	490w	495w	490w	ν(M-O)
--	450w	460w	455w	450w	ν(M-N)
--	370s	375s	375s	370s	ν(M-S)
--	260w	265w	265w	260w	ν(M-Cl)
--	215w	215w	215w	215w	ν(M-Br)

s = strong ; m = medium ; w = weak

I = [Ni(ACS)Cl(H$_2$O)]   ;   II = [Ni(ACS)Br(H$_2$O)]

III = [Cu(ACS)Cl(H$_2$O)]   ;   IV = [Cu(ACS)Br(H$_2$O)]

complexes of this ligand, position of this band remains unchanged indicating that the OH group does not take part in complexation. A broad band is observed in the region 2900-2950 cm^{-1} which is known to arise from the hydrogen bonded νOH.[107,108]

The ligands ACB and ACS can bind to the metal through the azomethine nitrogen and also through one or two sulphur atoms of the dithiocarboxylic acid group. Thus it is capable of acting as a tridentate ligand. In the spectra of both ACB and ACS ligands bands of medium intensity are observed at 1650 cm^{-1} and 1620 cm^{-1} respectively which may be attributed to νC = N. This band shifts towards lower frequencies in the spectra of the complexes indicating the donation of the nitrogen lone pair of the azomethine group to the central metal atom. Similar shifts to lower frequencies have been observed for Schiff base metal complexes by earlier workers also.[109] The region 900-1000 cm^{-1} is associated with the C-S stretching frequencies in dithiocarboxylic acid complexes. In the spectra of the complexes there are more than three bands in this region which might be due to the monodentate bonding of the dithiocarboxylic acid group. The band at 960 cm^{-1} in the ligand is bifurcated in the complexes at 930 and

990 cm^{-1} and may be attributed to νC-S and νC = S respectively.[110] Thus the Schiff base ligand in these complexes is acting only as a bidentate ligand coordinating through the nitrogen atom of the azomethine group and one of the sulphur atoms of the dithiocarboxylic acid group. A strong band seen around 380 cm^{-1} in all the complexes can be attributed to ν(M-S).[111] The bands observed at 450-460 cm^{-1} may be assigned to νM-N and that at 260-270 cm^{-1} might be due to metal-halogen (metal-chlorine or metal-bromine) vibrations.[111] A band observed at 490-500 cm^{-1} may be assigned to ν(M-O) of coordinated water molecule.[111]

3.3.4 EPR Spectra

The EPR spectra of Cu(II) complexes (Fig.3.9) were recorded in chloroform toluene mixture at liquid nitrogen temperature. In all the cases the g values were calculated using the Kneubuhl procedure.[61] For all the complexes three g values were observed which might be due to the slight deviations from the square planar structure and also due to the presence of different types of ligands in the complexes. The lowest g value is found to be less than 2.03; hence a compressed rhombic symmetry is indicated for these complexes.[82] The solid state spectrum of the complex [Cu(ACB)(Cl)(H$_2$O)] at room temperature also indicates three g values (Fig.3.10) for the complex. Further, for each

Table 3.6: EPR spectral data of Cu(II) complexes

Complex	g_1	g_2	g_3	A_1	A_2	A_3
[Cu(ACB)Cl(H$_2$O)*	2.09	2.22	2.29	--	--	--
[Cu(ACB)Cl(H$_2$O)	2.02	2.07	2.10	30	140	170
[Cu(ACS)Cl(H$_2$O)	2.01	2.08	2.24	30	140	180
[Cu(ACS)Br(H$_2$O)	2.01	2.09	2.23	30	130	180

* Powder spectra at room temperature
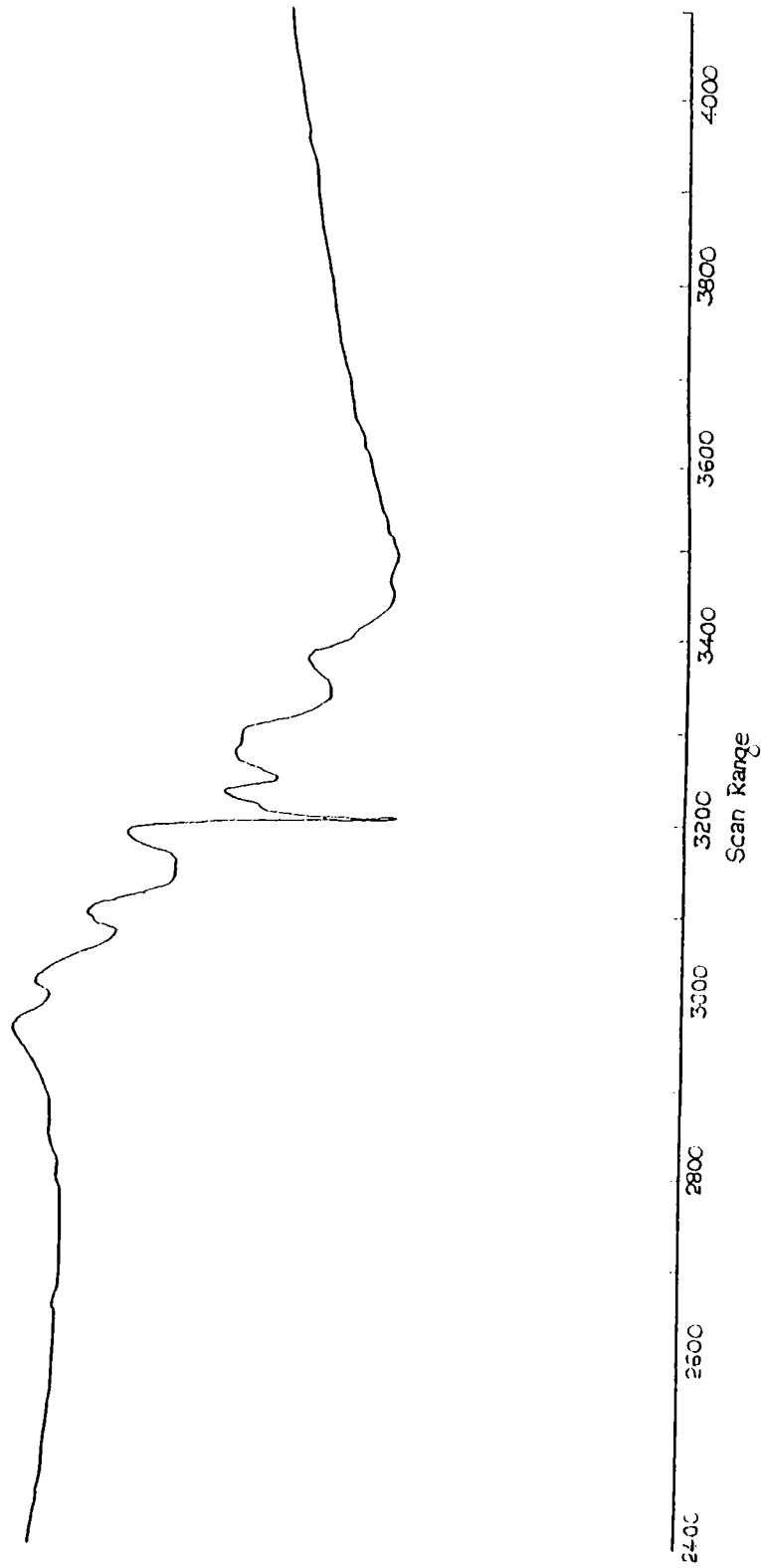
Fig.3.9: EPR spectrum of [Cu(ACS)Br(H$_2$O)] at liquid
nitrogen temperature
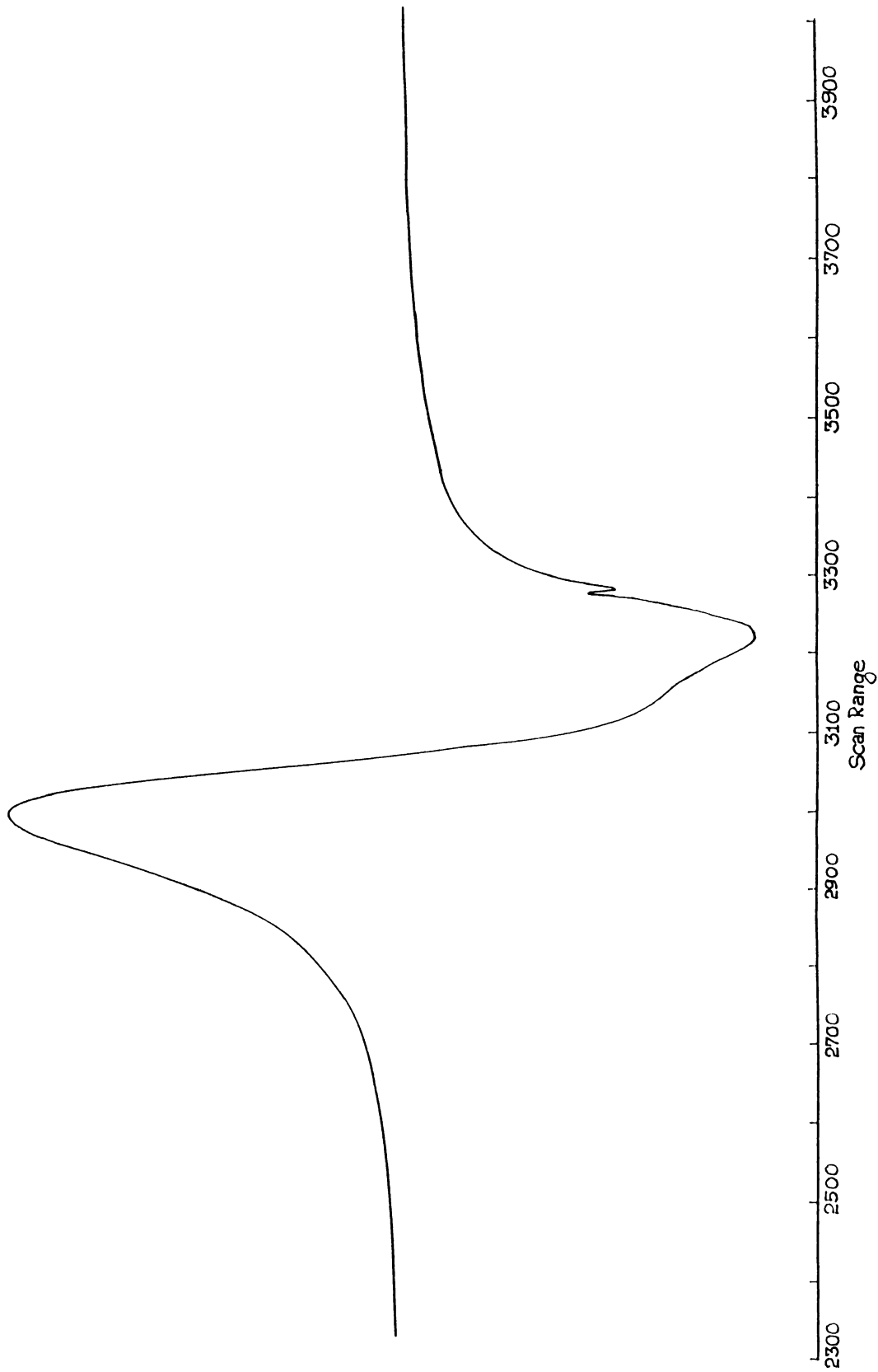
Fig.3.10: EPR Spectrum of [Cu(ACB)Cl(H$_2$O)]

at room temperature

Scan Range

2300 2500 2700 2900 3100 3300 3500 3700 3900
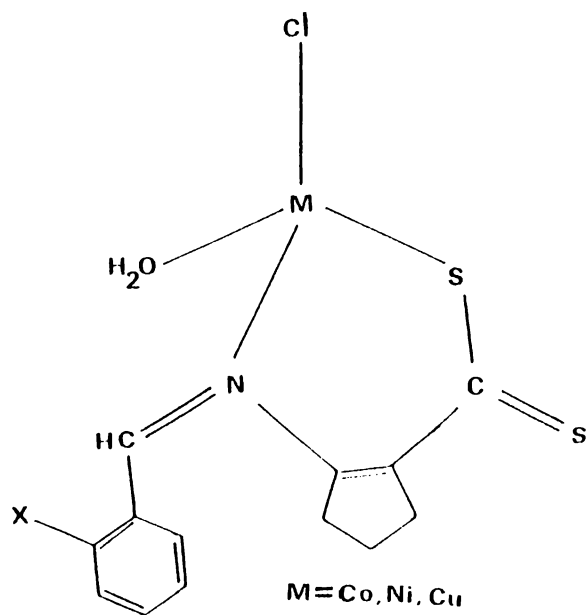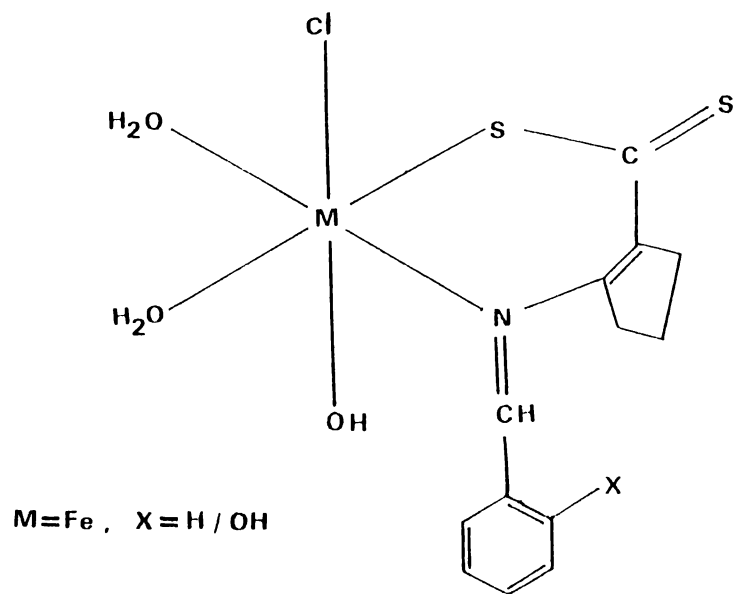
Fig.3.11: Proposed structures of the complexes

case, four hyperfine lines corresponding to the g_2 and g_3 values could be located; however the variations in the hyperfine line intensities and absence of few lines may be due to the superposition of the different hyperfine lines. From the EPR spectral data (Table 3.6) it can be seen that in most cases, the two g values have nearly the same value while the other is having a larger value. These results are typical of square planar Cu(II) complexes.[112] Further, the low g values (less than 2.3) observed in the present cases exclude the possibility of pseudotetrahedral structures for the complexes.[113]

Based on the elemental analysis and various physico-chemical studies, the structure shown in Fig.3.11 may be tentatively proposed for the present complexes.

Chapter 4

IRON(III), COBALT(II), NICKEL(II) AND COPPER(II) COMPLEXES OF A NEW SCHIFF BASE DERIVED FROM QUINOXALINE-2-CARBOXALDEHYDE AND 2-AMINOCYCLOPENT-1-ENE-1-DITHIOCARBOXYLIC ACID

4.1 INTRODUCTION

The Schiff base ACQ derived from quinoxaline-2-carboxaldehyde and 2-aminocyclopent-1-ene-1-dithiocarboxylic acid is more interesting than the Schiff bases ACB and ACS since it contains more potential donor sites. The nitrogen atom of the quinoxaline ring can also take part in coordination and this may lead to structurally interesting complexes. It was therefore considered worthwhile to synthesize a few complexes of this ligand and characterize them. The results of our studies on the synthesis and characterization of Fe(III), Co(II), Ni(II) and Cu(II) complexes of this ligand are described in this chapter.

4.2 EXPERIMENTAL

4.2.1 Materials

Details about the preparation and purification of the ligand ACQ are given in chapter 2.

4.2.2 Synthesis of the Complexes

The metal chelates were prepared by refluxing equimolar amounts of the ligand (0.01 mol, 3.24 g) and metal chlorides (0.01 mol -- 1.62 g of $FeCl_3$, 2.38 g of $CoCl_2 \cdot 6H_2O$, 2.36 g of $NiCl_2 \cdot 6H_2O$ or 1.7 g of $CuCl_2 \cdot 2H_2O$) in acetone on a water bath for 3-4 h. The complex separated was washed with acetone and dried over anhydrous $CaCl_2$ (Yield = 50-60% for the iron complex and 60-70% for the other complexes).

4.2.3 Analytical Methods

Details about the analytical methods and characterization techniques are given in chapter 2.

4.3 RESULTS AND DISCUSSION

All the complexes are brown crystalline substances. They are moderately soluble in nitrobenzene, acetonitrile, dimethylsulphoxide and dimethylformamide and slightly soluble in chloroform. The analytical data (Table 4.1) show that the complexes have the general empirical formulae [M(ACQ)Cl] for the Co(II), Ni(II) and Cu(II) complexes and [Fe(ACQ)Cl(OH)(H_2O)] for the Fe(III) complex. The molar conductance values suggest that all the complexes are non-electrolytes in nitrobenzene (Table 4.2).

Table 4.1: Analytical data

Complex	Colour	C (%) Found (Calc.)	H (%) Found (Calc.)	N (%) Found (Calc.)	M (%) Found (Calc.)	X (%) Found (Calc.)	S (%) Found (Calc.)
[Fe(ACQ)ClH$_2$O(OH)] C$_{15}$H$_{15}$ClFeN$_3$O$_2$S$_2$	Brown	42.00 (42.40)	3.53 (3.56)	9.84 (9.89)	13.00 (13.15)	8.20 (8.35)	14.92 (15.07)
[Co(ACQ)Cl] C$_{15}$H$_{12}$ClCoN$_3$S$_2$	Brown	45.80 (45.86)	3.19 (3.08)	10.68 (10.70)	14.84 (15.00)	9.00 (9.03)	16.40 (16.30)
[Ni(ACQ)Cl] C$_{15}$H$_{12}$ClNiN$_3$S$_2$	Brown	46.24 (45.89)	3.12 (3.08)	10.87 (10.70)	14.84 (14.96)	9.00 (9.03)	16.42 (16.31)
[Cu(ACQ)Cl] C$_{15}$H$_{12}$ClCuN$_3$S$_2$	Dark brown	47.10 (45.32)	3.12 (3.04)	10.48 (10.50)	15.84 (16.00)	8.78 (8.92)	16.32 (16.10)

Table 4.2: Molar conductance and magnetic moment data

Compound	Molar conductance $(ohm^{-1}cm^{2}mol^{-1})$	Magnetic moment (B.M)
[Fe(ACQ)ClH$_2$O(OH)]	2.0	3.5
[Co(ACQ)Cl]	1.5	4.4
[Ni(ACQ)Cl]	1.6	Diamagnetic
[Cu(ACQ)Cl]	2.2	1.7

4.3.1 Magnetic Susceptibility Measurements

Magnetic moment values of the complexes are presented in Table 4.2. For the iron complex the magnetic moment value was found to be 3.5 BM, which lies in between that expected for the high spin and low spin octahedral complexes. Such anomalous values were obtained in complexes, where the spin crossover behaviour occurs.[99] However, temperature dependent magnetic measurement studies have to be done, for attributing this behaviour to the present iron(III) complex. Unfortunately the facilities for such studies could not be made available to us.

The magnetic moment value of 4.4 BM for the Co(II) complex suggests it to have a tetrahedral structure.[100] The Ni(II) complex was found to be diamagnetic suggesting a square planar structure for the complex. The Cu(II) complex has a magnetic moment value of 1.7 BM which indicates that the complex is not tetrahedral and hence may have a square planar structure.

4.3.2 Electronic Spectra

Electronic spectra of the complexes in chloroform are shown in Figs.4.1 to 4.4 and the spectral data are
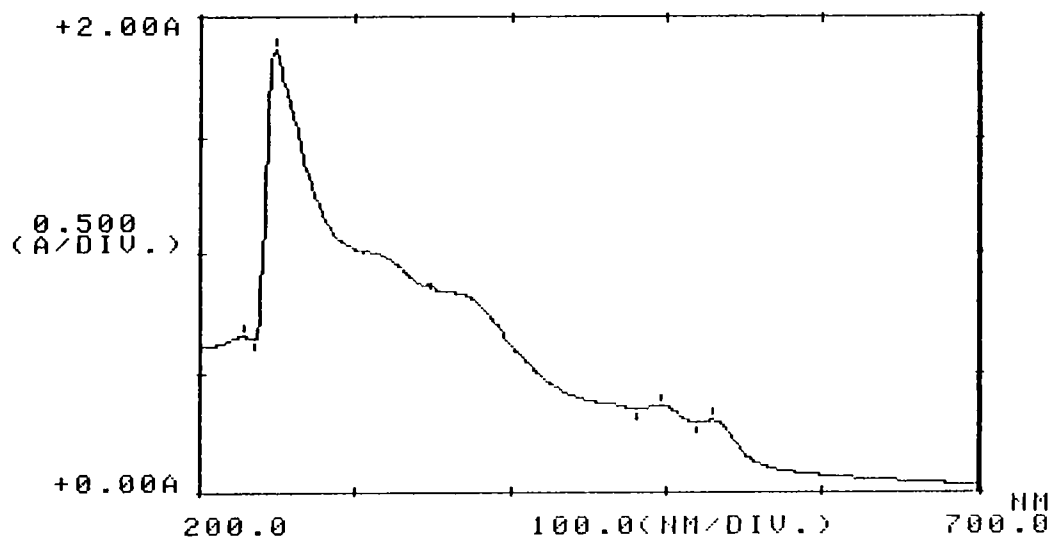
Fig.4.1: Electronic Spectrum of [Fe(ACQ)Cl(H$_2$O)(OH)]
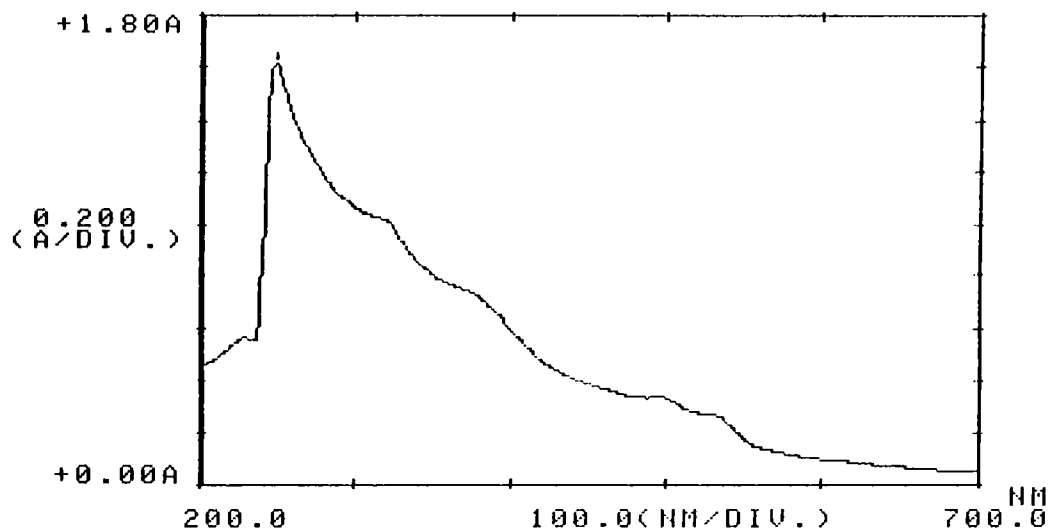
Fig.4.2: Electronic Spectrum of [Co(ACQ)Cl]
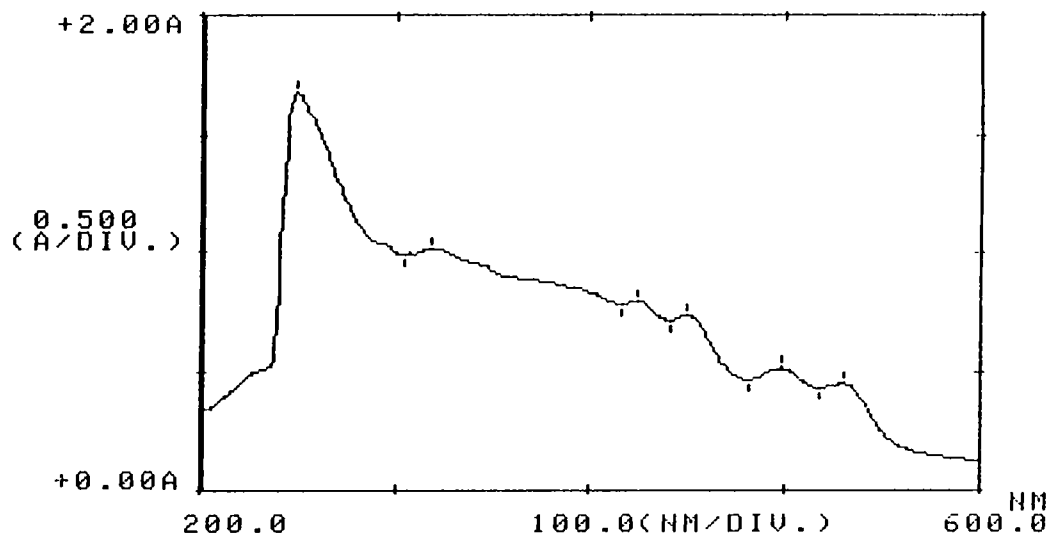
Fig.4.3: Electronic Spectrum of [Ni(ACQ)Cl]
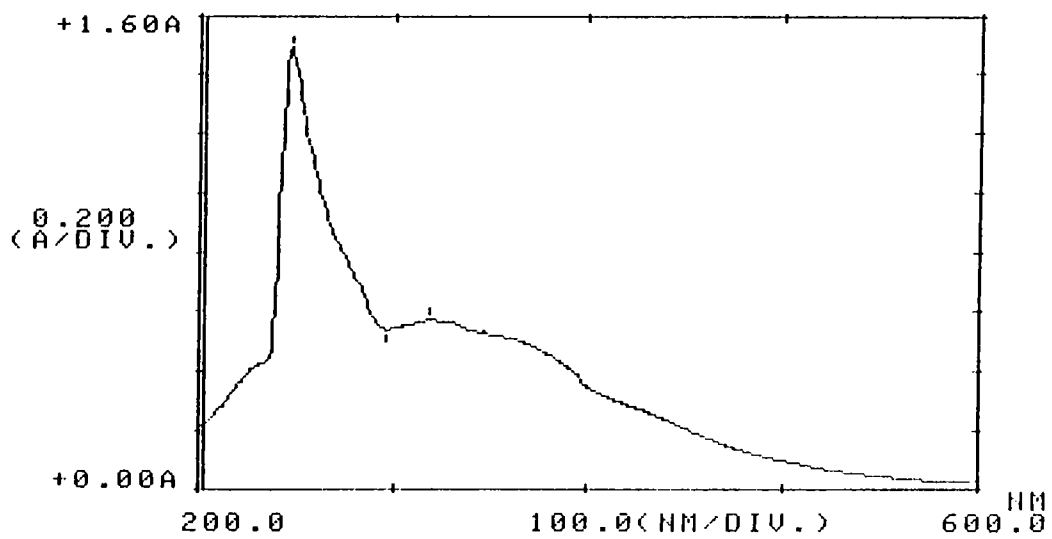
Fig.4.4: Electronic Spectrum of [Cu(ACQ)Cl]

given in Table 4.3. For the iron complex the bands observed at 43900 cm^{-1} and 40320 cm^{-1} may be assigned to the intra-ligand transitions and the bands at 31750 cm^{-1} and 26660 cm^{-1} to charge transfer transitions. The low intensity bands observed at 20200 cm^{-1} and 18900 cm^{-1} are due to the spin forbidden d-d transitions in the octahedral symmetry.[45]

The cobalt(II) complex exhibits bands at 43480 cm^{-1} and 40320 cm^{-1}, 26660 cm^{-1}, 20120 cm^{-1}, 18900 cm^{-1}, 7500 cm^{-1} and at 5200 cm^{-1}. The bands observed at 20120 cm^{-1} and 18900 cm^{-1} can be assigned to $^4A_2 \longrightarrow {}^4T_1(P)$ transition.[114] The broad absorption band around 7500 cm^{-1} may be assigned to $^4A_2 \longrightarrow {}^4T_1 F$. Bands observed at 26660 cm^{-1} and 40320 cm^{-1}, 43480 cm^{-1} are due to charge transfer and intra-ligand transitions respectively. Thus electronic spectrum of the cobalt(II) complex is in agreement with the magnetic moment value to suggest a tetrahedral structure for the complex.

The electronic spectrum of the square planar Ni(II) complex shows bands at 18870 cm^{-1}, 20080 cm^{-1} and 22220 cm^{-1} which may be assigned to $^1A_{1g} \longrightarrow {}^1E_g$, $^1A_{1g} \longrightarrow {}^1A_{2g}$, and $^1A_{1g} \longrightarrow {}^1B_{1g}$ transitions respectively.[102]

Table 4.3:   Electronic spectral data

Compound	Abs. Max (cm^{-1})	Tantative assignments
(1)	(2)	(3)
$[Fe(ACQ)ClH_2O(OH)]$	43900	Intra-ligand transition
	40320	"
	31750	Charge transfer transition
	26660	"
	20200	Forbidden d-d transition
	18900	"
$[Co(ACQ)Cl]$	43480	Intra-ligand transition
	40320	"
	26660	Charge transfer transition
	20120	$^4A_2 \longrightarrow {}^4T_1(P)$
	18900	
	7600	$^4A_2 \longrightarrow {}^4T_1(F)$
	5200	$^4A_2 \longrightarrow {}^4T_2$

(1)	(2)	(3)
[Ni(ACQ)Cl]	43480	Intra-ligand transition
	40485	"
	31545	Charge transfer transition
	22220	$^1A_{1g} \longrightarrow {}^1B_{1g}$
	20080	$^1A_{1g} \longrightarrow {}^1A_{2g}$
	18870	$^1A_{1g} \longrightarrow {}^1E_{g}$
[Cu(ACQ)Cl]	43480	Intra-ligand transition
	40485	"
	31350	Charge transfer transition
	27400	"
	22470	"

The bands at 31540 cm^{-1} and 40485 cm^{-1}, and at 43480 cm^{-1} can be assigned to charge transfer and intra-ligand transitions respectively.

For the copper(II) complex the bands observed at 43480 cm^{-1} and 40485 cm^{-1} are due to intra-ligand transitions. The very broad charge transfer bands observed at 31750 cm^{-1}, 27400 cm^{-1} and at 22470 cm^{-1} might have obscured the expected d-d transitions for square planar copper complex.[115]

4.3.3 Infrared Spectra

The infrared spectral data of the ligand and complexes are given in Table 4.4. For the iron complex, two bands are seen at 3400 cm^{-1} and 3060 cm^{-1} due to coordinated water molecule. The complex also shows a band at 1605 cm^{-1} due to the H-O-H deformation.[111] A band observed at 500 cm^{-1} may be assigned to ν(M-O) of coordinated water molecule.[111] Thus the IR spectra of the iron complex clearly shows the presence of coordinated water molecule and this is also confirmed from TG studies. However, these bands are not present in the spectra of other complexes.

Table 4.4:   Infrared absorption frequencies (cm^{-1})

ACQ	I	II	III	IV	Tentative Assignments of the more relevant bands
(1)	(2)	(3)	(4)	(5)	(6)
--	3400m	--	--	--	ν(O-H)
--	30̂60m	--	--	--	
1680m	1620m	1620m	1620m	1620m	ν(C=N)
--	1605m	--	--	--	δ(H-O-H)
1580m	1570m	1575m	1570m	1570m	ν(C=N) quinoxaline ring
1560m	1560m	1560m	1550m	1565m	
1535s	1530s	1530s	1535s	1540s	
1480m	1475m	1480m	1465m	1490m	
1440m	1445m	1450m	1440m	1440m	
1350m	1350m	1355m	1360m	1360m	
1290m	1295m	1290sh	1300m	1310m	
1250w	1250w	1250w	1250w	1240w	
1210m	1200m	1200m	1215m	1205m	
1120m	1120m	1120m	1120m	1120m	
1090m	1090m	1090sh	1095m	1095m	
1030m	1050w	1040w	1045w	1045w	
1010w	1010w	1010w	1000w	1010w	

(1)	(2)	(3)	(4)	(5)	(6)
--	980m	980m	970m	980m	
965m	--	--	--	--	γ(CSS)
--	950m	950m	950m	950m	
920m	920m	920m	915m	920m	
860w	855w	860w	860w	860w	
830w	830w	830w	830w	830w	
800w	790w	795w	800w	800w	
760s	755s	750s	760s	760s	
630w	580w	600w	605w	600w	
--	500m	--	--	--	γ(M-O)
--	450m	450m	450m	450m	γ(M-N)
--	390s	390s	390s	390s	γ(M-S)
--	260m	265m	260m	260m	γ(M-Cl)

s = strong ; m = medium ; w = weak ; sh = shoulder

I = [Fe(ACQ)ClH$_2$O(OH)] ; II = [Co(ACQ)Cl]

III = [Ni(ACQ)Cl] ; IV = [Cu(ACQ)Cl]

The ligand ACQ is capable of acting as a tetradentate ligand. It can bind to the metal through the azomethine nitrogen, the ring nitrogen and also through the two sulphur atoms of the dithiocarboxylic acid group. A band at 1680 cm^{-1} in the spectrum of the Schiff base may be attributed to $\gamma(C = N)$. This band shifts towards a lower frequency ($\sim$1620 cm^{-1}) in the spectra of the complexes indicating the donation of the nitrogen lone electron pair of the azomethine group of the Schiff base to the central metal atom.[109] The C = N (ring) stretching vibrations appear as a medium band around 1580 cm^{-1} in the ligand.[116] In the complexes this band is lowered to 1570 cm^{-1} showing that nitrogen atom of the quinoxaline ring is coordinated to the metal atom. The region 900-1000 cm^{-1} is associated with the C-S stretching frequencies in dithiocarboxylic acid complexes. In the spectra of the complexes there are more than three bands in this region which might be due to the monodentate bonding of the dithiocarboxylic acid group. The band at 965 cm^{-1} in the ligand is bifurcated in the complexes at 950 cm^{-1} and 980 cm^{-1} and may be attributed to γC-S and γC=S respectively.[110] Thus the Schiff base ligand in these complexes is acting as a tridentate ligand coordinating through the nitrogen atom of the azomethine group, through the nitrogen atom of the quinoxaline ring and
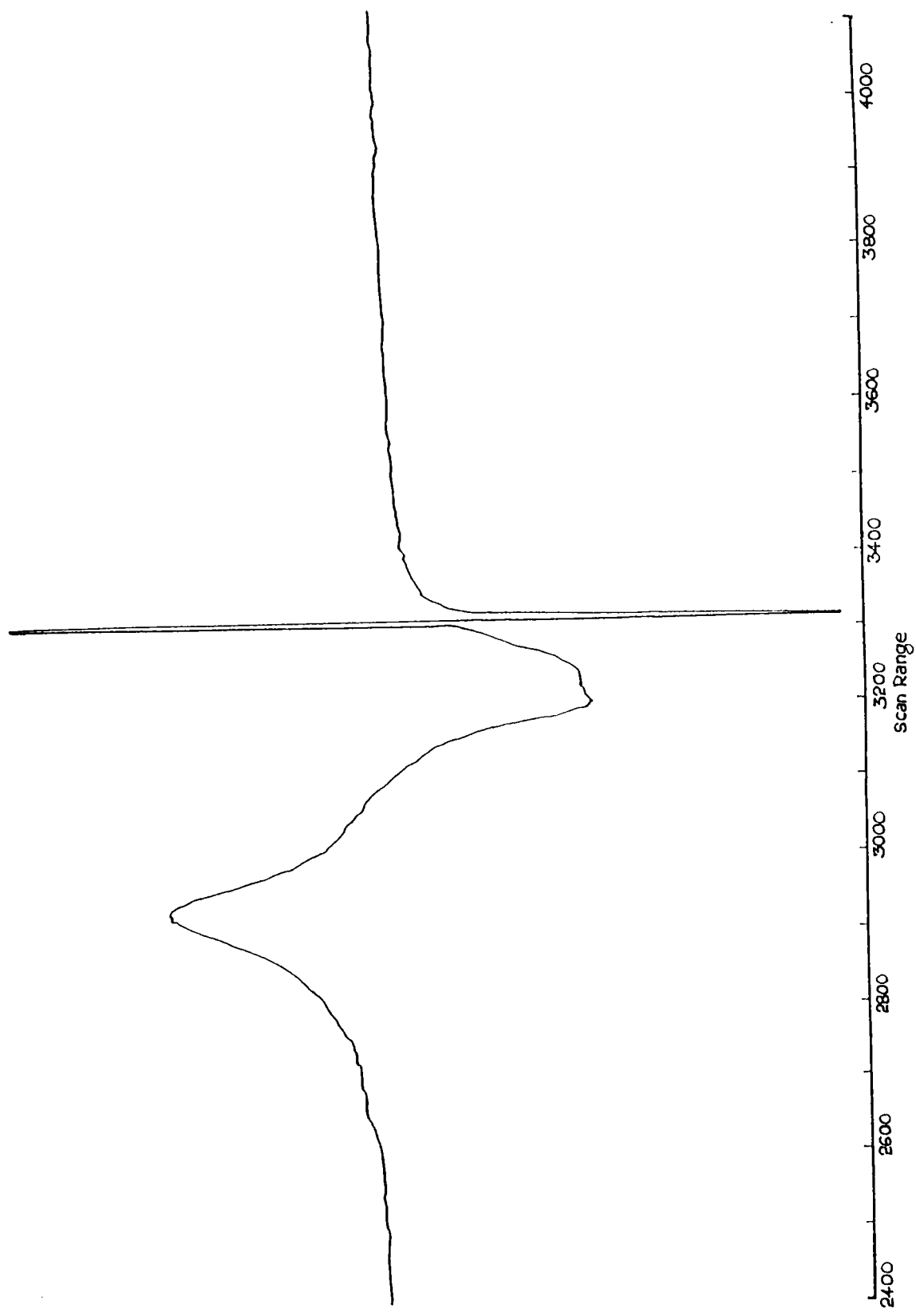
Fig.4.5: EPR Spectrum of [Cu(ACQ)Cl]

at room temperature
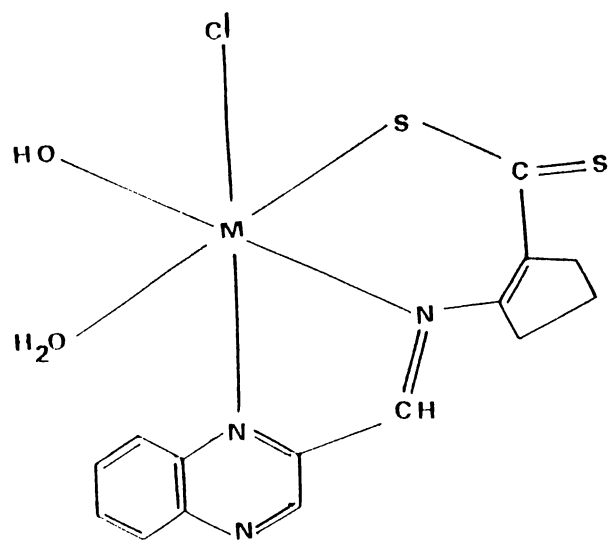
M = Fe
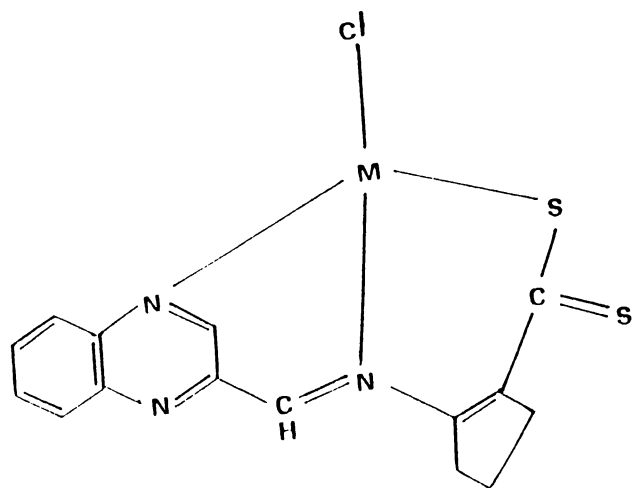
M = Co, Ni, Cu

Fig.4.6: Proposed Structures of the Complexes

one of the sulphur atoms of the dithiocarboxylic acid group. A strong band seen around 390 cm^{-1} in all the complexes can be attributed to $\gamma(M-S)$.[111] The band observed around 450 cm^{-1} due to $\gamma(M-N)$ and another band around 260 cm^{-1} due to $\gamma(M-Cl)$[117] are also observed in all the complexes. In the iron complex a band around 500 cm^{-1} due to $\gamma(M-O)$ is also observed.[111]

4.3.4 EPR Spectra

The solid state EPR spectrum of the Cu(II) complex (Fig.4.5) was recorded at room temperature. The g values were calculated using the Kneubuhl procedure.[61] The occurence of three g values, g_1 = 2.13, g_2 = 2.16, g_3 = 2.31, might be due to the slight deviations from the square planar structure and may also be due to the mixed ligand nature of the complex. As g_1 is almost equal to g_2 and g_3 is greater than the g_1 and g_2 values, square planar geometry can be assumed for the complex.[112] Three g values are expected for square planar complexes with elongated or compressed rhombic symmetry.[80,82] Besides, the possibility of having pseudo-tetrahedral structure can be excluded in the present case as all the g values are lower than 2.4.

Based on these results, the structure of the complexes may be assigned as shown in Fig.4.6.

IRON(III), COBALT(II), NICKEL(II) AND COPPER(II) COMPLEXES OF A NEW SCHIFF BASE DERIVED FROM POLYMER BOUND BENZALDEHYDE AND 2-AMINOCYCLOPENT-1-ENE-1-DITHIOCARBOXYLIC ACID

5.1 INTRODUCTION

The use of polymers as supports for chelates and catalysts as well as synthetic reagents has grown tremendously since Merrifield demonstrated the applications of polystyrene resins in peptide synthesis.[118-121] Varying degrees of success have been reported for incorporation of metal ions or metal complexes into polymer containing chelating groups of various sizes and donor sites. Polymer with nitrogen, oxygen, sulphur and phosphorus donors are commonly found as monodentate or bidentate ligands. There has been considerable interest in anchoring multidentate ligands to the polymer. Polymer bound multidentate amines would be valuable as the starting material for synthesizing many polymer bound chelates and macrocycles. Complete characterization of polymer bound metal complexes are often not possible. A knowledge of the environment around the metal which is necessary for the proper understanding of their involvement in catalytic reactions and other useful

technological applications, may be obtained from such studies. Further, synthesis and characterization of more and more new polymer bound metal complexes may lead to the development of new versatile heterogeneous catalysts. With this in view, iron(III), cobalt(II), nickel(II) and copper(II) complexes of a new polymer bound Schiff base derived from polymer bound benzaldehyde and 2-aminocyclo-pent-1-ene-1-dithiocarboxylic acid (PACB) have been synthesized. We report herein the details about the synthesis and characterization of the complexes of this polymeric Schiff base in this chapter.

5.2 EXPERIMENTAL

5.2.1 Materials

Details of the preparation of polymer bound Schiff base and other reagents and solvents employed are given in chapter 2.

5.2.2 Synthesis of the Complexes

All the polymer bound Fe(III), Co(II), Ni(II) and Cu(II) complexes were prepared by the same general

procedure. Polymer bound Schiff base was swollen in dimethylformamide and an excess of metal chlorides dissolved in DMF were added to the polymer bound Schiff base. The mixture is shaken for 5 h using a mechanical stirrer. The resulting polymer bound complexes were filtered, washed with DMF, ethanol, methanol and chloroform and dried in vacuo over anhydrous $CaCl_2$.

5.2.3 Analytical Methods

Details about the analytical methods and other characterization techniques are given in chapter 2.

5.3 RESULTS AND DISCUSSION

In the present study, chloromethylated polystyrene (2% crosslinked with divinyl benzene, (3.7 meq of chlorine/g) beads were used as the starting material. The chloromethyl group in polystyrene resin was converted to aldehyde group by refluxing a mixture of chloromethyl polystyrene and dimethylsulphoxide containing $NaHCO_3$ at 140°C following a literature procedure[84] as shown in Scheme 5.1.
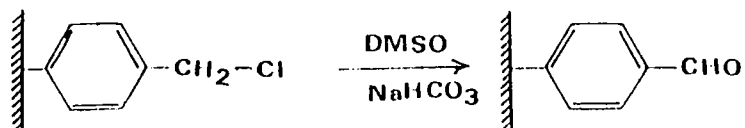
Scheme 5.1: Preparation of Aldehyde Resin

The resin gave yellow colour with Borsche's reagent which indicates the presence of aldehyde group. The residual chlorine content was found to be 0.1 meq. of chlorine/g which shows that almost all chloromethyl groups have been converted to the aldehyde. The formation of the aldehyde resin was further supported by the IR spectrum which showed peaks at 1680 cm^{-1} ν(C=O) and at 2725 cm^{-1} γ(C-H) characteristic of aldehyde group.

The polymer bound benzaldehyde was then condensed with ACDA to give polymer bound Schiff base as shown in Scheme 5.2.
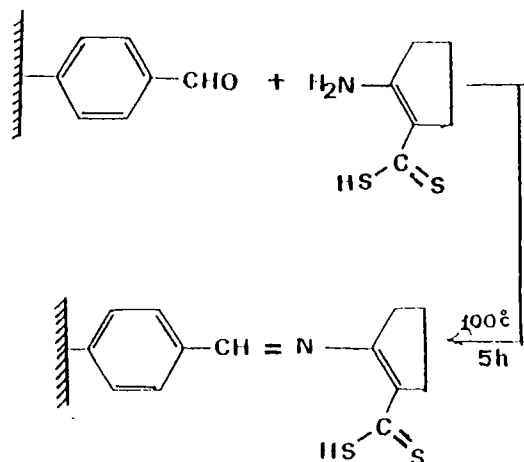
Scheme 5.2: Preparation of Schiff Base

The nitrogen analysis of the polymeric Schiff base indicated 0.28 meq. of the functionalized ligand per gram of the resin. Using the polymer bound Schiff base, complexes of Fe(III), Co(II), Ni(II) and Cu(II) were prepared. The reactions were facile and yielded various coloured resins, colour of which is same as that of the corresponding simple ACB complexes reported in chapter 3.

In arriving at probable structures of the various complexes the percentage nitrogen obtained from elemental analysis of the ligand has been taken as the standard.

Assuming that all the Schiff base units (0.28 meq) have participated in the complexation (vide section 5.3.3) the percentage of iron, chlorine and sulphur were calculated for various probable structures of the iron complex. It was found that the experimentally determined percentages of these elements (Table 5.1) did agree only with the values calculated for $[FeLCl_2(H_2O)_2]$ where L = PACB. By a similar procedure, empirical formulae of cobalt(II), nickel(II) and copper(II) complexes have been found to be $[MLClH_2O]$. However, microanalytical data for polymeric samples can be taken only as a qualitative rather than a quantitative guide.

Table 5.1: Analytical data

Complex	M (%) Found (Calc.)	X (%) Found (Calc.)	S (%) Found (Calc.)
$[Fe(PACB)Cl_2(H_2O)_2]$	1.48 (1.50)	1.60 (1.80)	1.74 (1.80)
$[Co(PACB)Cl(H_2O)]$	1.30 (1.59)	0.90 (0.96)	1.82 (1.80)
$[Ni(PACB)Cl(H_2O)]$	1.30 (1.59)	1.00 (0.96)	1.89 (1.80)
$[Cu(PACB)Cl(H_2O)]$	1.69 (1.72)	0.92 (0.96)	1.80 (1.80)

5.3.1 Magnetic Susceptibility Measurements

For the calculation of magnetic susceptibility of the complexes, VSM measurements were used. X_M values were calculated using the empirical formula weight for the anchored simple complex (for this calculation, molecular weight of the polymer back bone has not taken into consideration). The diamagnetic correction for the whole polymeric complex has been calculated and was subtracted from the X_M value to get X'_M values. When these X'_M values were used for the calculation of magnetic moments (Table 5.2), μ_{eff} values around 4.1 BM was obtained for the iron complex and 4.6 BM for the cobalt complex. Nickel complex was found to be diamagnetic. A μ_{eff} value of 1.7 BM was obtained for the copper(II) complex. For the Fe(III) complex, the low magnetic moment value may be due to the spin crossover behaviour of the complex.[99] The magnetic moment values indicate a tetrahedral structure for the cobalt(II) complex and square planar structures for the copper(II) and nickel(II) complexes.[94] Similar type of magnetic behaviour is exhibited by the corresponding simple complexes (vide chapter 3) section 3.3.1.

5.3.2 Electronic Spectra

The electronic spectra of the complexes are given in Figs.5.1 to 5.4 and the electronic spectral data are

given in Table 5.2. The data do not provide any conclusive evidence to assign the structure of these complexes. The spectrum of the iron(III) complex display bands at 46080 cm^{-1} and at 42550 cm^{-1} due to intra-ligand transitions and the bands at 37040 cm^{-1}, 32790 cm^{-1}, 28820 cm^{-1} and 24390 cm^{-1} may be due to charge transfer transitions. This charge transfer bands might have obscured the spin forbidden d-d transitions.[45]

The Co(II) complex exhibits only one d-d band at 20400 cm^{-1} which may be due to $^4A_2 \longrightarrow {}^4T_1(P)$ electronic transition.[100] The other low energy bands are not seen in the spectra of the complex. The bands observed at 25200 cm^{-1}, 29070 cm^{-1} and 33330 cm^{-1} are due to charge transfer and bands at 42550 cm^{-1}, 46500 cm^{-1} are due to intra-ligand transitions.

The electronic spectrum of the nickel(II) complex shows a band at 25510 cm^{-1} which may be assigned to the $^1A_{1g} \longrightarrow {}^1B_{1g}$ transition.[102] The bands at 28900 cm^{-1}, 32790 cm^{-1}, 37740 cm^{-1} and at 45045 cm^{-1} can be assigned to charge transfer and intra-ligand transitions respectively.

The electronic spectrum of Cu(II) complex shows a band at 46300 cm^{-1} due to intra-ligand transition. The expected
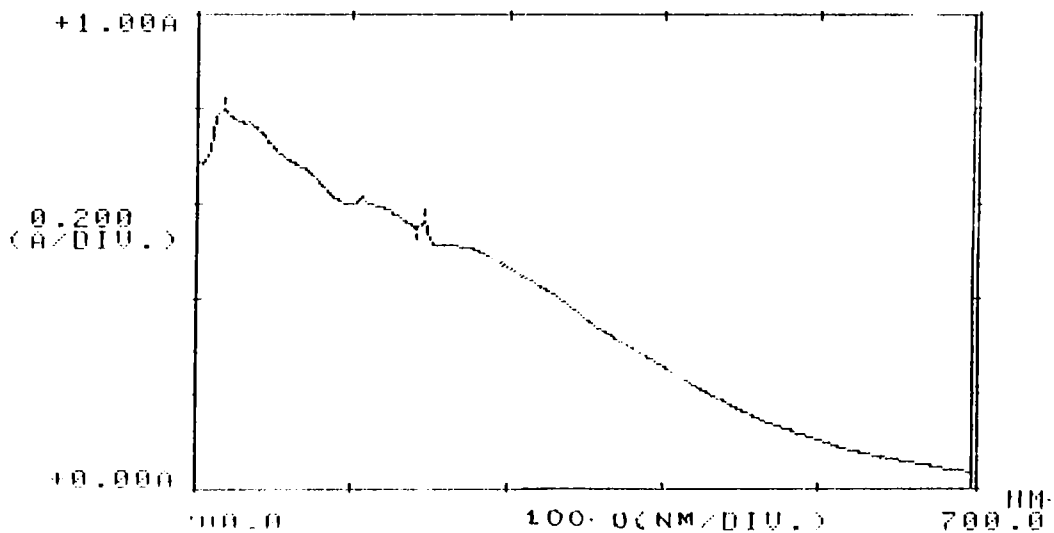
Fig.5.1: Electronic Spectrum of $[Fe(PACB)Cl(H_2O)_2]$
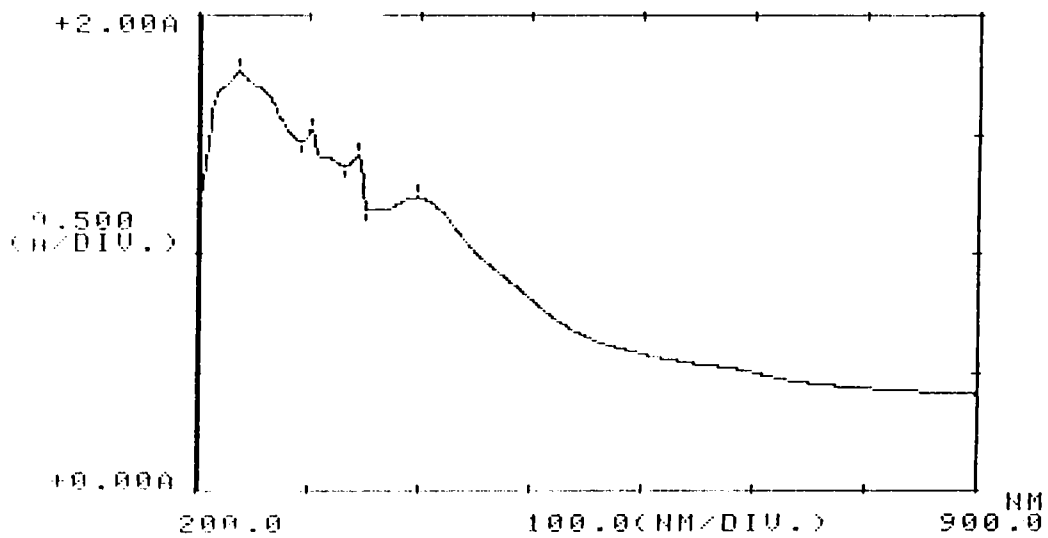
Fig.5.2: Electronic Spectrum of $[Co(PACB)Cl(H_2O)]$
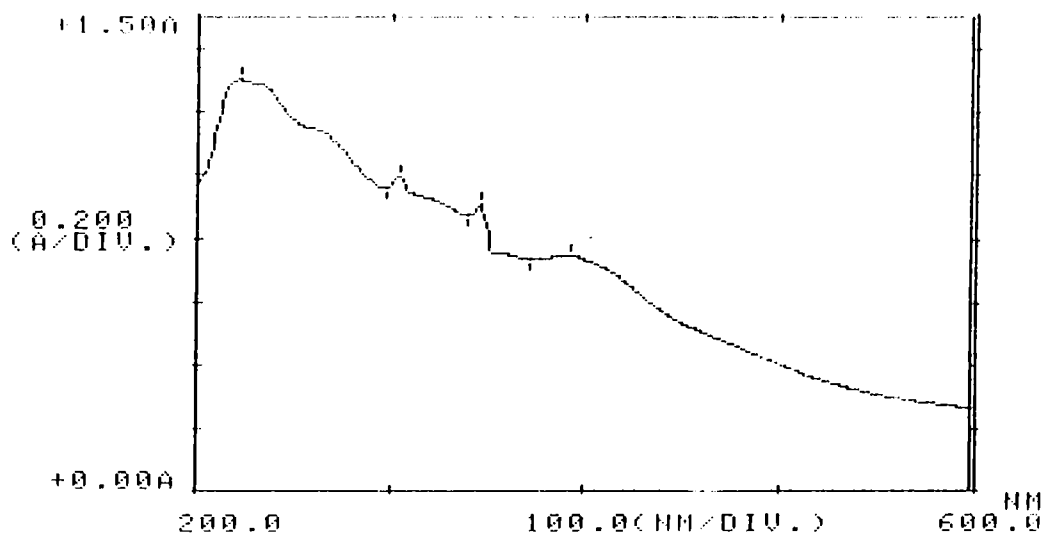
Fig.5.3: Electronic Spectrum of [Ni(PACB)Cl(H$_2$O)]
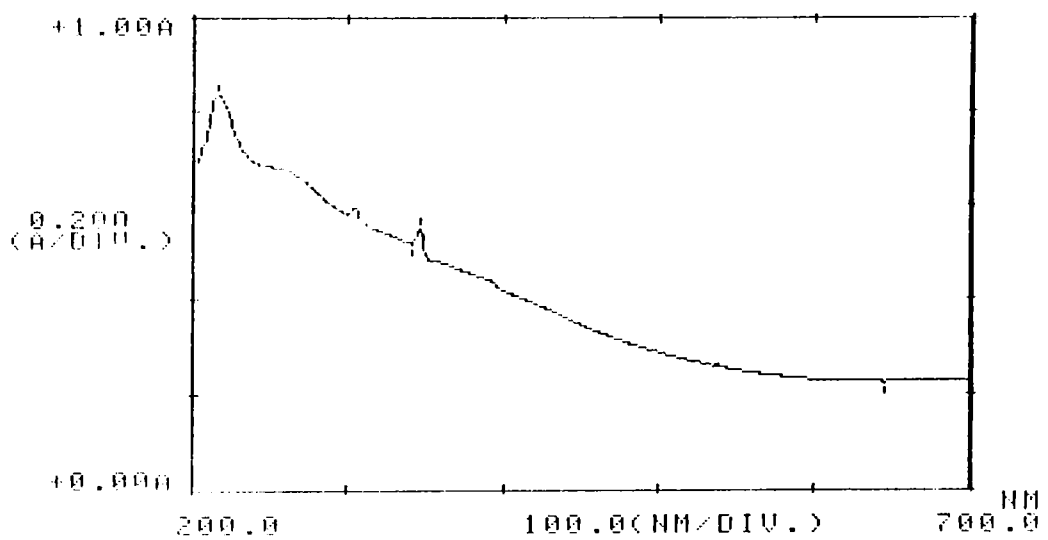
Fig.5.4: Electronic Spectrum of [Co(PACB)Cl(H$_2$O)]

Table 5.2:   Magnetic moment and electronic spectral data

Polymer complex	Magnetic moment (BM)	Abs.Max. (cm^{-1})	Tentative Assignments
(1)	(2)	(3)	(4)
$[Fe(PACB)Cl_2(H_2O)_2]$	4.1	46080	Intra-ligand transition
		42550	"
		37040	Charge transfer transition
		32790	"
		28820	"
		24390	"
$[Co(PACB)Cl(H_2O)]$	4.6	46500	Intra-ligand transition
		42550	"
		33330	Charge transfer transition
		29070	"
		25200	"
		20400	$^4A_2 \longrightarrow {}^4T_1(P)$

(1)	(2)	(3)	(4)
[Ni(PACB)Cl(H$_2$O)]	Diamagnetic	45045	Intra-ligand transition
		37740	Charge transfer transition
		32790	"
		28900	"
		25510	$^1A_{1g} \longrightarrow {}^1B_{1g}$
[Cu(PACB)Cl(H$_2$O)]	1.7	46300	Intra-ligand transition
		38460	Charge transfer transition
		33000	"
		28820	"

d-d transitions for square planar complex are not obtained. The charge transfer band observed at 38460 cm^{-1} might have obscured the d-d transitions.

5.3.3 Infrared Spectra

The infrared spectral data are given in Table 5.3. All the complexes show a band in the region 3200-3400 cm^{-1} due to γOH of water molecule.[104] A sharp band at 840 cm^{-1} is also seen in the spectra of the complexes, which may be due to the presence of coordinated water molecule.[105] The complexes show a band at 1650-1660 cm^{-1} due to H-O-H deformation.[111] Thus the IR spectra clearly reveal the presence of coordinated water molecule. A band observed both in the ligand and complexes at 2725 cm^{-1} is due to C-H stretching vibration of unconverted aldehyde group. The band at 1700 cm^{-1} due to the C-O stretching vibration of the aldehyde.[122] is also observed in the complexes, suggesting the presence of unreacted aldehyde groups in the complexes. The ligand can act as a tridentate ligand by coordinating through the azomethine nitrogen and also through the two sulphur atoms of the dithiocarboxylic acid group. The shifting of the strong band observed at 1630 cm^{-1} towards a lower frequency (1600-1605 cm^{-1}) in the spectra of the complexes indicates the participation of the

Table 5.3: Infrared absorption frequencies (cm^{-1})

PACB	I	II	III	IV	Tentative Assignments of the more relevant bands
(1)	(2)	(3)	(4)	(5)	(6)
--	3400m	3400m	3400m	3400m	γ(H-O-H)
--	3200m	3200m	3200m	3200m	
2950m	2950m	2950m	2950m	2950m	
2725m	2725m	2725m	2725m	2725m	γ(C-H)
1700m	1700m	1700m	1700m	1700m	γ(C=O)
--	1660s	1650m	1640m	1650m	δ(H-O-H)
1630s	1600s	1600s	1605s	1605s	γ(C=N)
1510m	1505m	1510m	1510m	1510m	
1490m	1490m	1490m	1490m	1490m	
1440m	1440m	1440m	1440m	1440m	
1420m	1420m	1420m	1420m	1420m	
1370m	1370s	1380m	1370m	1370m	
1250m	1250m	1240m	1240m	1235m	
1215w	1210w	1210w	1210w	1210w	
1105w	1110w	1110w	1110w	1110w	
1010m	1015m	1010m	1110m	1015m	

(Contd...)

(1)	(2)	(3)	(4)	(5)	(6)
--	975m	985m	980m	980m	
960m	--	--	--	--	$\gamma(CSS)$
--	910m	905m	910m	915m	
--	840m	840m	840m	840m	$\gamma(H-O-H)$
775w	770w	760w	760w	760w	
715s	720s	700s	720s	720s	
--	550m	550m	550m	550m	$\gamma(M-N)$

s = strong ; m = medium ; w = weak ;

I = $[Fe(PACB)Cl_2(H_2O)_2]$; II = $[Co(PACB)Cl(H_2O)]$

III = $[Ni(PACB)Cl(H_2O)]$; IV = $[Cu(PACB)Cl(H_2O)]$
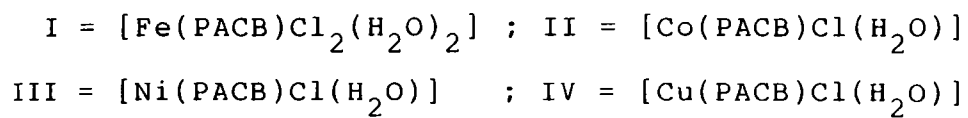
azomethine nitrogen.[109]   The disappearance of the band at

1630 cm^{-1} and the appearance of a new band at $\sim$1600 cm^{-1}

in the complexes suggests that all the Schiff base units

take part in coordination.   Besides, more than one band in

the region (900-1000 cm^{-1}) associated with the C-S

stretching frequencies indicate monodentate bonding of the

dithiocarboxylic acid group.[110]   Thus the polymeric Schiff

base ligand acts as a bidentate ligand coordinating through

the nitrogen atom of the azomethine group and one of the

sulphur atoms of the dithiocarboxylic acid group.

Definite assignments could not be made for metal-

ligand vibrations in the far IR spectra of polymer

supported complexes, due to the presence of the difference

bands of the polymer ligand in this region.

5.3.4 EPR Spectra

The powder spectra of the polymer bound Cu(II)

complex (Fig.5.5) was recorded at room temperature.   Three

g values were obtained: g_1 = 2.08; g_2 = 2.18 and g_3 = 2.3.

These results are in agreement with those obtained for the

complex [Cu(ACB)Cl(H$_2$O)] reported in chapter 3.   Therefore,

symmetry around the metal ion in the polymer anchored
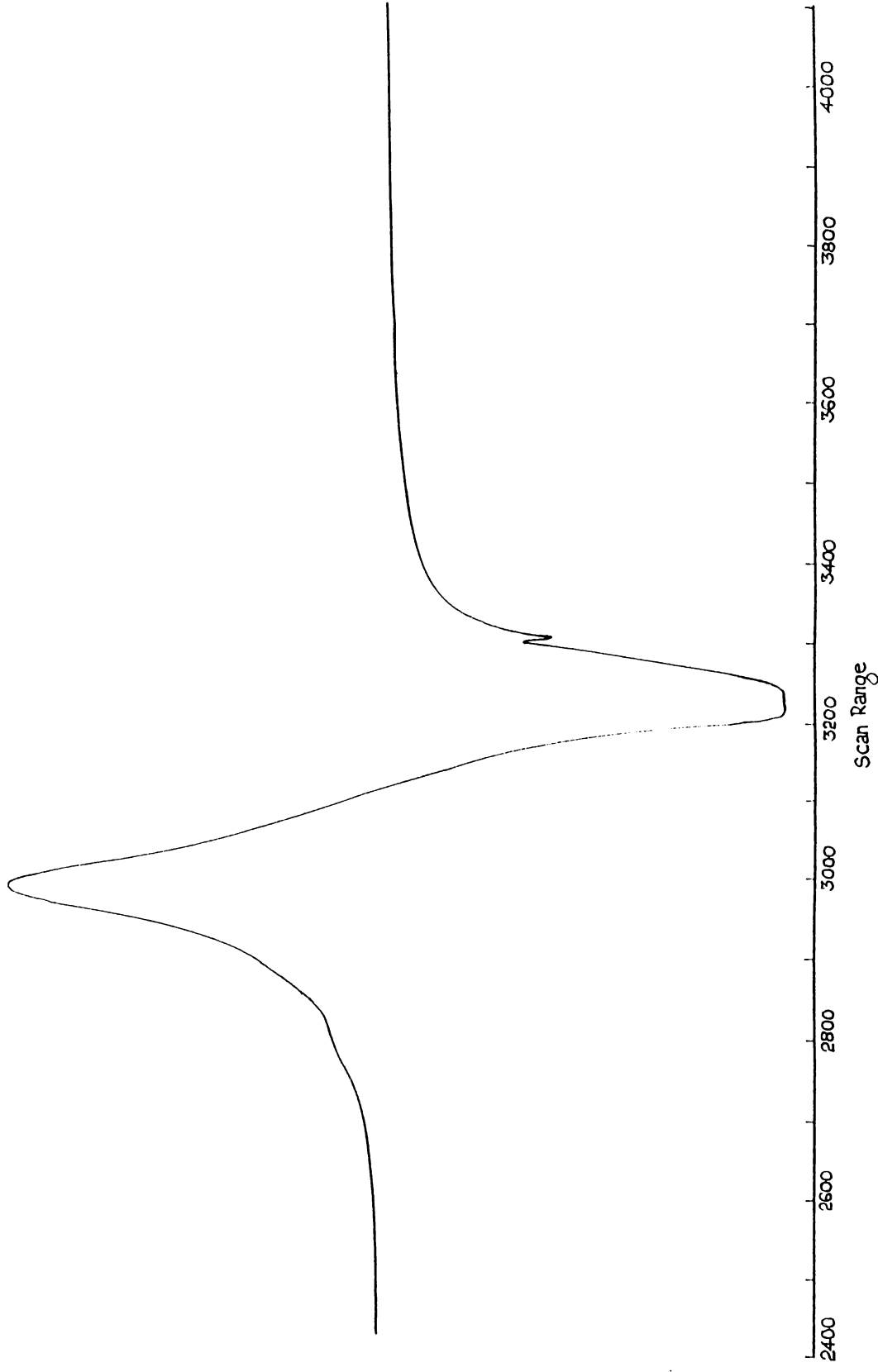
Fig.5.5: EPR Spectrum of [Cu(PACB)Cl(H$_2$O)]
at room temperature

Scan Range

complex may be same as that of the simple complex and (vide section 3.3.4) and square planar structure with compressed rhombic symmetry[112] may be assigned for this complex also.

5.3.5 Thermal Studies of the Complexes

The TG/DTG/DSC curves for all the complexes are given in Fig.5.6. Thermoanalytical data for the complexes are presented in Table 5.4. The complexes are stable upto 160°C. The DTG curves indicate that the thermal decomposition of the Fe(III), Co(II) and Cu(II) complexes occurs in three stages. The mass loss during the first stage of decomposition might be due to the removal of water molecule. The mass loss for the second stage does not correspond to any particular group. Probably the functionalized groups might have been removed at this stage along with the partial decomposition of the polymer. For all the complexes the last stage of decomposition represents the complete decomposition of the polymer part.

The DTG curve for the nickel(II) complex exhibits only two peaks. The second peak is the strongest and occurs at $\sim 540°C$. This peak represents the decomposition of the polymer part and functional groups. The first peak may be due to the removal of coordinated water. Only one
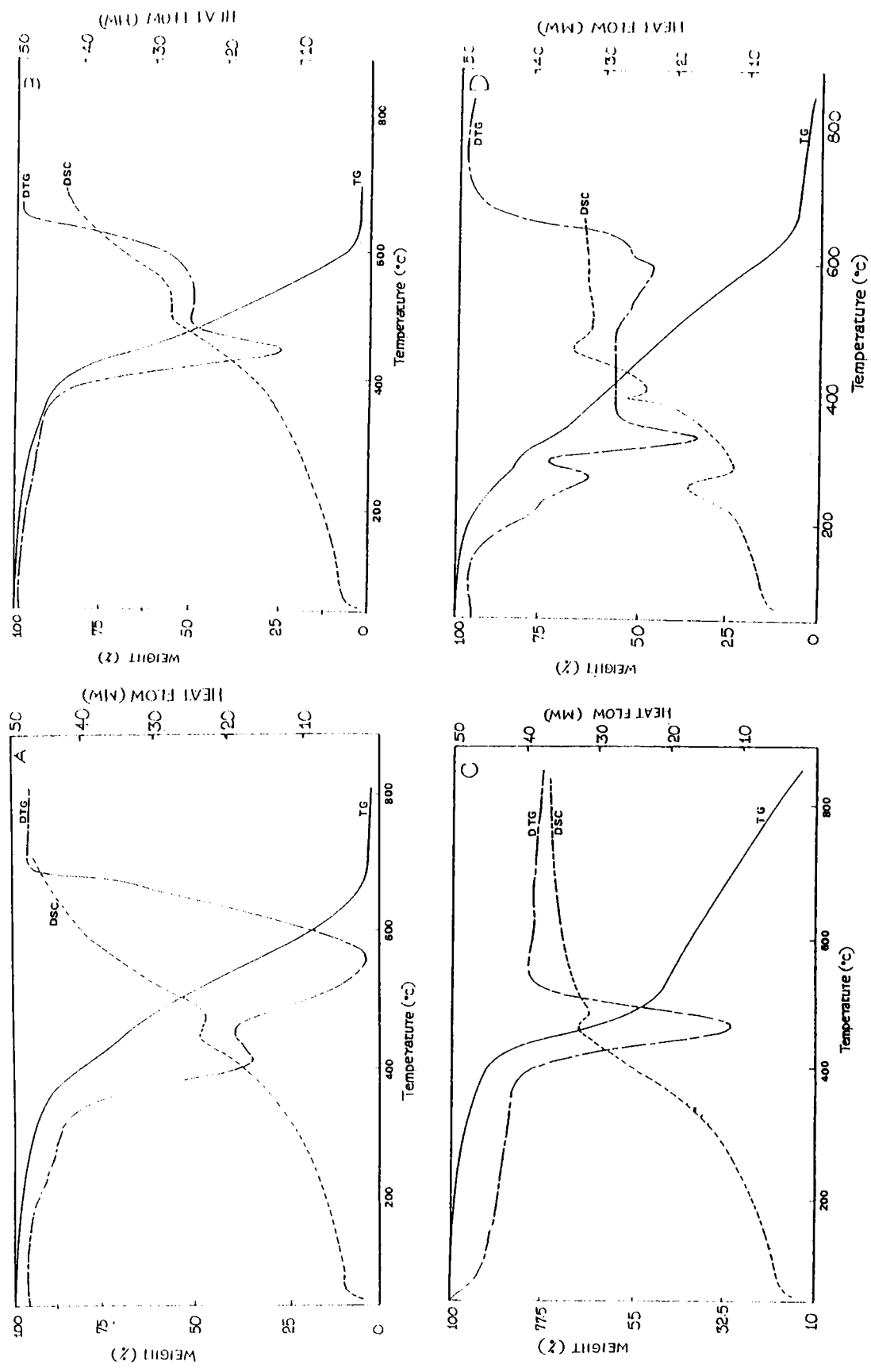
Fig.5.6: TG/DTG/DSC traces of the complexes

Table 5.4:   Thermal decomposition data

Compound	Stage of decomposition	Temp. range in DTG (°C)	Peak Temp. in DTG (°C)	Peak Temp. in DSC (°C)
$[Fe(PACB)Cl_2(H_2O)_2]$ (A)	I	160–415	325	
	II	415–565	460	450
	III	565–780	700	
$[Co(PACB)Cl(H_2O)]$ (B)	I	160–450	390	
	II	450–520	490	460
	III	520–680	550	
$[Ni(PACB)Cl(H_2O)]$ (C)	I	160–460	355	
	II	460–860	540	470
$[Cu(PACB)Cl(H_2O)]$ (D)	I	160–340	300	260
	II	340–425	390	360
	III	425–860	500	465

DSC exothermic peak was observed in the case of the complexes other than that of Cu(II). For the copper(II) complex the DSC exothermic peaks occurs at 260°C, 360°C and 460°C for the first, second and third stages respectively and the DSC pattern agrees with the data obtained for TG curve. The presence of only one DSC peak in the case of other complexes may be due to absence of well defined stages.

IRON(III), COBALT(II), NICKEL(II) AND COPPER(II) COMPLEXES OF THE SCHIFF BASE LIGAND DERIVED FROM QUINOXALINE-2- CARBOXALDEHYDE AND POLYSTYRENE FUNCTIONALIZED WITH AMINO GROUP

6.1   INTRODUCTION

Details about the synthesis and   characteriza-
tion of complexes of a polymer bound Schiff base are
described in chapter 5.   In this chapter we describe the
synthesis and characterization of some complexes of another
interesting   Schiff   base   ligand   (PSBQC)   prepared   by
condensing   quinoxaline-2-carboxaldehyde   with   polystyrene
functionalized with amino group.

6.2 EXPERIMENTAL
6.2.1 Materials

Details of the preparation of polymer bound Schiff
base and other reagents and solvents employed are given in
chapter 2.

6.2.2 Synthesis of the Complexes

All   the   polymer   bound   metal   complexes   were
prepared by the following general procedure: Polymer bound

Schiff base was swollen in dimethylformamide for 2 h and an excess of metal acetate dissolved in DMF was added to the Schiff base. The mixture was shaken for 5 h using a mechanical stirrer. The resulting polymer bound complex was filtered, washed with DMF, ethanol, methanol and chloroform and dried in vacuo over anhydrous $CaCl_2$.

6.2.3 Analytical Methods

Details about the analytical methods and other characterization techniques are given in chapter 2.

6.3 RESULTS AND DISCUSSION

Chloromethylated polystyrene (2% crosslinked with divinylbenzene, 3.7 meq. of chlorine/g) beads were used as the starting material in the present study. The chloromethyl groups in the polystyrene resin was converted to amino group. This is a polymer analogous extension of Delepine reaction in which activated halides react with hexamethylenetetramine in a non-aqueous medium to form an iminium salt which is hydrolysed by ethanolic HCl to produce the corresponding amine hydrochloride.[85]
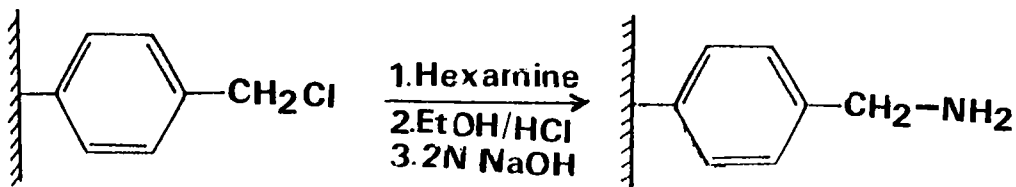
Scheme 6.1: Preparation of Amino Methyl Polystyrene

The conversion was more efficient and quick when the reaction was carried out in the presence of potassium iodide in DMF (2.3% conversion). Under these conditions a mixture of chloromethyl resin, hexamine and potassium iodide in DMF was used. The amino resin gave deep blue colour with ninhydrin reagent characteristic of the amino group.

The amino capacity of the resin was determined. Almost satisfactory results were obtained when the amino resins were reacted with excess standard HCl and back titrated the excess acid. The amino capacity in this case was found to agree with the results of percentage nitrogen

content (1.2 mmol/g) obtained from microanalysis. Then the aminopolystyrene was condensed with quinoxaline-2-carboxaldehyde to give polymer bound Schiff base as shown in Scheme 6.2.
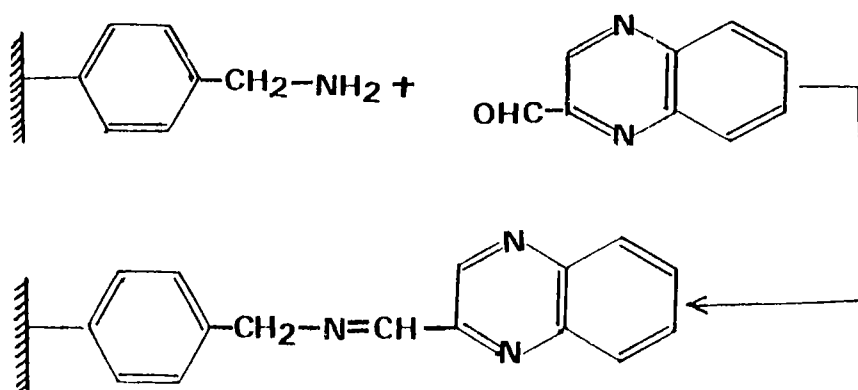
Scheme 6.2: Preparation of Schiff Base

Nitrogen analysis of the polymer was carried out and it was found that 1.2 mmols of nitrogen was present in the Schiff base ligand. Using this polymer bound Schiff base, complexes of Fe(III), Co(II), Ni(II) and Cu(II) were prepared.

Both nickel(II) and copper(II) complexes are light green in colour and the other complexes have almost the

Table 6.1: Analytical data

Complex	M (%) Found (Calc.)
$[Fe(PSBQC)(OAc)_3(H_2O)_2]$	2.00 (2.03)
$[Co(PSBQC)(OAc)_2(H_2O)]$	1.98 (2.10)
$[Ni(PSBQC)(OAc)_2(H_2O)]$	1.97 (2.10)
$[Cu(PSBQC)(OAc)_2(H_2O)]$	2.18 (2.30)

same colour as that of the cobalt(II) and iron(III) complexes reported in chapter 4.

The percentage of metal ions present in the complexes were determined by the colorimetric methods mentioned in chapter 2 (Table 6.1). The percentage of nitrogen obtained from elemental analysis of the ligand has been taken as the standard for obtaining the empirical formula and probable structures of the complexes, as has been done in chapter 5 (vide section 5.3). Thus $[FeL(OAc)_3(H_2O)_2]$ is the empirical formula obtained for the iron(III) complex and $[(ML(OAc)_2H_2O]$ for the cobalt(II), nickel(II) and copper(II) complexes, where L = PSBQC and OAc = acetato group.

6.3.1 Magnetic Susceptibility Measurements

The magnetic moment values are given in Table 6.2. VSM measurements were used for the calculation of magnetic susceptibility of the complexes. A magnetic moment value around 5.8 BM is obtained for the Fe(III) complex which indicates an octahedral structure for the complex.[101] The μ_{eff}. value for the Co(II) complex was around 4.4 BM which indicates a tetrahedral structure.[100] The nickel(II)

Table 6.2: Magnetic moment and electronic spectral data

Polymer complex	Magnetic moment (BM)	Abs. max (cm^{-1})	Tentative Assignments
$[Fe(PSBQC)(OAc)_3(H_2O)_2]$	5.8	45870	Intraligand transition
		39215	Charge transfer transition
		33300	"
		29000	"
		25640	"
$[Co(PSBQC)(OAc)_2(H_2O)]$	4.4	45870	Intraligand transition
		39690	Charge transfer transition
		33300	"
		28570	"
		22280	$^4A_2 \longrightarrow {}^4T_1(P)$
$[Ni(PSBQC)(OAc)_2(H_2O)]$	dia-magnetic	45870	Intraligand transition
		38020	"
		33300	"
		28820	"
		25600	$^1A_{1g} \longrightarrow {}^1B_{1g}$
$[Cu(PSBQC)(OAc)_2(H_2O)]$	1.7	45870	Intraligand transition
		39370	Charge transfer transition
		33300	"
		29070	"
		25980	"

complex was found to be diamagnetic and the magnetic moment value obtained for copper(II) complex was 1.7 BM, which indicate square planar structures for these two complexes.

6.3.2 Electronic Spectra

The electronic spectra of the complexes are given in Figs.6.1 to 6.4 and the electronic spectral data are given in Table 6.2. The data do not provide any conclusive evidence to assign the structure of these complexes. The spectrum of the iron(III) complex shows band at 45870 cm^{-1} due to intra-ligand transition. The bands at 39215 cm^{-1}, 33300 cm^{-1}, 29000 cm^{-1} and 25640 cm^{-1} may be due to charge transfer transitions and these bands might have obscured the spin forbidden d-d transitions.[101]

The Co(II) complex shows only one d-d band at 22280 cm^{-1} which may be due to $^4A_2 \longrightarrow {}^4T_1(P)$ electronic transition.[114] The other low energy bands are not seen in the spectra of the complex. The bands observed at 28570 cm^{-1}, 33300 cm^{-1} and 39690 cm^{-1} are due to charge transfer and band at 45870 cm^{-1} is due to intra-ligand transition.

The Ni(II) complex shows a band at 25600 cm^{-1} which may be assigned to $^1A_{1g} \longrightarrow {}^1B_{1g}$ transition.[102] The
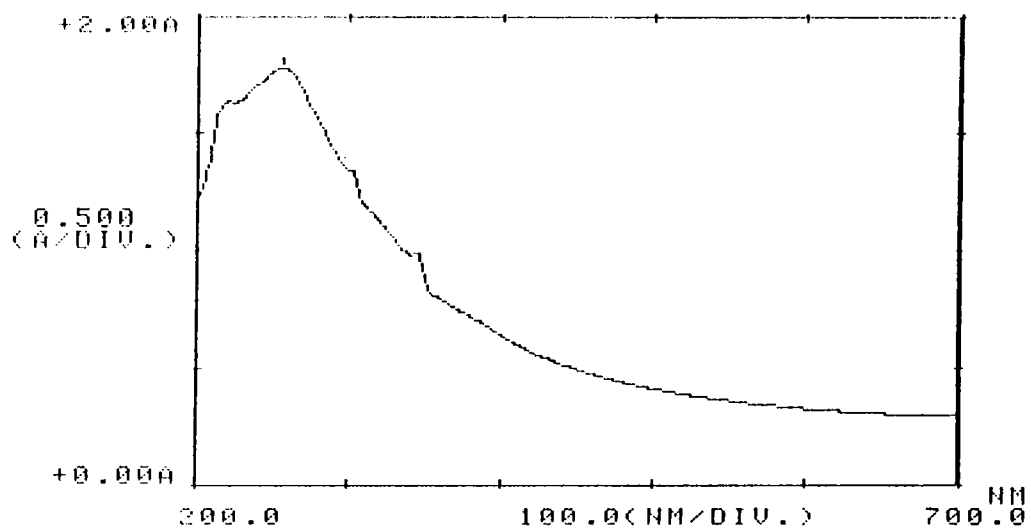
Fig.6.1: Electronic Spectrum of $[Fe(PSBQC)(OAc)_3(H_2O)_2]$
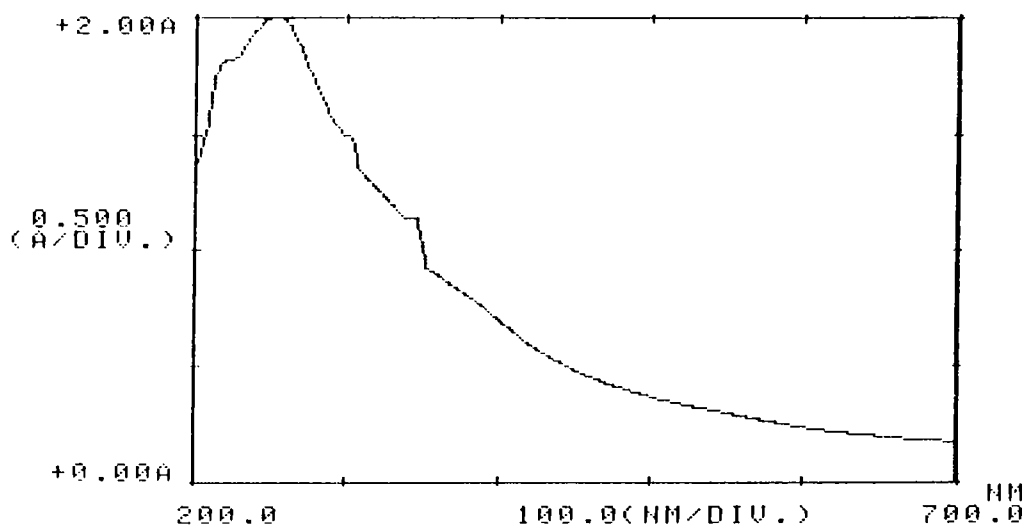
Fig.6.2: Electronic Spectrum of $[Co(PSBQC)(OAc)_2(H_2O)]$
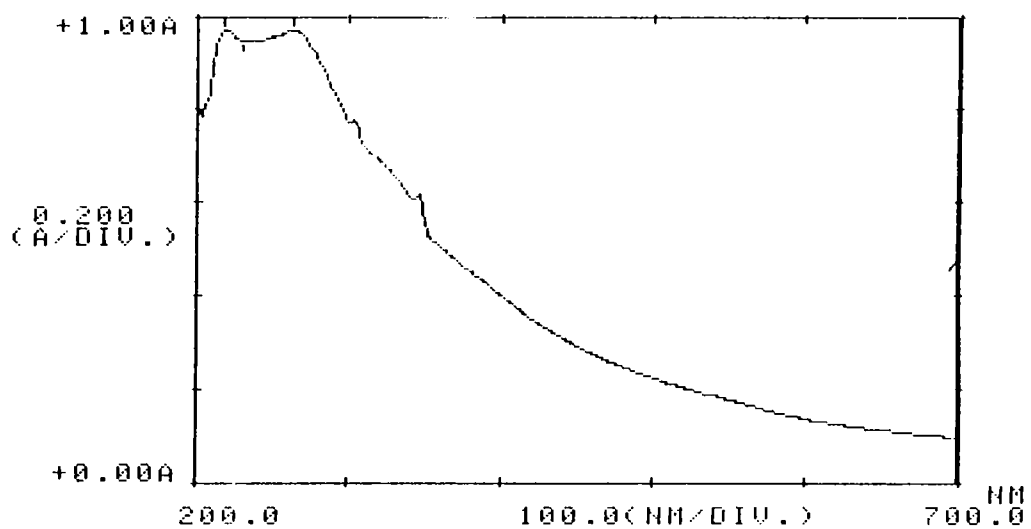
Fig.6.3: Electronic Spectrum of [Ni(PSBQC)(OAc)$_2$(H$_2$O)]
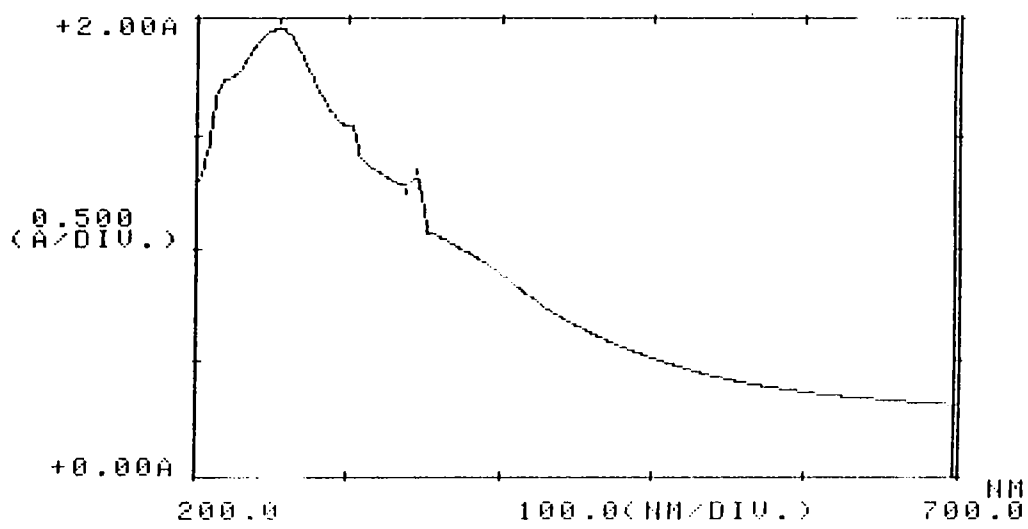
Fig.6.4: Electronic Spectrum of [Cu(PSBQC)(OAc)$_2$(H$_2$O)]

bands at 28820 cm^{-1}, 33300 cm^{-1} and 38020 cm^{-1} and the band at 45870 cm^{-1} can be assigned to charge transfer transitions and intra-ligand transition respectively.

The Cu(II) complex shows a band at 45870 cm^{-1} due to intra-ligand transition. The expected d-d bands for square planar complex are not observed. The charge transfer bands observed at 25980 cm^{-1}, 29070 cm^{-1}, 33300 cm^{-1} and 39370 cm^{-1} might have obscured the d-d transitions.[115]

6.3.3 Infrared Spectra

The infrared spectral data of the ligand and the complexes are given in Table 6.3. All the complexes show bands in the region 3200-3400 cm^{-1} due to γOH of water molecule.[104] A band at 840 cm^{-1} due to coordinated water molecule is also seen in the complexes.[105] A band observed at 1630 cm^{-1} in the spectrum of the ligand is shifted to 1620 cm^{-1} in the spectra of all the complexes indicating coordination of the azomethine nitrogen.[109] The band due to γ(C-N) of the quinoxaline ring appears almost at the same position suggesting the non-participation of the ring nitrogen atom.

Table 6.3:   Infrared absorption frequencies (cm^{-1})

PSBQC	I	II	III	IV	Tentative Assignments of the more relevant bands
(1)	(2)	(3)	(4)	(5)	(6)
--	3400m	3400m	3400m	3400m	γ(H-O-H)
--	3200m	3200m	3200m	3200m	
2905m	2905m	2905m	2930m	2930m	
2830m	2810m	2810m	2830m	2820m	
1690m	1690m	1690m	1690s	1690s	
1630m	1620m	1620m	1620m	1620m	γ(C=N)
--	1605m	1605m	1605m	1605m	γ_a(COO)
1580w	1580m	1580m	158 0m	1580m	γ(C=N) (ring)
1500m	1505m	1500m	1505m	1500m	
1490m	1490s	1490m	1490m	1490w	
1450s	1450s	1455s	1450s	1450s	
1415m	1420m	1415m	1415m	1415m	
--	1375s	1375s	1380s	1380s	γ_s(COO)
1365m	1340sh	1340sh	1355s	1355s	
1215m	1210m	1210m	1210m	1200m	
1165m	1165m	1160m	1170m	1165m	
1105m	1110m	1110m	1105m	1120m	
1015w	1020w	1015w	1015m	1010m	

(Contd.. .)

(1)	(2)	(3)	(4)	(5)	(6)
--	970w	990w	990w	990w	
--	940w	965w	970w	970w	δ(COO)
--	920w	920w	920w	920w	
890w	890w	890w	890w	890w	
--	840m	840m	840m	845m	ρ(H-O-H)
825m	825m	820m	820m	820m	
775w	760w	765w	760w	785w	
720m	720m	720m	720m	720m	
620m	620m	620m	620m	625m	
550w	550w	550w	550w	535w	

s = strong ;   m = medium ;   w - weak

$I = [Fe(PSBQC)(OAc)_3(H_2O)_2]$; $II = [Co(PSBQC)(OAc)_2(H_2O)]$

$III = [Ni(PSBQC)(OAc)_2(H_2O)]$; $IV = [Cu(PSBQC)(OAc)_2(H_2O)]$
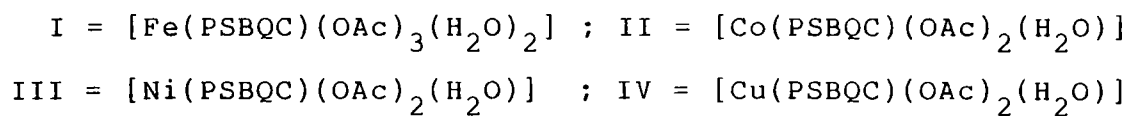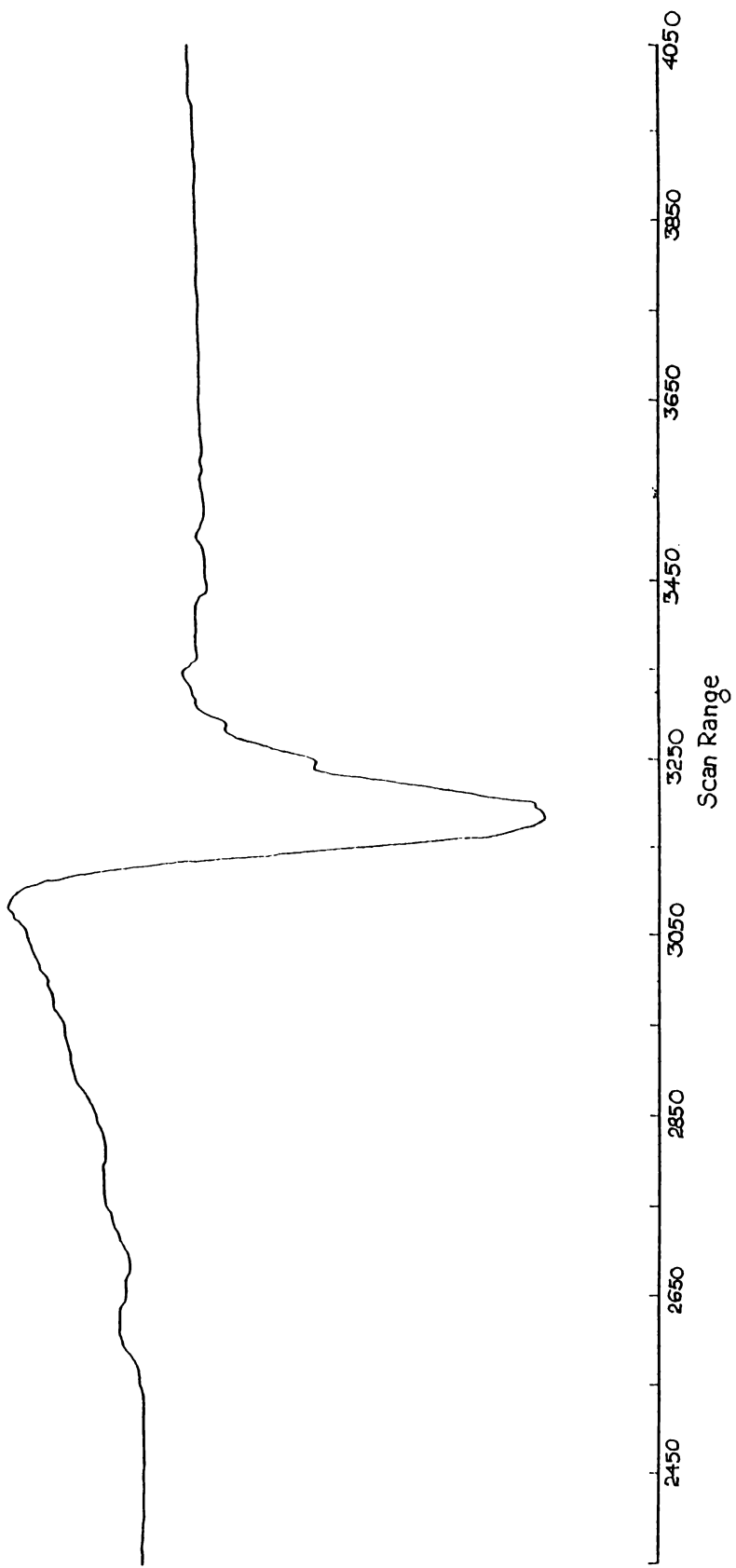
Fig.6.5: EPR Spectrum of $[Cu(PSBQC)(OAc)_2(H_2O)]$

The acetate group in the complexes acts as unidentate ligand and this is supported by the appearance of two new bands at 1605 cm^{-1} and 1380 cm^{-1} which may be attributed to ν_a(COO) and ν_s(COO) respectively.[111] Further three bands are seen in the region 920-990 cm^{-1} of the spectra of the complexes. These bands are not observed in the spectrum of the ligand.

6.3.4 EPR Spectra

The powder spectra of the polymer bound Cu(II) complex (Fig.6.5) was recorded at room temperature. The $g_{\parallel}$ value of 2.4 and $g_{\perp}$ value of 2.08 obtained for this complex suggest a square planar structure for the Cu(II) complex.[112] Further the lowest g value was found to be greater than 2.04, which is usually observed for a copper(II) complex ion in axial symmetry with all the principal axes aligned parallel. The G value ($g_{\parallel}$ -2/$g_{\perp}$-2) of the complex was found to be 5 which further indicates that the local tetragonal axes are only slightly misaligned.

6.3.5 Thermal Studies of the Complexes

The TG/DTG/DSC curves for all the complexes are given in Fig.6.6. Thermoanalytical data for the complexes

Table 6.4: Thermal decomposition data

Compound	Stage of decomposi-tion	Temp. range in DTG (°C)	Peak Temp. in DTG (°C)	Peak Temp. in DSC (°C)
[Fe(PSBQC)(OAc)$_3$(H$_2$O)$_2$] (A)	I	140–225	200	
	II	225–430	300	
	III	430–620	460	460
[Co(PSBQC)(OAc)$_2$(H$_2$O)] (B)	I	140–220	220	
	II	220–450	350	
	III	450–620	475	450
[Ni(PSBQC)(OAc)$_2$(H$_2$O)] (C)	I	140–435	180	
	II	435–780	495	455
[Cu(PSBQC)(OAc)$_2$(H$_2$O)] (D)	I	140–220	165	
	II	220–440	295	
	III	440–620	450	450

5·7 1·49 : [542.261/·28 : 546·88]

K ᴬ ᴬ
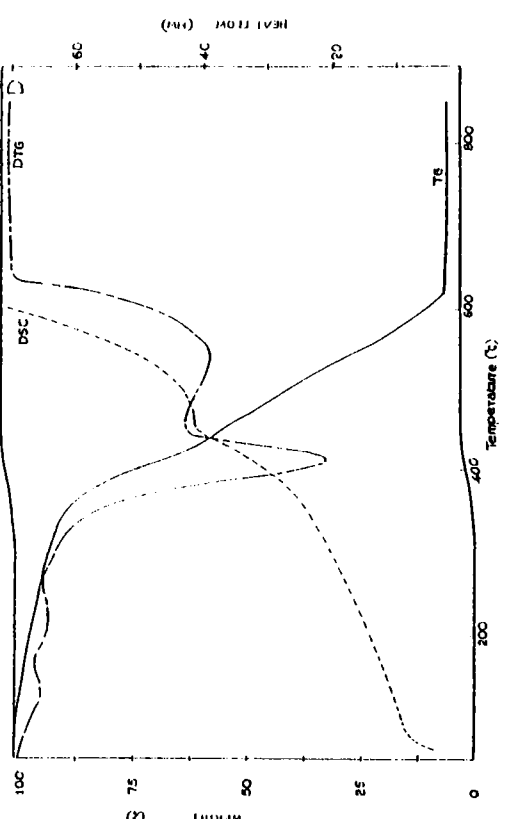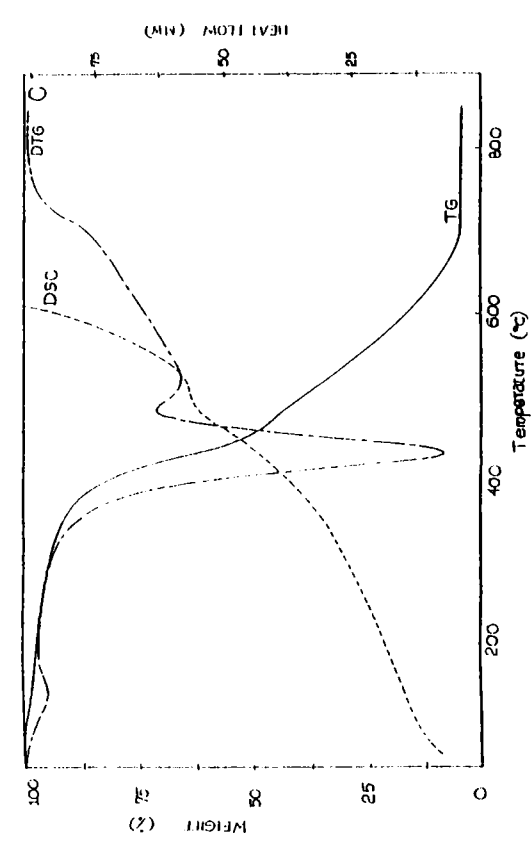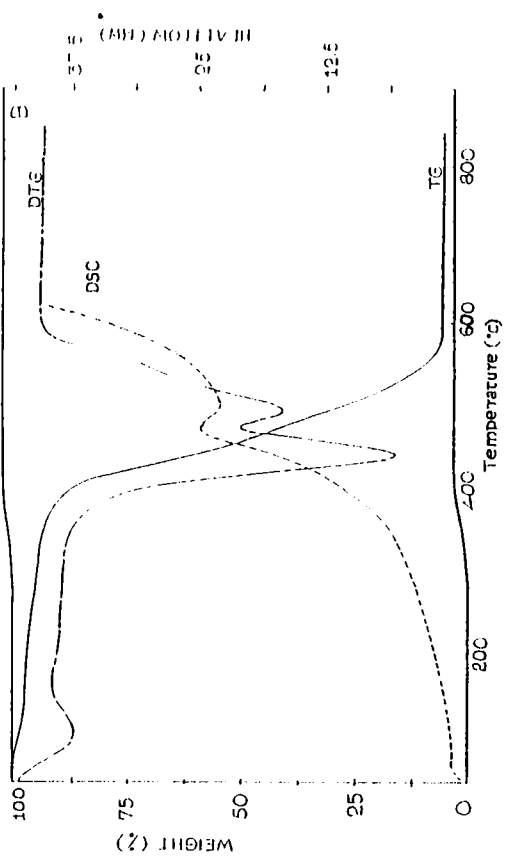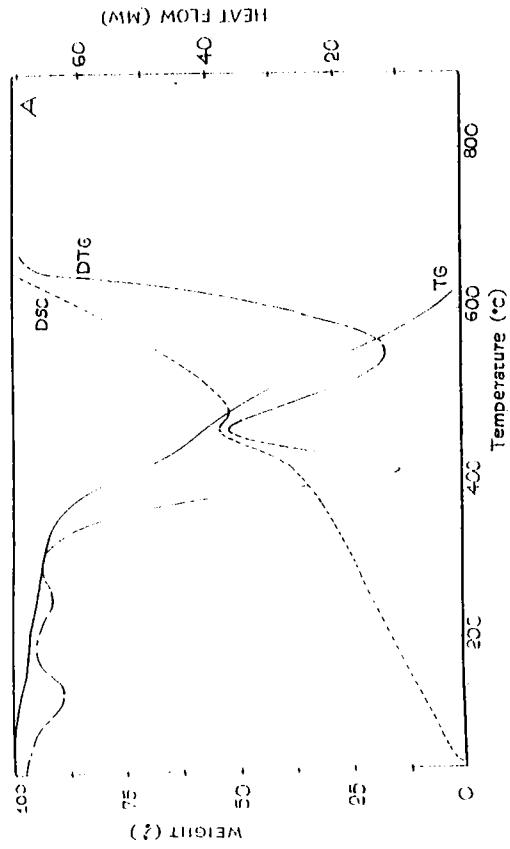
Fig.6.6: TG/DTG/DSC traces of the complexes

are presented in Table 6.4. The complexes are stable upto ~140°C, above which they start slowly decomposing. The DTG curves indicates that there are three stages involved in the thermal decomposition of the Fe(III), Co(II) and Cu(II) complexes. The mass loss at the first stage of decomposition corresponds to the removal of water molecule. It is difficult to predict the groups expelled during the second stage as the mass loss does not correspond with the removal of any particular group, probably acetate and Schiff base unit might have been removed at this stage, along with the partial decomposition of the polymer. The last stage corresponds with the complete decomposition of the polymer part, which is indicated by the fact that this decomposition happens nearly in the same temperature region for all the present polymer complexes.

In the case of Ni(II) complex the DTG curve shows only two peaks. The first one may be due to the removal of water molecule. The second peak is the strongest and occurs at ~495°C. It represents the decomposition of the polymer part and also the functional groups. In all the above three cases only one DSC exothermic peak was observed. This may be due to the overlapping of the different stages involved in the decomposition reaction.

MIXED LIGAND COMPLEXES OF IRON(III) CONTAINING

N,N'-BIS(SALICYLALDEHYDE)ETHYLENEDIIMINE AND

2-AMINOCYCLOPENT-1-ENE-1-DITHIOCARBOXYLIC ACID OR

ITS ALKYL DERIVATIVES

7.1   INTRODUCTION

Mixed   ligand   complexes   of   iron(III)   containing dithio   ligands   have   attracted   much   interest   because   of their   unusual   electronic   and   structural   properties.[123] Many   fascinating   mixed   ligand   complexes   of   iron(III)   have been   synthesized.   Among   them   are   the   five   coordinate complexes   like   halogenobis(dialkyldithiocarbamato)iron(III), dithiocarbamato-xanthato   cobalt(III)   complex   and   iron(III) complexes   containing   a   dithiocarbamate   group   and   a   Schiff base   ligand.[124,125]   We   have   synthesized   hitherto   unknown mixed   ligand   complexes   of   iron(III)   containing   the   Schiff base   ligand,   salen   and   ACDA   or   its   alkyl   derivatives, i-PrACDA,   n-BuACDA.   The   results   of   our   studies   are presented   in   this   chapter.

7.2   EXPERIMENTAL

7.2.1   Materials

Details   about   the   preparation   and   purification   of the   ligands,   ACDA   and   its   alkyl   derivatives,   i-PrACDA   or

n-BuACDA) and N-N'-bis(salicylaldehyde)ethylenediimine (salen) are given in chapter 2.

7.2.2 Synthesis of the Complexes

7.2.2.1 Synthesis of [Fe(Salen)Cl]

The complex [Fe(Salen)Cl] is prepared according to the following procedure: Equimolar amounts of salen (0.01 mol, 2.68 g) and ferric chloride (0.01 mol, 1.62 g) in benzene solution were refluxed for 4 h on a water bath. The dark brown product formed was washed with methanol and ether and dried over anhydrous $CaCl_2$.

7.2.2.2 Synthesis of [Fe(Salen)L] (L = ACDA, i-PrACDA, n-BuACDA)

[Fe(Salen)Cl] (0.01 mol, 3.59 g) dissolved in methanol (50 ml) and the ligand (0.01 mol, 1.58 g ACDA or 1.99 g i-PrACDA or 2.25 g n-BuACDA) dissolved in methanol (50 ml) were mixed and refluxed for 4 h on a water bath. The reaction mixture was allowed to stand for some time. The dark brown crystals separated out were collected, washed with ether and dried over anhydrous $CaCl_2$.

7.2.3 Analytical Methods

Details about the analytical methods and other characterization techniques are given in chapter 2.

Table 7.1:   Analytical data

Complex	Colour	C (%) Found (Calc.)	H (%) Found (Calc.)	N (%) Found (Calc.)	M (%) Found (Calc.)	S (%) Found (Calc.)
[Fe(Salen)(ACDA)] [$C_{22}H_{22}N_3FeS_2$]	Dark brown	54.98 (55.1)	4.62 (4.60)	8.62 (8.76)	10.98 (11.65)	13.45 (13.36)
[Fe(Salen)i-PrACDA)] [$C_{25}H_{28}N_3FeS_2$]	Dark brown	57.00 (57.57)	5.38 (5.41)	7.99 (8.05)	10.51 (10.71)	12.30 (12.28)
[Fe(Salen)n-BuACDA)] [$C_{26}H_{30}N_3FeS_2$]	Dark brown	57.00 (57.02)	5.49 (5.52)	7.59 (7.67)	1C.28 (10.20)	11.72 (11.69)

7.3 RESULTS AND DISCUSSION

All the complexes are dark brown coloured crystalline substances and are stable in air. They are soluble in nitrobenzene, chloroform, acetone, acetonitrile, dimethylsulphoxide and dimethylformamide and slightly soluble in methanol and ethanol. The analytical data (Table 7.1) show that the complexes have the general formula [Fe(Salen)L] where L = ACDA, i-PrACDA or n-BuACDA. The molar conductance values suggest that all the complexes are non-electrolytes in nitrobenzene (Table 7.2).

7.3.1 Magnetic Susceptibility Measurements

Magnetic moment values of the complexes are presented in Table 7.2. The values (around 5.9 BM) indicate a high spin Fe(III) octahedral structure for all the complexes.[94]

7.3.2 Electronic Spectra

Solid state electronic spectra of the complexes are given in Fig.7.1 to 7.3 and the spectral data are given in Table 7.3. Bands observed around 40600 cm^{-1} and 37500 cm^{-1} may be assigned to intra-ligand transitions and band at 31200 cm^{-1} is due to charge transfer transition.

Table 7.2: Molar conductance and magnetic moment data

Compound	Molar conductance $(ohm^{-1}cm^2mol^{-1})$	Magnetic moment (BM)
[Fe(Salen)ACDA]	2.1	5.9
[Fe(Salen)i-PrACDA]	2.8	5.8
[Fe(Salen)n-BuACDA]	2.3	5.9
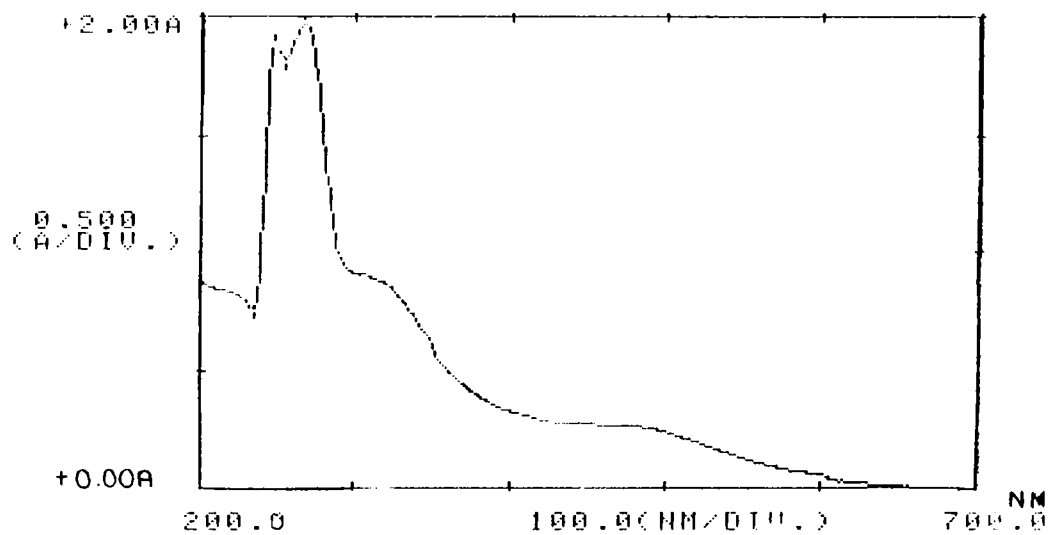
Fig.7.1: Electronic Spectrum of [Fe(Salen)ACDA]
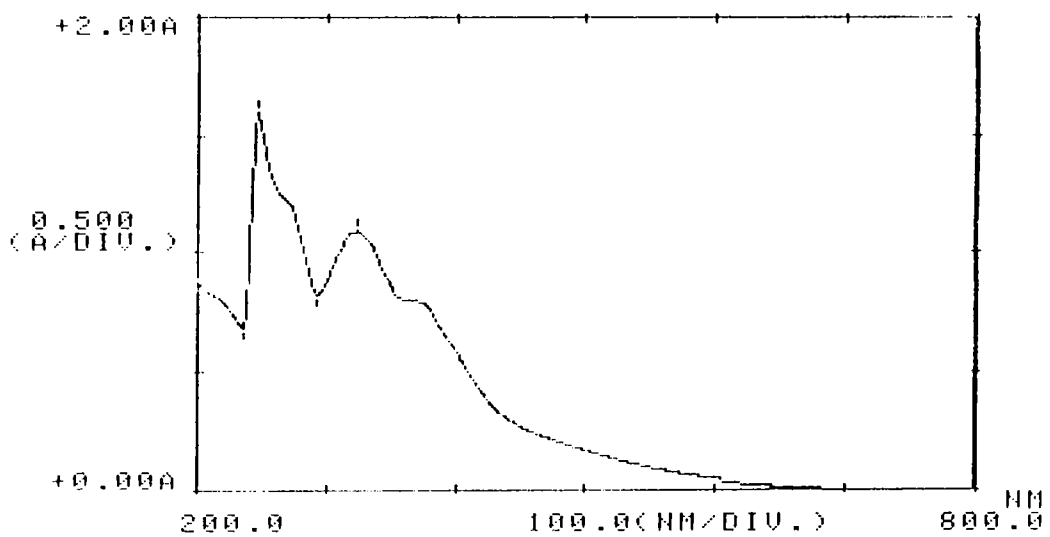
Fig.7.2: Electronic Spectrum of [Fe(Salen)i-PrACDA]
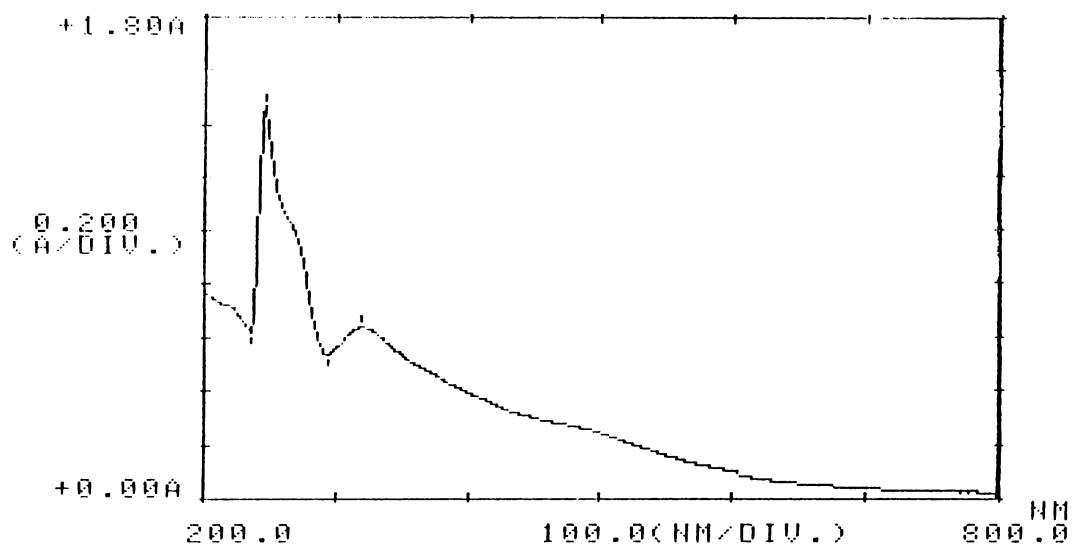
Fig.7.3: Electronic Spectrum of [Fe(Salen)n-BuACDA]

Table 7.3: Electronic spectral data

Compound	Abs.Max. (cm^{-1})	Tentative Assignments
[Fe(Salen)ACDA]	40500	Intra-ligand transition
	37450	"
	31750	Charge transfer transition
	20400	d-d transition
[Fe(Salen)i-PrACDA]	40650	Intra-ligand transition
	37000	"
	31250	Charge transfer transition
	25000	d-d transition
[Fe(Salen)n-BuACDA]	40650	Intra-ligand transition
	37750	"
	31250	Charge transfer transition
	20000	d-d transition

The shoulder band observed around 20000-25000 cm^{-1} in the spectra of all the complexes may be due to d-d transitions in the octahedral symmetry.[37,115]

7.3.3 Infrared Spectra

The infrared spectra of the ligands and complexes are given in Table 7.4. In the spectra of the complexes some of the characteristic bands of both the ligands appear in the same region. Such composite bands resulting from the overlap of the bands of the two different ligands are usually observed in the spectra of mixed ligand complexes and assignments of these bands are often difficult. The bands observed around 3080 cm^{-1} can be attributed to $\mathcal{V}$(N-H) of ACDA.[126] Further $\mathcal{V}$(C=C) of ACDA appears as a strong band[127] around 1610-1630 cm^{-1}. The bands observed around 1540 cm^{-1} in the spectra of salen and mixed ligand complexes may be assigned to $\mathcal{V}$(C-O) band stretching of salen ligand.[128] The medium bands observed at 1380 cm^{-1} and 1330 cm^{-1} can be assigned to the imino group.[129] A band is seen in the region 900-1000 cm^{-1}, which is usually associated with the C-S stretching frequencies of dithio-carboxylic acid complexes.[111] Further, presence of only one band in this region ($\sim$970 cm^{-1}) indicates bidentate

Table 7.4:   Infrared absorption frequencies (cm^{-1})

I	II	III	IV	V	VI	VII	Tentative Assignments of the more relevant bands
(1)	(2)	(3)	(4)	(5)	(6)	(7)	(8)
3080w	3080w	3080w	--	3080w	3080w	3080w	γN-H
2990m	2990m	2980m	2990m	2990m	2990m	2980m	γ(C-H)
2800w	2800w	2820w	2830w	2830w	2830w	2830w	
--	--	2720w	2715m	2715m	2715m	2715m	
--	--	--	2380w	2380w	2380w	2380w	
1610s	1615s	1620s	1630s	1630s	1625s	1630s	γ(C=C)
--	--	--	1605s	1595s	1595s	1600s	
1570s	1570s	1570s	1570m	1570m	1570sh	1570sh	δ(CNH)
--	--	--	1545s	1535sh	1540sh	1530s	γ(C-O) Salen
1470s	1470s	1460m	1465m	1465m	1465s	1465m	γ(C=C) + δCH$_2$
--	--	--	1440s	1440m	1440s	1440m	
1370m	1370m	1370s	1380m	1380m	1380m	1380m	
--	--	--	1355s	1360s	1360s	1360m	
1330m	1330m	1330s	1330m	1330m	1330m	1330m	γ(C-N)+γ(C-S)
1310sh	1305w	1305w	1295w	1300m	1305m	1290m	
1280s	1265m	1270m	1260sh	1260m	1260m	1270m	γ(C-S)+γ(C-N)
--	--	--	1250w	1250w	1245sh	1290sh	
--	--	--	1230w	1230w	1220w	1220w	
--	--	1200w	1190w	1200w	1200w	1190w	

(Contd...)

(1)	(2)	(3)	(4)	(5)	(6)	(7)	(8)
1155m	1155m	1155m	1140m	1130m	1145m	1150m	
1130w	1130w	1120w	1120m	1130m	1130w	1120m	
--	--	--	1085w	1085w	1085w	1080w	
1060w	1060w	1060w	--	1045w	1045w	1060w	
1020w	1020w	1020w	1025m	1000m	1000w	1000w	
970m	950m	980m	965m	965m	970m	970m	ν_a(CSS)
880m	870m	855w	855w	855w	850w	850w	
800w	800w	800w	795m	810m	795m	790w	
760m	785s	760m	760m	760m	755m	750s	
710w	700w	720w	700w	680w	700w	680w	
615m	610m	610w	620m	620w	620m	610m	
--	--	--	585w	585w	585w	580w	
--	--	--	535w	530w	520w	530w	
475w	470w	475w	470w	475w	450w	450w	ν(M-O)
--	--	--	430m	415m	420m	425m	ν(M-N)
--	--	--	--	385m	390m	385m	ν(M-S)
--	--	--	365m	--	--	--	ν(M-Cl)

s = strong ;   m = medium ;   w = weak ;   sh = shoulder

I = ACDA ;   II = i-PrACDA ;   III = n-BuACDA ;

IV = [Fe(Salen)Cl]   ;   V = [Fe(Salen)ACDA] ;

VI = [Fe(Salen)i-PrACDA] ;   VII = [Fe(Salen)n-BuACDA]

bonding of the ACDA ligand through the sulphur atoms.[111,130-133] Further indication about this is obtained from the presence of a strong ν(M-S) band around 385 cm^{-1}. The bands seen at 450-470 cm^{-1} and 425 cm^{-1} are due to ν(M-O) and ν(M-N) respectively.[111]

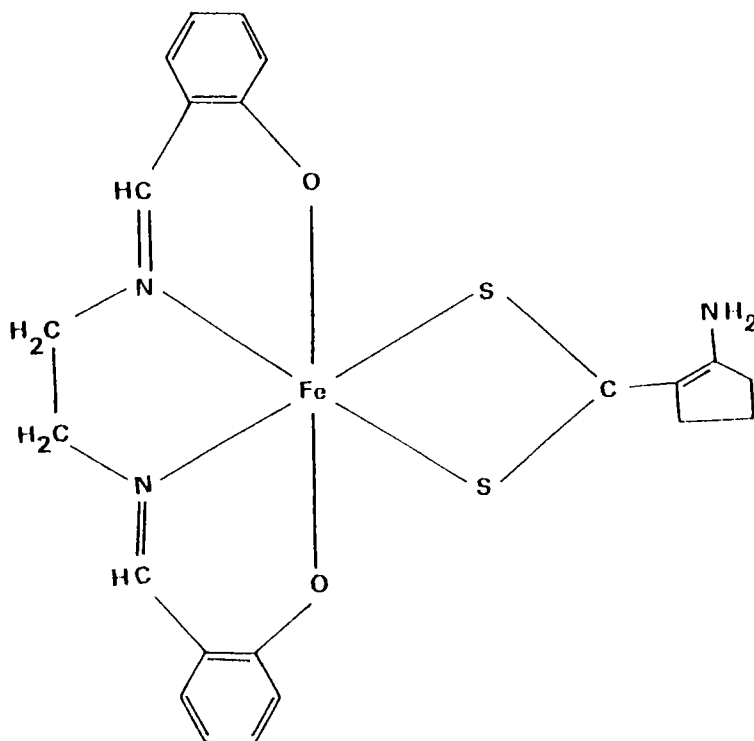Fig.7.4: Schematic Structure of [Fe(Salen)ACDA]

Based on these studies, the structure shown in Fig.7.4 may be tentatively proposed for the present complexes.

SYNTHESIS,   CHARACTERIZATION   AND   THERMAL   DECOMPOSITION
KINETICS   OF   MIXED   LIGAND   COMPLEXES   OF   COBALOXIME   WITH   A
BULKY   LIGAND   1-BENZYL-2-PHENYLBENZIMIDAZOLE

SECTION A: SYNTHESIS AND CHARACTERIZATION

8.1   INTRODUCTION

Cobaloximes are complexes containing the $Co(DH)_2^+$ moiety[134] (DH is the monoanion of dimethylglyoxime, DH_2). They are known to simulate closely the reactions of Vitamin B_{12}, and are of importance in Vitamin B_{12} "model chemistry".[135,136] They are useful reagents in synthetic organic chemistry and are used as protecting groups in the synthesis of amino acids.[137] Cobaloximes are also reported to act as catalysts for oxidation reactions.[138] Several mixed ligand cobaloxime complexes of the type, trans-$[Co(DH)_2 L X]$, where L = imidazole or benzimidazole or their substituted derivatives, and X = Cl, SCN, N_3, ClO_4 or BF_4 have been reported.[139-142] However, mixed ligand cobaloxime complexes with a bulky ligand like 1-benzyl-2-phenylbenzimidazole (BPBI) have not yet been reported. The derivative BPBI is interesting from the structural point of view because of its bulky nature and steric effects.

The results of our studies on the synthesis and character-
ization of such complexes and thermal decomposition kinetic
studies are described in this chapter.

8.2 EXPERIMENTAL

8.2.1 Materials

Details regarding the preparation and purification
of the ligand BPBI are given in chapter 2.

8.2.2 Synthesis of the Complexes

Synthesis of [Co(DH)$_2$BPBI)X], X = Cl or Br

To a hot solution of $CoX_2 \cdot 6H_2O$ (0.005 mol, 1.2 g)
in 15 ml of n-butanol, was added a hot solution of DH_2
(0.01 mol, 1.16 g) in 25 ml of n-butanol followed by BPBI
(0.005 mol, 1.42 g) in 15 ml hot n-butanol. Air was
bubbled through the reaction mixture for 5 h keeping the
system on a boiling water bath. The whole solution was
kept at room temperature for 24 h. The crystals formed
were filtered, washed with n-butanol, ether and was finally
dried over anhydrous $CaCl_2$.

Synthesis of [Co(DH)$_2$(BPBI)X] (X = I or SCN)

CoX_2' was obtained by metathetic reaction of
$Co(NO_3)_2 \cdot H_2O$ (0.005 mol, 1.47 g) and KX' (0.01 mol, 1.66 g

of KI or 0.972 g KSCN) in butanol. The precipitated KNO_3 was filtered off and washed with n-butanol. The filtrate was concentrated to a small volume and was used as the source of COX_2. To this was added a hot solution of 0.01 mol of DH_2 and then a hot solution of 0.005 mol of BPBI. The rest of the synthetic procedure was same as that described above.

8.2.3 Analytical Methods

Details about the analytical methods and other characterization techniques are given in chapter 2.

8.3 RESULTS AND DISCUSSION

We have attempted the synthesis of the complexes by the usual procedure of treating BPBI with DH_2 and cobalt salts in ethanol or methanol in the presence of air. However, no solid compound was separated from the reaction medium. The formation of mixed chelate complexes are known to be affected by solvent.[143] The complexation reaction was then tried in several solvents. The formation of the present complexes take place only on refluxing and bubbling air through a solution containing cobalt(II) salt, DH_2 and BPBI (1:2:1 ratio), in hot n-butanol. The complexes formed

Table 8.1: Analytical data

Complex	Colour	M.P °C	C (%) Found (Calc.)	H (%) Found (Calc.)	N (%) Found (Calc.)	Co (%) Found (Calc.)	X (%) Found (Calc.)	S (%) Found (Calc.)
[Co(DH)$_2$(BPBI)Cl] [C$_{28}$H$_{30}$ClCoN$_6$O$_4$]	Brown	190	54.90 (55.20)	4.82 (4.92)	13.50 (13.80)	9.70 (9.70)	5.80 (5.80)	--
[Co(DH)$_2$(BPBI)Br] [C$_{28}$H$_{30}$BrCoN$_6$O$_4$]	Brown	194	51.00 (51.44)	4.39 (4.50)	12.76 (12.80)	9.01 (9.02)	12.16 (12.20)	--
[Co(DH)$_2$(BPBI)I] [C$_{28}$H$_{30}$ICoN$_6$O$_4$]	Greyish brown	215	47.53 (47.99)	4.16 (4.28)	.11.70 (11.90)	8.50 (8.40)	17.40 (18.12)	--
[Co(DH)$_2$BPBI)SCN] [C$_{29}$H$_{30}$CoN$_7$O$_4$S]	Light brown	170	54.80 (55.10)	4.65 (4.75)	15.50 (15.52)	9.21 (9.33)	--	5.30 (5.06)

without passing air through the system exhibited magnetic moment much lower than that expected for six or four coordinated cobalt(II), which indicate partial oxidation of Co(II) to Co(III).

All the complexes are coloured crystalline substances. They are non-hygroscopic and are quite stable in air. The complexes are soluble in methanol, aceto-nitrile, chloroform, dimethylsulphoxide and nitrobenzene. They can be recrystallized from their hot methanol solutions. The analytical data of the complexes are presented in Table 8.1. The data reveal that the complexes have the general empirical formula $[Co(DH)_2(BPBI)X]$, where X = Cl, Br, I or SCN. These complexes were found to be diamagnetic suggesting that they are low-spin cobalt(III) octahedral complexes. The molar conductance values suggest that all the complexes are non-electrolytes in nitrobenzene (Table 8.2).

8.3.1 Electronic Spectra

The electronic spectral bands along with their probable assignments are given in Table 8.2. The complexes show bands around 41000 cm^{-1} (Fig.8.1 to 8.4) due to intra-ligand $\pi - \pi^*$ transition in the coordinated dimethyl-
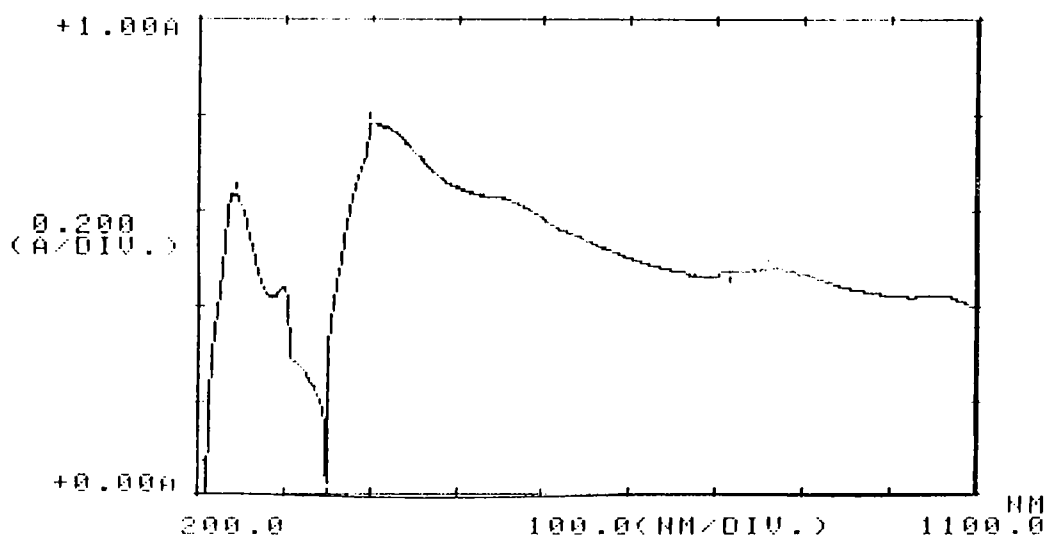
Fig.8.1: Electronic Spectrum of [Co(DH)$_2$(BPBI)Cl]
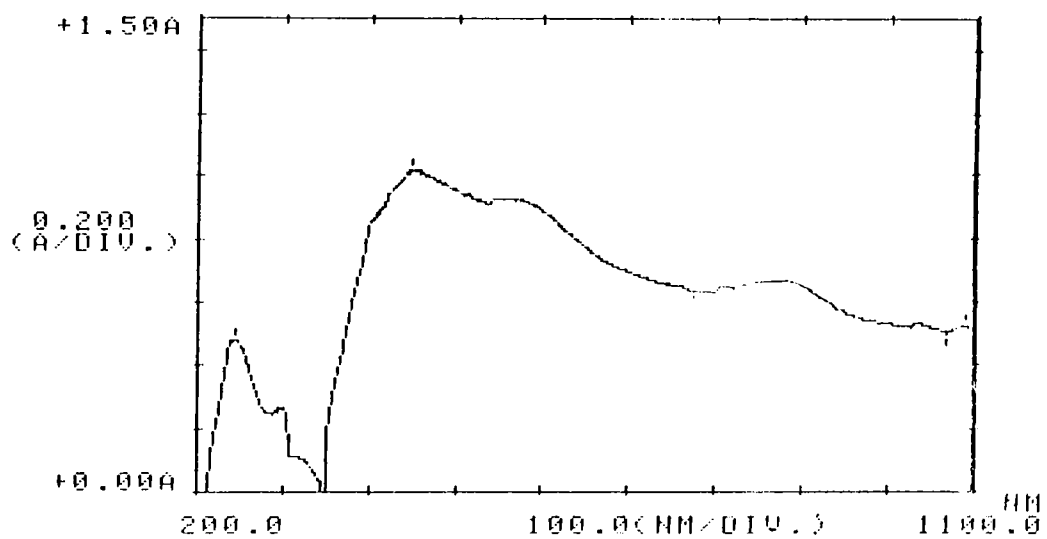
Fig.8.2: Electronic Spectrum of [Co(DH)$_2$(BPBI)Br]
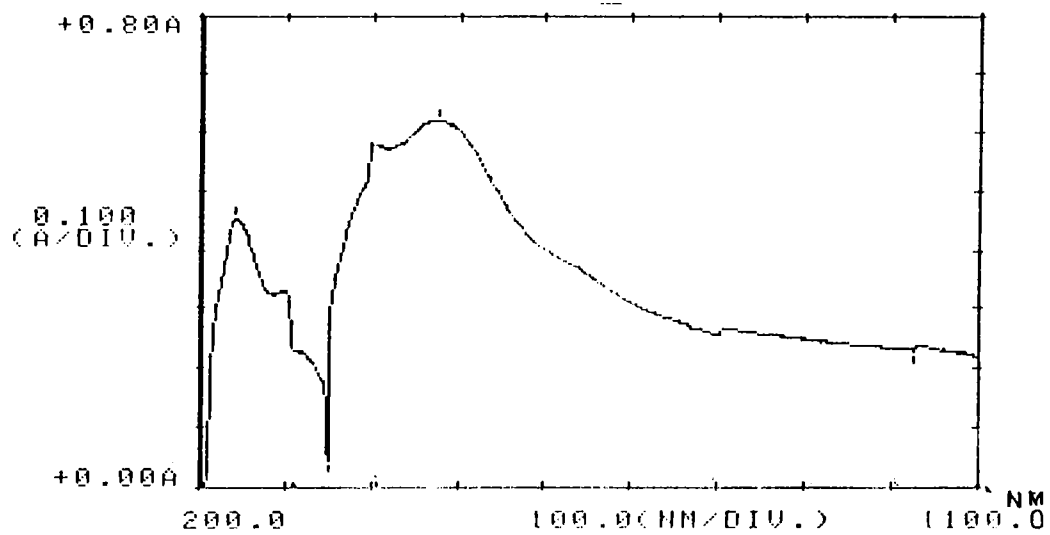
Fig.8.3: Electronic Spectrum of [Co(DH)$_2$(BPBI)I]
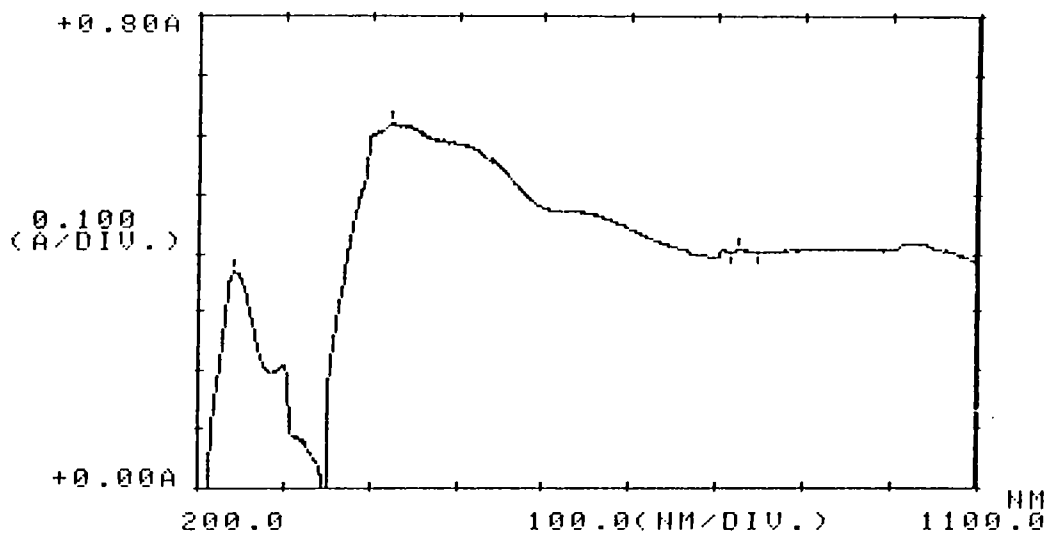
Fig.8.4: Electronic Spectrum of [Co(DH)$_2$(BPBI)SCN]

Table 8.2: Molar conductance and electronic spectral data

Compound	Molar conduct-ance $(ohm^{-1}cm^{2}mol^{-1})$	Abs.Max. (cm^{-1})	Tentative Assignments
$[Co(DH)_2(BPBI)Cl]$	1.1	40980	Intra-ligand transition
		33330	Charge transfer transition
		25130	"
		18000	$^1A_{1g} \longrightarrow {}^1T_{1g}$
$[Co(DH)_2(BPBI)Br]$	2.2	41150	Intra-ligand transition
		33330	Charge transfer transition
		22200	"
		18000	$^1A_{1g} \longrightarrow {}^1T_{1g}$
$[Co(DH)_2(BPBI)I]$	2.2	41300	Intra-ligand transition
		33000	Charge transfer transition
		21000	"
		16700	$^1A_{1g} \longrightarrow {}^1T_{1g}$
$[Co(DH)_2(BPBI)SCN]$	2.8	41300	Intra-ligand transition
		33000	Charge transfer transition
		23600	"
		18520	$^1A_{1g} \longrightarrow {}^1T_{1g}$

glyoxime.[144] Bands occuring at 33300 cm^{-1} and 21000-25000 cm^{-1} are assigned to the charge transfer transitions dπ (Co) $\rightarrow \pi$*(DH)(MLCT) and BPBI $\rightarrow$ Co(LMCT) transitions respectively.[144] Because of the high intensity of the above mentioned bands the d-d transitions are almost masked. However, a shoulder is seen around 18000 cm^{-1}. Assuming a distorted octahedral structure, this can be assigned to the $^1A_{1g} \longrightarrow ^1T_{1g}$ transition. A similar assignment has been made for a band at 18000 cm^{-1} in the case of trans-[Co(DH)$_2$XIm] complexes, where Im is imidazoles.[115,145,146]

8.3.2 Infrared Spectra

The infrared spectral data of the ligand and complexes are given in Table 8.3. The infrared spectra of the complexes show most of the bands due to the BPBI and DH$_2$ ligands. The ν(C=N) of DH$_2$ is seen at 1565 cm^{-1} in the spectra of the complexes. This band is known to occur around 1620 cm^{-1} in the case of non-coordinated DH$_2$. The ν(C=N) band at 1500 cm^{-1} of the free BPBI is observed in the present complexes at 1475 cm^{-1} suggesting the coordination of the N-3 atom of BPBI ligand to the metal.[146] The N-O stretching frequency of the DH$_2$ ligand occurs as a very

Table 8.3: Infrared absorption frequencies (cm^{-1})

BPBI	I	II	III	IV	Tentative Assignments of more relevant bands
(1)	(2)	(3)	(4)	(5)	(6)
3040w	3060w	3060w	3050w	3060w	
2930w	2940w	2940w	2920w	2920w	
2860w	2860w	2860w	2860w	2860w	
--	--	--	--	2100s	γ(C-N)(thio-cyanate
--	1780m	1785m	1780m	1785m	γ(O-H-O)(bridging group)
1610w	1615w	1620m	1625m	1605m	
--	1560s	1565s	1560s	1545m	γ(C=N)(dimethyl glyoxime)
1500m	1475s	1470s	1475s	1465s	γ(C=N)(benzimidazole)
1400s	1425s	1425s	1430m	1415m	
1380s	1360s	1370m	1385m	1385m	
1340w	1340w	1325w	1330w	1330w	
1290m	1290m	1275m	1275m	1290m	
1260m	1255m	1250m	1255m	1250m	
--	1230s	1235s	1230s	1230s	γ(N-O)(dimethyl-glyoxime)
1190w	1205m	1195m	1170m	1170m	
1080m	1085s	1090s	1085s	1100s	

(Contd...)

(1)	(2)	(3)	(4)	(5)	(6)
1040m	1030m	1025m	1030m	1030m	
1010m	980m	980m	980w	980w	
930m	930w	930w	930w	925w	
850m	845w	835w	850w	850w	
800s	800w	815w	815w	825w	
780m	760s	760s	755m	755s	
740s	740s	740s	735m	740s	
720s	725m	690s	700s	700s	
710s	690s	695s	685s	685s	
650w	670w	625w	625w	635w	
580w	580w	565w	550w	590w	
--	510s	510s	510s	510s	ν(Co-N)(dimethyl-glyoxime)
420s	420s	425s	420s	420s	
--	--	--	--	380m	ν(Co-S)
--	350m	340m	340m	350m	ν(Co-N)(benzi-midazole)
--	270m	--	--	--	ν(Co-Cl)
--	--	240m	--	--	ν(Co-Br)
210m	210m	210m	210m	210m	

s = strong ;   m = medium ;   w = weak

I = [Co(DH)$_2$(BPBI)Cl] ; II = [Co(DH)$_2$(BPBI)Br]

III = [Co(DH)$_2$(BPBI)I] ; IV = [Co(DH)$_2$(BPBI)SCN]

strong band around 1235 cm^{-1} in the spectra of complexes.[147] There is an intense and sharp band at 2100 cm^{-1} in the case of the thiocyanato complex which might be due to the ν(C-N) of the thiocyanate group,[111] as this band is absent in the other complexes. Moreover, the intensity and sharpness of this band suggests Co-SCN bonding. Such a band is seen in the thiocyanato complexes where the bonding of -NCS group to the metal is through the sulphur atom.[148,149] This indicates a soft acid nature for cobalt(III). Similar observations have been made by earlier workers.[139] A weak band due to ν(C-S) is expected in the region 720-690 cm^{-1} for the S-bonded thiocyanato complexes,[111] however, this band could not be identified in the present case, as it is obscured by other bands in this region. Furthermore, all the complexes show a broad band due to the deformation mode of the O-H...O bridging group around 1780 cm^{-1} and this also suggests a trans configuration for the complexes.[150,151]

All the complexes show a strong band at ~510 cm^{-1} and a medium band at ~345 cm^{-1} which can be assigned to ν(Co-N) of DH$_2$ and ν(Co-N) of BPBI respectively. A band at 270 cm^{-1} is seen only for the chloro complex, so it might be due to the Co-Cl stretching vibration. The intense band at 240 cm^{-1} observed for the bromo complex can be assigned

X = Cl, Br, I or SCN

Y =
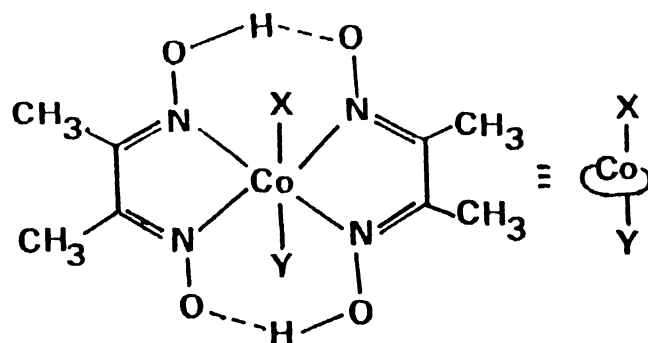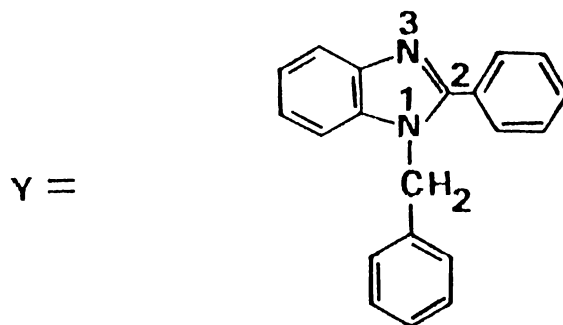

Fig.8.5: Schematic structure of trans-[Co(DH)$_2$(BPBI)X]

to the Co-Br stretching frequency. In the spectra of the thiocyanato complex, there is a band at 380 cm^{-1} which can be attributed to γ(Co-S).[117] Based on these results, the following structure (Fig.8.5) can be assigned to the complexes.

8.3.3 ^{1}H NMR Spectra

The ^{1}H NMR spectra of the complexes in CDCl$_3$ were found to be in complete agreement with the above proposed structure (Table 8.4). The complexes show the signal due to O-H...O protons at δ 8.8-8.5 ppm. Signals due to CH$_3$ group of DH$_2$ appear as very sharp singlet at δ 2.30-2.35-ppm. This indicates the equivalence of the four methyl groups in the complexes and hence a trans structure. Signals due to CH$_2$ protons of BPBI appear at δ 5.40-5.65 ppm and those due to aromatic protons as a multiplet which is centered around δ 7.50 ppm. The integrated area for each signal is found to be in agreement with the number of protons responsible for the signal.

8.3.4 Cyclic Voltammogram

The cyclic voltammetric behaviour of [Co(DH)$_2$(BPBI)Cl] in acetonitrile using LiClO$_4$ as supporting electrolyte

Table 8.4: Proton NMR data for ligands and complexes in $CDCl_3$*

Compound	CH_3 protons DH_2	CH_2 protons (BPBI)	Aromatic ring protons (BPBI) centered at	O-H-O protons
DH_2	2.30	--	--	--
BPBI	--	5.40	7.4	--
[Co(DH)$_2$(BPBI)Cl]	2.30	5.65	7.6	8.80
[Co(DH)$_2$(BPBI)Br]	2.35	5.65	7.6	8.85
[Co(DH)$_2$(BPBI)I]	2.35	5.60	7.5	8.85
[Co(DH)$_2$(BPBI)SCN]	2.35	5.55	7.5	8.80

* The chemical shifts are expressed in ppm. TMS was used as an internal standard.
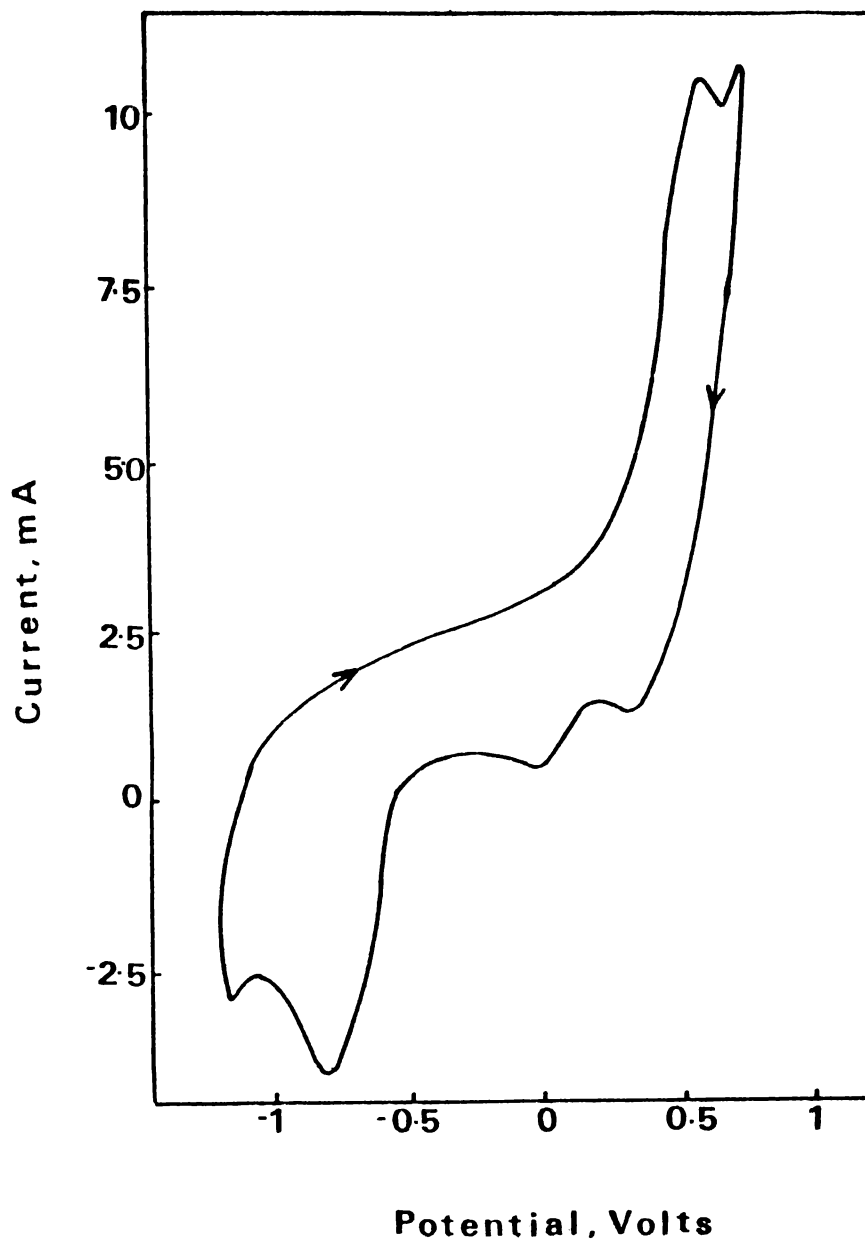
Fig.8.6: Cyclic voltammogram of trans-[Co(DH)$_2$(BPBI)Cl]

was studied. The potential was cycled from -1.2 V to 0.9 V vs. saturated calomel electrode (SCE). Fig.8.6 shows the cyclic voltammogram of the complex. The complex gives one anodic peak and three cathodic peaks. The anodic peak at 0.57 V is due to the oxidation of Co(III) to Co(IV) and the cathodic peaks at 0.46 V, 0.1 V and -0.72 V are due to the reduction of Co(IV) $\longrightarrow$ Co(III), Co(III) $\longrightarrow$ Co(II) and Co(II) $\longrightarrow$ Co(I) respectively.[152] The peak current dependence of the cathodic potential at 0.46 V vs. the square root of scan rate give a straight line showing that the reduction of Co(IV) $\longrightarrow$ Co(III) is reversible. All these observations clearly indicate the existence of cobalt in the +3 oxidation state.

SECTION B: THERMAL DECOMPOSITION KINETICS

8.4 INTRODUCTION

A literature survey revealed that TG studies of cobaloxime complexes have been done only in a few cases[153] and thermal decomposition kinetic studies have not yet been reported on any of these complexes. Thermal decomposition kinetics of the cobaloxime complexes described in the Section A of this chapter have been studied and the results of these studies are presented in this section.

The thermal decomposition of solids is a very complicated process, involving the decomposition of one chemical compound and the formation of others, the destruction of initial crystal lattice, the formation of crystallization centres and their growth, the adsorption and desorption of gaseous products, the diffusion of gases, heat transfer and many other elemental processes. The overall process is influenced by many procedural variables such as heating rate, the heat conductivities of furnace atmosphere, the sample and the sample holder, the static or dynamic character of the atmosphere, the physical state of the sample, sample weight, compactness, particle size etc. Owing to the complexity of thermal decomposition reactions, there is no chance of describing whole process theoretically at once. Therefore, successive approaches are needed for understanding these processes. Application of formal kinetics of homogeneous reactions may be considered as a first approach. In fact, all the methods for deriving the kinetic parameters, n, E_a, ΔS and A from TG curves recorded under dynamic temperature conditions are based on the relation taken from the formal kinetics of homogeneous reactions. In the present investigation Coats Redfern method[154] has been used for the calculation of the parameters, as it is simple and gives reliable results.

8.5 EXPERIMENTAL

Details about the instruments used are given in chapter 2.

8.5.1 Treatment of Data

<u>Thermogravimetry</u>

The TG and DTG curves obtained were used as such. From the TG and DTG curves, the following information was obtained.

1. Temperature ranges of stability

2. Decomposition peak temperature

3. Decomposition temperature ranges and

4. Probable composition of the expelled groups.

For the evaluation of kinetic parameters, the Coats-Redfern equation was used in the form,

$$\log g(\infty)/T^2 \quad = \quad \log (AR/\emptyset E) - E/2.303 \; RT$$

(Details about the equation and the evaluation procedures are given in the Appendix of this chapter. In the present study, the evaluation of the parameters was based on a computer program which was developed for use on a Busybee PC, PC/XT computer (HCL Ltd.).

Differential Thermal Analysis

The instrumental DTA curves were used as such. From these curves the following information were obtained. (1) Endothermic and exothermic peak temperature. (2) Peak base widths, ie., phase change or decomposition temperature ranges. These values have also been tabulated in every case along with the corresponding TG data.

8.6 RESULTS AND DISCUSSION

8.6.1 Thermal Behaviour

The TG/DTG/DTA curves for all the complexes are shown in Fig.8.7. Thermoanalytical data for the complexes are presented in Table 8.5. The percentage mass loss and the probable compositions of the expelled groups are also given in this table. All the complexes have a fairly wide stability range and have almost the same pattern of thermal decomposition. The DTG curves show three peaks for all the complexes. All the DTG peaks have their parallel DTA peaks. The DTA peak corresponding to the first stage is a weak endothermic peak followed by an exothermic peak. A similar behaviour in nitrogen has been reported for the first stage thermal decomposition of organo(aquo)cobaloxime and organo(pyridine)cobaloxime complexes.[153] The endo-
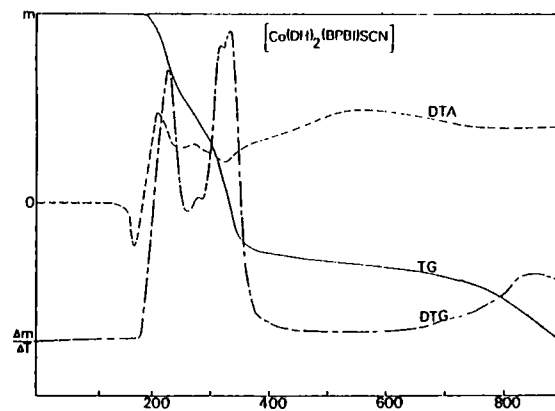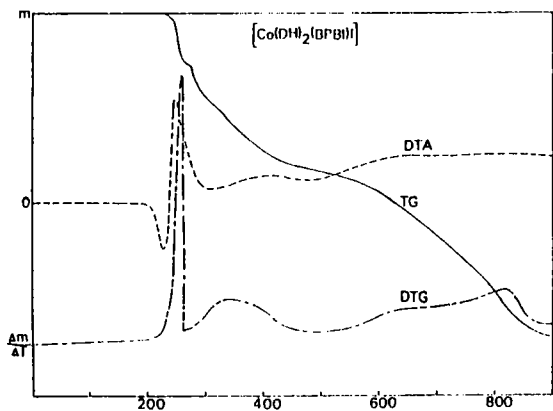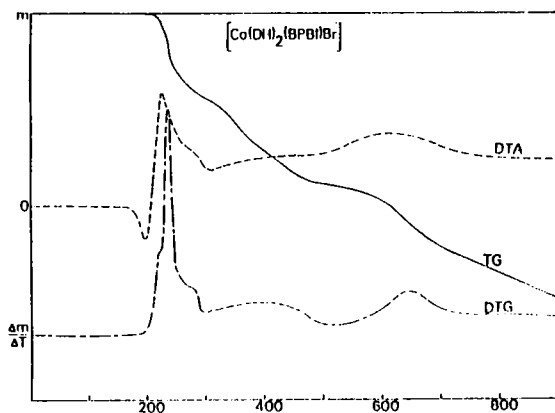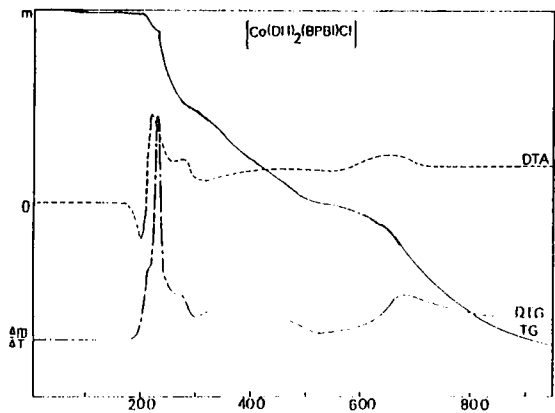
Fig.8.7: TG/DTG and DTA curves of complexes

Table 8.5: Thermal decomposition data

Compound	Peak temperature in DTA (°C)	Temperature range in DTA(°C)	Peak temperature in DTG (°C)	Temperature range in DTG(°C)	Stage of decomposition	Loss (%) from TG (Calc.)	Probable composition of expelled group
$[Co(DH)_2(BPBI)Cl]$	215 exo(s)	190–220	220(s)	190–230	I	5.94 (5.82)	Cl
	260 exo(m)	230–520	255(m)	230–520	II	43.56 (46.66)	BPBI
	640 exo(m)	520–890	675(m)	550–890	III	36.44 (37.76)	DMG core
$[Co(DH)_2(BPBI)Br]$	225 exo(s)	190–240	230(s)	190–240	I	11.22 (12.24)	Br
	265 exo(m)	240–480	265(m)	240–480	II	32.74 (43.48)	BPBI
	630 exo(m)	480–900	650(m)	480–900	III	30.84 (35.25)	DMG core
$[Co(DH)_2(BPBI)I]$	240 exo(s)	210–260	250(s)	210–260	I	13.96 (18.10)	I
	380 exo(m)	260–450	340(m)	260–460	II	27.36 (40.56)	0.7 BPBI
	660 exo(m)	530–900	820 (m)	530–900	III	43.30 (32.88)	0.3 BPBI and DMG core
$[Co(DH)_2(BPBI)SCN]$	215 exo(s)	170–230	225(s)	170–230	I	15.66 (9.34)	SCN
	270 exo(m)	230–380	333(m)	230–380	II	46.32 (45.00)	BPBI
	540 exo(m)	520–900	850(m)	520–900	III	22.64 (36.79)	DMG core

thermic peak may be due to the melting of the complexes. Independent studies revealed that the complexes decompose just after melting.

The mass loss at the first stage of decomposition corresponds with the expulsion of halogen atom in the case of the halogeno complexes and SCN group in the case of the thiocyanato complex. The unexpected exothermic nature of the decomposition step may be due to the subsequent reactions involving the halogen or thiocyanate radical formed during this stage. The residue left after the first stage was isolated and analysed. The intermediate complexes were found to have an approximate composition of $[Co(DH)_2(BPBI)]$. The IR spectra of these complexes show the presence of DH and BPBI. Furthermore, magnetic susceptibility measurements were also carried out on these complexes. Their μ_{eff} values around 4.6 BM indicates that these intermediate complexes are 5-coordinate Co(II) complexes. In all the complexes the first DTG peak is followed by a medium DTG peak. The mass loss at this stage corresponds to the removal of BPBI molecule, except in the case of the iodo complex. For the iodo complex, the mass loss corresponds to the expulsion of 0.7 BPBI only. The temperature range for the last stage of decomposition is

almost same for all the complexes. This might be due to
the thermal break down of the common core complex,
$[Co(DH)_2]$. For the iodo complex 0.3 BPBI is also removed
at this stage. In all the cases the residue after the
final stage of decomposition was found to be CoO.

8.6.2 Decomposition Kinetics

The kinetic parameters, n, E_a, ΔS and A, calcul-
ated using the Coats-Redfern equation are presented in
Table 8.6. In the present study, the parameters, E_a and
ΔS, have been evaluated for similar compounds using the
same equation for nearly same experimental conditions (same
heating rate, furnace atmosphere, sample weight etc.) and
hence can be used for the comparison of the decomposition
processes.[155] But, the order 'n' does not provide any
meaningful information about the mechanism of complexes.[155]

The activation energies for the first stage of the
decomposition are seen to decrease in the following order:
the thiocyanato complex > the chloro complex > the bromo
complex > the iodo complex. This order is almost similar
to that of the Co-X bond strength, which indicate that in
all the cases the dissociation of the Co-X bond takes place
during this stage. The stoichiometry of the intermediate

Table 8.6:   Kinetic data

Compound	Stage of decompo-sition	Order (n)	E_a (KJ mol^{-1})	ΔS (KJ mol^{-1}K^{-1})	A (s^{-1})
[Co(DH)$_2$(BPBI)Cl]	I	0.15	141	-189	1.216×10^3
	II	1.99	26	-123	3.948×10^6
	III	1.61	112	-192	1.755×10^3
[Co(DH)$_2$(BPBI)Br]	I	1.12	124	-81	6.139×10^8
	II	1.34	31	-255	6.300×10^{-1}
	III	1.26	47	-264	3.016×10^{-1}
[Co(DH)$_2$(BPBI)I]	I	1.81	63	-223	2.395×10^1
	II	1.66	63	-193	9.417×10^2
	III	1.03	71	-241	5.828×10^0
[Co(DH)$_2$(BPBI)SCN]	I	0.56	159	+35	7.321×10^{14}
	II	0.82	76	-167	2.223×10^4
	III	0.28	35	-287	2.226×10^{-2}

complex formed after the first stage of decomposition (vide Table 8.6) also indicates this aspect.

Eventhough the intermediate complexes after the first stage of decomposition have nearly the same composition, $[Co(DH)_2(BPBI)]$, the different kinetic parameters for the second stage of decomposition of the chloro, bromo, iodo and thiocyanato complexes indicate that the decomposition mechanisms are different for these complexes. This might be due to the subsequent reactions of the gaseous products and also due to slight differences in stoichiometries of the intermediate complexes involved in these decomposition steps. Such slight differences in composition and structure are known to alter the rate in many catalytic reactions.[156]

The E_a values for the second stage of decomposition are found to be smaller than those for the first stage in the case of all the complexes, indicating an increased rate of decomposition during the second stage. This might be due to the catalytic activity of the intermediate five coordinate complex, which, due to its vacant coordination site, can adsorb gaseous products and thus facilitate easy decomposition. The E_a values for the third stage also

suggest increased rate of reaction, especially for the thiocynato complex. Here also the increased rate may be due to the catalytically active four coordinate $[Co(DH)_2]$ complex formed after the second stage.

Negative ΔS values for the first stage of decomposition suggest that the activated complexes have a more ordered structure than the reactions which are in the liquid state just before the decomposition. The more ordered nature may be due to polarisation of bonds in the activated state, which might happen through charge transfer electronic transitions. The ΔS values for the second and third stages are found to be more negative, except for the chloro complex, than those for the first stage, which might be due to the chemisorption of the gaseous decomposition products by the intermediate complexes with vacant coordination sites involved in these respective steps. The five coordinate complex, $[Co(DH)_2(BPBI)]$, formed after the first stage of decomposition and the four coordinate complex, $[Co(DH)_2]$, formed after the second stage have vacant coordination sites. In fact, these type of complexes are known to act as catalysts in many oxidation reactions.[138]

SUMMARY

The thesis deals with the studies on some metal
complexes of interesting Schiff bases and also on some
mixed ligand complexes. The Schiff base ligands used in
the present study are those formed by the condensation of
2-aminocyclopent-1-ene-1-dithiocarboxylic acid (ACDA) with
benzaldehyde, salicylaldehyde, quinoxaline-2-carboxalde-
hyde, or with polymer bound benzaldehyde. A polymer
Schiff base ligand derived from quinoxaline-2-carboxal-
dehyde and crosslinked polystyrene functionalized with
amino group PSBQC, is also used in the present study. The
ligands involved in the synthesis of the mixed ligand
complexes are dimethylglyoxime, 1-benzyl-2-phenyl-
benzimidazole (BPBI), 2-alkyl derivatives of ACDA and
N,N'-bis(salicylaldehyde)ethylenediimine (Salen).

The thesis is divided into eight chapters.
Chapter 1 is a brief discussion on the stereochemistry
and electronic properties of iron(III), cobalt(II),
cobalt(III), nickel(II) and copper(II) metal ions. Scope
of the present investigation is also given in this
chapter. The details of the preparation and purification
of the ligands, reagents etc., employed in the study are

given in chapter 2. Furthermore, the various character-
ization techniques employed are also described in this
chapter.

Chapter 3 deals with synthesis and characteriza-
tion of Fe(III), Co(II), Ni(II) and Cu(II) complexes of a
new Schiff base ligand synthesized by condensing ACDA with
benzaldehyde (ACB) and also deals with Cu(II) and Ni(II) complexes
of another Schiff base ligand synthesized by condensing
ACDA with salicylaldehyde (ACS). The analytical data show
that the complexes have the general empirical formulae
[ML Cl(H_2O)], when L = ACB and M = Co(II), Ni(II) or
Cu(II) and [ML'X(H_2O)] when L' = ACS; X = Cl or Br and M =
Cu(II) or Ni(II). The iron complex has the empirical
formulae [Fe(ACB)Cl(OH)(H_2O)$_2$]. All the complexes are
coloured crystalline substances. The complexes of ACB are
moderately soluble in nitrobenzene, dimethylformamide,
dimethylsulphoxide, acetonitrile and are slightly soluble
in chloroform. The complexes of ACS are insoluble in most
of the solvents but slightly soluble in DMSO, DMF and
nitrobenzene. All these complexes behave as non-
electrolytes in nitrobenzene. Infrared spectra of the
complexes suggest that both the ACS and ACB are acting as
bidentate ligands coordinating through one of the sulphur

atoms and through the azomethine nitrogen atom. Magnetic moment value (3.6 BM) for the iron(III) complex indicates spin crossover behaviour for the complex. Square planar structures have been assigned to Cu(II) and Ni(II) complexes and tetrahedral structure to the Co(II) complex. The EPR spectra of the copper(II) complexes have been studied and g values suggest a square planar environment with rhombic distortion around Cu(II) ion.

Chapter 4 is a discussion on the synthesis and characterization of Fe(III), Co(II), Ni(II) and Cu(II) complexes of the Schiff base derived from ACDA and quinoxaline-2-carboxaldehyde (ACQ). The analytical data show that the complexes have the general formula [M(ACQ)Cl] for the Co(II), Ni(II) and Cu(II) complexes and [Fe(ACQ)Cl(OH)(H$_2$O)] for the Fe(III) complex. Octahedral and square planar structures have been assigned for the Fe(III) and Ni(II), Cu(II) complexes respectively, while the Co(II) complex has a tetrahedral structure. The ACQ acts as a tridentate ligand coordinating through one of the sulphur atoms, the azomethine nitrogen atom and also through nitrogen atom of the quinoxaline ring. EPR spectra of the Cu(II) complex shows three g values expected for a square planar complex with elongated or compressed rhombic symmetry.

Chapter 5 deals with synthesis and characterization of polymer bound Fe(III), Co(II), Ni(II) and Cu(II) complexes of a Schiff base ligand (PACB) derived from polymer bound benzaldehyde and ACDA. From the analytical data, the empirical formula arrived for the iron(III) complex is [Fe L $Cl_2(H_2O)_2$] (where L = PACB part containing one Schiff base unit) and that for Co(II), Ni(II) and Cu(II) complexes is [ML Cl H_2O]. Infrared spectral studies show that the ligand bonds through one of the sulphur atoms. EPR studies of Cu(II) complex suggest a square planar structure with a compressed rhombic symmetry. Magnetic studies indicate a spin crossover behaviour for the Fe(III) complex. Based on these studies octahedral and tetrahedral structures have been assigned for Fe(III) and Co(II) complexes respectively and square planar for Ni(II) and Cu(II) complexes. Thermal behaviour of these complexes was investigated by the technique of non-isothermal thermogravimetry (TG), derivative thermo-gravimetry (DTG) and by differential scanning calorimetry (DSC). The main decomposition peaks and probable composition of expelled groups and residue were noted from TG.

Chapter 6 deals with synthesis and characterization of Fe(III), Co(II), Ni(II) and Cu(II) complexes of

another Schiff base ligand (PSBQC) derived from quino-
xaline-2-carboxaldehyde and polystyrene functionalized
with amino group. The empirical formula for the iron(III)
complex is [Fe L(OAc)$_3$(H$_2$O)$_2$] and that for Co(II), Ni(II)
and Cu(II) complexes is [ML(OAc)$_2$H$_2$O] where L = PSBQC
containing one Schiff base unit. IR spectra indicate that
in all the complexes acetate group acts as a unidentate
ligand. Further the spectra indicate that the bonding of
the Schiff base unit to the metal in all the complexes
is through the azomethine nitrogen atom and not through the nitrogen
atom in the quinoxaline ring. Based on the electronic spectra
and magnetic behaviour, octahedral and tetrahedral
structures have been assigned for the Fe(III) and Co(II)
complexes and square planar structures for the Ni(II) and
Cu(II) complexes.

Mixed ligand complexes of Fe(III) containing
N-N'-bis(salicylaldehyde)ethylenediimine (Salen) and ACDA or its
alkyl derivatives such as isopropyl and n-butyl were
synthesized and characterized and studies on these
complexes are presented in chapter 7. Analytical and
molar conductance values suggest that the complexes have
the empirical formulae [Fe(Salen)L] where L = ACDA;
i-PrACDA or n-BuACDA. Magnetic and spectral data suggest
an octahedral structure for the complexes.

Chapter 8 of the thesis deals with the studies of some mixed ligand complexes which are synthesized by reacting cobaloxime with a bulky ligand, 1-benzyl-2-phenylbenzimidazole. This chapter has two sections. Section A deals with the synthesis and characterization of the complexes. These complexes were prepared by reacting 1-benzyl-2-phenylbenzimidazole (BPBI) with CoX_2 and dimethylglyoxime (DH_2) in n-butanol in the presence of air. The complexes are of the type $trans-[Co(DH)_2(BPBI)X]$, where X = Cl, Br, I or SCN. These complexes were characterized by elemental analyses, conductivity measurements, spectral (electronic, IR and NMR), TG and cyclic voltammetric studies. The infrared spectra indicate bonding of the BPBI ligand through the N-3 atom in all the complexes. In $[Co(DH)_2(BPBI)SCN]$, the sulphur atom of the thiocyanate group is bonded to the metal. All the complexes are shown to possess a distorted octahedral structure. Cyclic voltammetric studies of the chloro complex shows three reductive waves and an oxidative wave confirming a +3 oxidation state for the cobalt atom.

Section B deals with thermal decomposition kinetic studies. The complexes were subjected to a systematic TG/DTG/DTA analysis. All the complexes decompose just

after melting, and the decomposition process consists
essentially of three stages. The final residue in all the
cases was found to be CoO. The mass loss data indicate
the formation of intermediate complexes with an approxi-
mate composition of $[Co(DH)_2(BPBI)]$ at the end of the
first stage of decomposition. The kinetic parameters were
calculated using the Coats-Redfern equation. The E_a
values for the first stage of the decomposition are seen
to decrease in the following order; the thiocyanato
complex > the chloro complex > the bromo complex > the iodo
complex. The E_a and ΔS values for the second and third
stages of decomposition indicate catalytic activity of the
intermediate complexes formed during these stages.

KINETIC PARAMETERS FROM NONISOTHERMAL THERMOGRAVIMETRY

The specific rate equation for the thermal decomposition of a single solid giving another solid and a volatile product:

$$A \text{ (solid)} \longrightarrow B \text{ (solid)} + C \text{ (gas)}$$
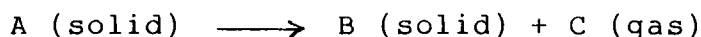
can be written in the form,

$$d\alpha/dt = kf(\alpha) \tag{A.1}$$

where α is the fraction decomposed at time t, $f(\alpha)$ is a function of α and can have various forms; k is the specific reaction rate. In the derivation of almost all the well known kinetic equations developed for evaluating kinetic parameters, simplified form of $f(\alpha)$; $f(\alpha) = (1-\alpha)^n$ is used. Eventhough, n is usually identified as the order of the reaction, it does not have much physical significance in solid state reactions, which are usually heterogeneous.[157-160]

For the decomposition reaction with a constant linear heating rate, $\emptyset$, (where $\emptyset = dT/dt$) equation (A.1) may be rewritten as,

$$d\alpha/dT \ = \ (k/\emptyset) \ f(\alpha) \ = \ (k/\emptyset)(1-\alpha)^n \qquad (A.2)$$

Substituting the Arrhenius equation, ie.,

$$k \ = \ A \ e^{-E_a/RT} \qquad (A.3)$$

into the equation (A.2), we get an equation, which is the fundamental equation employed in non-isothermal TG.

$$d\alpha/dT \ = \ (A/\emptyset) \ e^{-E_a/RT} \ (1-\alpha)^n \qquad (A.4)$$

where A is the pre-exponential factor and E_a is the energy of activation.

The methods for evaluating the kinetic parameters using the equation (A.4) can be broadly classified into three groups:[161] (1) differential methods; (2) approximation methods and (3) integral methods. Integral methods are considered to be most accurate and give quite reliable values.[162,163] Among them, Coats-Redfern method is the most reliable one and in the present investigation this method has been used for the evaluation of kinetic parameters. Therefore, only details about the Coats-Redfern method are included here.

The Coats-Redfern Method

This method employs the integrated form of the equation (A.4). Coats and Redfern used the equation (A.4) in the following form:

$$d\alpha/(1-\alpha)^n = (A/\emptyset)\ e^{-E_a/RT}\ dT \qquad (A.5)$$

The integration of the left hand side (LHS) of equation (A.5) with limits 0 to α is easy, but the integration of the right hand side (RHS) with limits 0 to T poses some difficulty, as it has no exact solution. The integral of LHS, denoted by the function $g(\alpha)$, can be written as,

$$g(\alpha) = [1-(1-\alpha)^{1-n}]/(1-n) \qquad (A.6)$$

when $n \neq 1$, and

$$g(\alpha) = -\ln(1-\alpha) \qquad (A.7)$$

when $n = 1$. Coats and Redfern evaluated the RHS of equation (A.5), ie., the temperature integral, with the aid of the Rainville function.[164] The final form of the equation derived by them was,

$$\log g(\alpha)/T^2 = (\log AR/\emptyset E_a)(1-2RT/E_a) - E_a/2.303\ RT \qquad (A.8)$$

The term $2RT/E_a$ is negligible in comparison with unity and can therefore be neglected. Therefore equation (A.8) can be written in the form,

$$\log g(\alpha)/T^2 = \log AR/\emptyset E_a - E_a/2.303\ RT \qquad (A.9)$$

The $g(\alpha)$ values can be calculated only if value of n is known. For determining the best value of n, the following procedure is adopted: first a value of n is selected and $g(\alpha)$ values are calculated. The best values of intercept (a) and slope (b) of the equation (A.9) for this value of n are found out by the method of least squares. Using these values of a and b, the $g(\infty)$ values are calculated employing the equation (A.9). Then, the sum of the squares of deviation of these values from the $g(\alpha)$ values, S, is calculated and the whole procedure is repeated for various values of n until S is a minimum. The value of n which gives the minimum value of S is taken as the best value.

A plot of $\log g(\alpha)/T^2$ vs. $1/T$ will be linear and the slope of this plot will give the value of $-E_a/2.303\ R$ from which activation energy value (E_a) can be calculated.

Knowing E_a, the value of pre-exponential factor (A) can be found out from the intercept.

The entropy of activation, ΔS is calculated using the relation, $A = (kT/h)e^{\Delta S/R}$, where k is the Boltzmann constant, h is the Plank's constant and R is the gas constant. The DTG peak temperature is usually taken as the value of temperature term T in the above equation.

REFERENCES

1. N.Kitajima, H.Fukui and Y.Moro-oka, J. Chem. Soc. Chem. Commun., 485 (1988).

2. M.Faraj and C.L.Hill, J. Chem. Soc. Chem. Commun., 1487 (1987).

3. M.M.Taqui Khan, Oxidn. Commun., 9, 15 (1986).

4. R.A.Sheldon and J.K.Kochi, "Metal Catalyzed Oxidation of Organic Compounds", Academic Press, New York (1981).

5. M.M.Taqui Khan and A.E.Martell, "Homogeneous Catalysis by Metal Complexes", Academic Press, New York (1974).

6. M.M.Taqui Khan, H.C.Bajaj, R.S.Shukla and S.A.Mirza, J. Mol. Catal., 45, 5 (1988).

7. J.E.Lyons, in R.Ugo (Ed.), "Aspects of Homogeneous Catalysis", Vol.3, Reidal, Dordrecht (1977).

8. J.C.Bailar, Catal. Rev. Sci. Eng., 10(1), 17 (1974).

144

9. R.H.Crubbs and L.C.Kroll, J. Am. Chem. Soc., **94**, 3062 (1971).

10. P.Hodge and D.C.Sherrington, "Polymer Supported Reactions in Organic Synthesis", Wiley, New York, Brisbane, Chichester, Toronton (1980).

11. E.M.Cernia and M.Graziani, J. Appl. Polym. Sci., **18**, 2725 (1974).

12. T.B.D.Wohrle, G.S.Ekloff and A.Andreev, J. Mol. Catal., **70**, 259 (1991).

13. W.L.K.Schwoyer, "Polyelectrolytes for Water and Waste Water Treatment", CRC Press Inc., Florida (1981).

14. A.I.Vogel, "A Text Book of Quantitative Inorg. Analysis", Fourth Edition, ELBS Longman, England (1978).

15. J.Aggett and R.A.Kichardson, Anal. Chim. Acta., **50**, 269 (1970).

16. D.Hall, H.J.Morgan and T.N.Waters, J. Chem. Soc. A, 677 (1966).

17. C.R.Clark, D.Hall and T.N.Waters, J. Chem. Soc. A, 223 (1968).

18. B.R.Karas and A.B.Ellis, J. Am. Chem. Soc., 102, 968 (1980).

19. H.Green, "Recent Uses of Liquid Ion Exchangers in Inorganic Analysis", Talanta, 11, 1561.

20. U.Landau, E.Yeager and D.Kortan, "Electrochemistry in Industry", (Eds.), Plenum Press, New York (1982).

21. F.Beck, J. Appl. Electro. Chem., 7, 239 (1977).

22. H.G.Tanner (to E.I), Du Pont de Numours & Co., US Patent 2, 163, 768 June 27 (1939).

23. Ciba Ltd., British Patent 685, 582 (Jan. 7, 21953).

24. P.S.Harikumar and V.N.Sivasankara Pillai, J. Mater. Sci. Lett.,8(18), 969 (1989).

25. E.M.Engler, Chemtech., 542 (1987).

26. Y.Yamada, J. Appl. Phys., **26**, L865 (1987).

27. P.M.May and R.A.Bulman, Prog. Med. Chem. **20**, 225 (1983).

28. M.B.Chenoweth, Pharmacol. Rev., **8**, 57 (1956).

29. D.D.Perrin, "Topics in Current Chemistry", Springer Verlag, New York, 64 (1976).

30. J.P.Collman, Acc. Chem. Res., **10**, 265 (1977).

31. C.K.Chang, T.G.Traylor, J. Am. Chem. Soc., **95**, 5819 (1973).

32. J.P.Collman, K.S.Suslick, Pure Appl. Chem., **50**, 951 (1978).

33. R.D.Jones, D.A.Summerville and F.Basolo, Chem. Rev., 79 (1979).

34. C.McLendon and A.E.Martell, Coord. Chem. Rev., **79**, 1 (1976).

35. W.M.Coleman and L.T.Taylor, Coord. Chem. Rev., **32**, 1 (1980).

36. E.C.Niederhoffer, J.H.Timmons and A.E.Martell, Chem. Rev., **84**, 137 (1984).

37. F.A.Cotton and C.Wilkinson, "Advanced Inorganic Chemistry", Fifth Edition, John Wiley & Sons, New York (1988).

38. J.S.Griffith, J. Inorg. Nucl. Chem., 2, 1 (1956).

39. J.S.Griffith, Discuss. Faraday. Soc., 26, 81 (1958).

40. R.L.Martin and A.H.White, Inorg. Chem., 6, 712 (1967).

41. B.N.Figgis, M.Gerloch and R.Mason, Proc. Roy. Soc., Ser.A. 309, 91 (1969).

42. B.N.Figgis, Trans. Faraday Soc., 57, 199 (1961).

43. P.Ganguli, V.R.Marathi and S.Mitra, Inorg. Chem., 14, 970 (1975).

44. D.N.Hendrickson, Inorg. Chem., 25, 160 (1986).

45. S.A.Cotton, Coord. Chem. Rev., 8 (1972).

46. S.Holt and R.Dingle, Acta. Chem. Scand., 22, 1091 (1968).

47. A.H.Ewald, R.L.Martin, E.Sinn and A.H.White, Inorg. Chem., 8, 1837 (1969).

48. N.N.Greenwood and A.Earnshaw, "Chemistry of the Elements", Pregamon Press (1984).

49. D.F.Shriver, P.W.Atkins and C.H.Langford, "Inorganic Chemistry", Oxford University Press (1990).

50. I.Bertini, M.Ciampolini and D.Catteschi, Inorg. Chem., 12, 693 (1973).

51. M.Divaira and P.L.Orioli, Inorg. Chem., 6, 955 (1967).

52. J.S.Wood, J. Chem. Soc., A. 1582 (1969).

53. M.Ciampolini and I.Bertini, J. Chem. Soc., A. 2241 (1968).

54. M.Gerloch, J.Kohl, J.Lewis and W.Urland, J. Chem. Soc., A. 3283 (1970).

55. M.Divaira and P.L.Orioli, Acta Crystallogr. Sect., B. 24, 595 (1968).

56. I.Bertini, M.Ciampolini, P.Dapporto and D.Gatteschi, Inorg. Chem., 11, 2254 (1972).

57. M.J.Norgett and L.M.Venanzi, Inorg. Chim. Acta., 2, 107 (1968).

58. M.Gerloch, J.Kohl, J.Lewis and W.Urland, J. Chem. Soc., A. 3269 (1970).

59. C.Furlani, A.Flamini, A.Sgamellotti and C.Bellitto, J. Chem. Soc. Dalton. Trans., 2404 (1973).

60. R.H.Sands, Phys. Rev., 99, 1222 (1955).

61. F.K.Kneubuhl, J. Chem. Phys., 33, 1074 (1960).

62. R.Neiman and D.Kivelson, J. Chem. Phys., 35, 156 (1961).

63. T.Vanngard and R.Aasa, in W.Low (Ed.), Paramagnetic Resonance, Vol.2, Academic Press, 509 (1963).

64. F.K.Kneubuhl and B.Natterer, Helv. Phys. Acta., 34, 710 (1961).

65. V.S.Korolkov and A.K.Potapovich, Optics and Spectroscopy, 16, 251 (1964).

66. T.S.Johnston and H.G.Hecht, J. Mol. Spec., 17, 98 (1965).

67. J.W.Searl, R.C.Smith and S.J.Wyard, Proc. Phys. Soc., 78, 1174 (1964).

68. J.E.Geusic and L.Carlton-Brown, Phys. Rev., 112, 64 (1958).

69. D.S.Schonland, Proc. Phys. Soc., 73, 788 (1959).

70. D.E.Billing and B.J.Hathaway, J. Chem. Phys., 50, 2258 (1969).

71. H.Abe and K.Ono, J. Phys. Soc. Japan, 11, 947 (1956).

72. D.E.Billing and B.J.Hathaway, J. Chem. Phys., 50, 1476 (1969).

73. I.M.Procter, B.J.Hathaway and P.Nicholls, J. Chem. Soc., A. 1678 (1968).

74. R.C.Slade, A.A.G.Tomlinson and B.J.Hathaway and D.E.Billing, J. Chem. Soc., A. 81 (1968).

75. M.C.M.O'Brain, Proc. Roy. Soc., A. 281, 323 (1969).

76. B.J.Hathaway, M.J.Bew, D.E.Billing, R.J.Dudley and P.Nicholls, J. Chem. Soc., A. 2312 (1969).

77. B.J.Hathaway, M.J.Bew and D.E.Billing, J. Chem. Soc., A. 1090 (1969).

78. J.C.Eisenstein, J. Chem. Phys., 28, 323 (1958).

79. H.G.Von, Schnering, Z.Anorg. Allgem. Chem., 353, 13 (1967).

80. B.Morosin, Acta. Cryst., B. 24, 19 (1969).

81. G.A.Barclay, B.F.Hoskins and C.H.L.Kennard, J. Chem. Soc., 5691 (1963).

82. C.K.Proust, R.A.Armstrong, J.R.Carruthers, J.G.Forrest P.Murray Rust and F.J.C.Rossotti, J. Chem. Soc., A. 2791 (1968).

83. C.L.Leese and H.N.Rydon, J. Chem. Soc., 303 (1955).

84. J.M.J.Frechet and K.E.Haque, Macromolecules., 8, 130 (1975).

85. K.S.Devaki, V.N.R.Pillai, Eur. Polym. J., 24, 209 (1988).

86. A.Weissberger, P.S.Proskaner, J.A.Riddich and E.E.Troops, "Organic Solvents", Interscience, New York, Vol.7 (1956).

87. T.Takeshima, M.Yokoyama, T.Imamoto, M.Akano and M.Asaba, J. Org. Chem., 34, 730 (1969).

88. B.Bordas, P.Sobar, G.Matolcsy and P.Bachesi, J. Org. Chem., 37, 1727 (1972).

89. D.J.Aymes, M.R.Paris, J. Chem. Educ., 66, 854 (1989).

90. N.V.Subha Rao and C.V.Ratnam, Proc. Indian Acad. Sci., 43A, 174 (1956).

91. B.N.Figgis and R.S.Nyholm, J. Chem. Soc., 4190 (1958).

92. B.N.Figgis and J.Lewis, "Modern Coordination Chemistry", J. Lewis and R.G.Wilkins, (Eds.), Interscience, New York (1960).

93. P.W.Selwood, "Magnetochemistry", Interscience, New York (1958).

94. A.Earnshaw, "Introduction to Magnetochemistry", Academic Press, New York (1968).

95. B.N.Figgis and J.Lewis, "Progress in Inorganic Chemistry", F.A.Cotton, (Ed.), Interscience, New York, Vol.4 (1964).

96. L.N.Venanzi, G.Dyer and J.G.Hartley, J. Chem. Soc., 1293 (1965).

97. D.Coucouvanis, Prog. Inorg. Chem., 11, 234 (1970).

98. R.P.Burns, F.P.McCullough and C.A.McAuliffer, "Advances in Inorganic Chemistry and Radiochemistry", Vol.23, 211 (1980).

99. E.Kokot and G.A.Ryder, Aust. J. Chem. 24, 649 (1971).

100. M.Goodgame and F.A.Cotton, J. Am. Chem. Soc., 84, 1543 (1962).

101. R.S.Drago, "Physical Methods in Chemistry", Saunders, Philadelphia (1969).

102. S.I.Shupack, E.Billing, R.J.M.Clarle, R.Williams and H.B.Gray, J. Am. Chem. Soc., 86, 4594 (1964).

103. L.Sacconi and M.Giampolini, J. Chem. Soc., A. 273 (1974).

104. J.R.Ferraro and W.R.Wacker, Inorg. Chem., 4, 1382 (1965).

105. T.Gamo, Bull. Chem. Soc. Japan, 34, 760 (1961).

106. L.J.Bellamy, "The Infrared Spectra of Complex Molecules", Chapman and Hall, London (1978).

107. J.J.Charette, Spectrochim. Acta., 19, 1275 (1965).

108. H.H.Freedmann, J. Amer. Chem. Soc., 83, 2900 (1961).

109. G.R.Burns, Inorg. Chem., 7, 277 (1968).

110. K.Nag and D.S.Johrdar, Inorg. Chim. Acta., 14, 133 (1975).

111. K.Nakamoto, "Infrared Spectra of Inorganic and Coordination Compounds", Wiley Interscience, New York (1990).

112. R.Williams, E.Billig, J.H.Waters and H.B.Gray, J. Am. Chem. Soc., 88(1), 43 (1966).

113. B.N.Figgis, G.A.Melson, "Transition Metal Chemistry", Vol.8, Marcel Dekker, Inc. New York and Basel.

114. K.K.M.Yusuff and R.Sreekala, Thermochim. Acta., 159, 357 (1990).

115. A.B.P.Lever, "Inorganic Electronic Spectroscopy", Elsevier, New York (1968).

116. N.Nakanishi and P.H.Solomon, "Inorganic Absorption Spectroscopy", Holden-Day, San Fransisco (1977).

117. D.M.Adams, "Metal-ligand and Related Vibrations", Arnold, London (1967).

118. Bailar C.John, J. Catal. Rev. Sci. Eng., 10, 17 (1974).

119. C.C.Legnoff, Chem. Soc. Rev., 3, 65 (1974).

120. C.V.Pittman, G.V.Evans, Chemtech., 560 (1973).

121. J.I.Crowley and H.Rapoport, Acc. Chem. Res., 9, 135 (1976).

122. A.K.Saxena, S.Saxena and A.K.Rai, Synth. React. Inorg. Met. Org. Chem., 20, 21 (1990).

123. A.Tsipis, C.C.Hadjikostas and C.E.Manoussakis, Inorg. Chim. Acta. 23, 163 (1977).

124. R.L.Martin   and   A.H.White,   Inorg.   Chem.,   6,   712 (1967).

125. D.Petridis, A.Simopoulos and A.Kostikas, Phys. Rev. Lett., 27, 1171 (1971).

126. S.N.Choi   and   J.R.Wasson,   Inorg.   Chem.,   14,   1964 (1975).

127. R.D.Bereman   and   J.R.Dorfman,   Polyhedron,   2,   1013 (1983).

128. C.E.Batley and D.P.Graddon, Austral. J. Chem., 20, 877 (1967).

129. P.P.Singh and N.B.Singh, Polyhedron, 9, 557 (1990).

130. S.B.Kumar   and   M.Chaudhury,   J.   Chem.   Soc.   Dalton Trans., 3043 (1978).

131. M.Chaudhury, Inorg. Chem., 24, 301 (1985).

132. M.Chaudhury, Inorg. Chem., 23, 4434 (1984).

133. M.Chaudhury, J. Chem. Soc. Dalton Trans., 115 (1984).

134. G.N.Schrauzer, Acc. Chem. Res., 97, 1 (1968).

135. G.N.Schrauzer and G.Kiatel, Angew. Chem., 77, 180 (1965).

136. G.N.Schrauzer and R.J.Windgassen, J. Am. Chem. Soc., 88, 3738 (1966).

137. H.Eckert, G.N.Schrauzer and I.Ugi, Tetrahedron, 31, 1399 (1975).

138. L.I.Simandi, S.Nemeth, Z.Szeverenyi, Inorg. Chim. Acta., 44, 4107 (1980).

139. J.K.Das and K.C.Dash, Polyhedron, 4, 1109 (1985).

140. J.D.Das and K.C.Dash, Synth. React. Inorg. Met. Org. Chem., 15, 839 (1985).

141. J.K.Das and K.C.Dash, Indian J. Chem., 244, 387 (1985).

142. J.K.Das and K.C.Dash, Proc. Natl. Acad. Sci. India, 56A, 14 (1986).

143. T.Ohya, K.Iwamoto and M.Sato, J. Chem. Soc. Dalton Trans., 987 (1985).

144. Y.Yamano, I.Masuda and K.Shimura, Bull. Chem. Soc. Japan., **44**, 1581 (1972).

145. J.K.Das and K.C.Dash, Polyhedron, 5, 1857 (1986).

146. K.C.Bose and C.C.Patel, J. Inorg. Nucl. Chem., 32, 1141 (1970).

147. R.Blinc and D.Hadzi, J. Chem. Soc., 4536 (1958).

148. A.H.Norbury, D.E.Shaw and A.I.P.Sinha, J. Chem. Soc. Dalton Trans., 742 (1975).

149. A.V.Ablov, N.N.Proskina, A.Bologna and N.M.Samus, Russ, J. Inorg. Chem.,15, 1245 (1970).

150. R.B.Gillard and G.Wilkinson, J. Chem. Soc., 6041 (1963).

151. D.G.Batyr, M.P.Starysh, V.N.Shafranskii and Y.Y.Kharitonov, Russ. J. Inorg. Chem., 19, 417 (1974).

152. J.Popich and J.Halpern, Inorg. Chem., 18, 1339 (1979).

153. K.L.Brown, G.Jang, R.Segal and K.Rajeswar, Inorg. Chim. Acta., 128, 197 (1987).

154. A.W.Coats and J.P.Redfern, Nature, 68, 201 (1964).

155. C.N.Natu, S.B.Kulkarni and P.S.Dhar, J. Therm. Anal., 23, 101 (1982).

156. R.Pearce and W.R.Patterson, "Catalysis and Chemical Processes", Blackle and Sons Ltd. (1981).

157. W.B.Hillig, "Kinetics of High Temperature Processes", W.D.Kingery, (Ed.), Wiley, New York (1959).

158. W.Gomes, Nature, 192, 865 (1961).

159. T.A.Clarke and J.M.Thomas, Nature, 219, 1149 (1968).

160. T.A.Clarke, E.L.Evans, K.G.Robins and J.M.Thomas, Chem. Commun., 266 (1969).

161. J.Sestak, A.Brown, V.Rihak and G.Berggren, "Thermal Analysis", R.F.Schwenker Jr. and P.D.Garn, (Eds.), Academic Press, New York, Vol.2 (1969).

162. J.P.Redfern, "Differential Thermal Analysis", R.C.Mackenzie, (Ed.), Academic Press, New York, Vol.1 (1970).

163. J.Sestak, Talanta, 13, 567 (1966).

164. D.Rainville, "Special Functions", Macmillan & Co., New York (1960).